201

EFFECT OF PARTICLE SIZE DISTRIBUTION ON ACTIVATED CARBON ADSORPTION

by

THOPPIL JOJO KUNJUPALU

B.E., College of Engineering, Guindy, Madras University
India, 1983

A MASTER'S THESIS

submitted in partial fulfillment of the

requirements for the degree

MASTER OF SCIENCE

Department of Civil Engineering

KANSAS STATE UNIVERSITY
Manhattan, Kansas

1986

Approved by :

Alexander J. McNeil

Major Professor

A11202 965184

LD
2668
.T4
1986
K86
c. 2

Table of contents

Page

LIST OF TABLES III

LIST OF FIGURES VI

NOTATIONS IX

CHAPTER 1 INTRODUCTION 1

1.1 Discussion of problem 1
1.2 Methods of removal 3
1.2.1 Aeration 3
1.2.2 Adsorption 4
1.3 Factors that influence adsorption ... 5
1.4 Objectives of study 5

CHAPTER 2 ESTIMATION OF PARTICLE SIZE 7

2.1 Methods of sizing 7
2.1.1 Microscopial measurment 8
2.1.2 Sedimentation 8
2.1.3 Sieving 9
2.1.3.1 Types of sieves 10
2.1.3.2 Sieving errors 10
2.2 Particle shape and equivalent diameters 11
2.3 Particle size distribution 15
2.4 Determination of particle diameters. 19

CHAPTER 3 REVIEW OF RELATED LITERATURE 28

3.1 Isotherm 28
3.1.1 Single solute monolayer adsorption 28
3.1.2 Single solute multilayer adsorption 31
3.1.3 Multisolute equilibrium models. 32
3.2 Adsorption kinetics 36
3.2.1 Single solute batch modelling . 37
3.2.2 Single solute kinetics for Fixed beds 39
3.2.3 Single solute fixed bed models with two or more adsorbents ... 40
3.2.4 Multisolute modelling for batch systems 41
3.2.5 Multisolute modelling for fixed beds 43

CHAPTER 4 EXPERIMENTAL MATERIALS AND METHODS .. 46

4.1 Materials 46
4.1.1 Solutes 46
4.1.2 Adsorbent 46
4.2 Methods 49
4.2.1 Analytical methods 49
4.2.2 Analysis of particle diameters. 50
4.3 Experimental methods 50
4.3.1 Equilibrium experiments 50
4.3.2 Batch experiments 54
4.3.3 Fixed bed experiments 58

CHAPTER 5 KINETIC MODEL 63

5.1 Model equations 63
5.1.1 Model equations for finite batch reactor 64
5.1.2 Model equations for fixed bed model 65
5.2 Solution of the model 67

CHAPTER 6 RESULTS AND DISCUSSION 71

6.1 Equilibrium studies 71
6.1.1 Single solute isotherm studies for phenol and PCP 71
6.2 Single solute rate studies for single sizes 76
6.3 Single solute rate studies for mixture of sizes 90
6.4 Single solute fixed bed studies for single sizes 108
6.5 Single solute fixed bed studies for mixture of sizes 122
6.6 Multicomponent adsorption 135
6.6.1 Experimental methods 135
6.6.2 Equilibrium studies 135
6.6.3 Batch studies 139
6.6.4 Fixed bed studies 144

CHAPTER 7 SUMMARY AND CONCLUSIONS 151

APPENDIX 155

REFERENCES 169

ABSTRACT .....

LIST OF TABLES

Page

2.1 Values of and p_r for various shapes 16

2.2 Values for and C for for various geometrical forms and also for irregular particles 16

2.3 Particle size distribution of Carborandum 17

2.4 Mean proporties of particles for individual size fractions based on Quantimet image analysis 20

2.5 Mean diameters based on number and mass. 25

2.6 Carbon size fractions and diameters using area of the particle 26

2.7 Carbon size fractions and diameters using perimeter of the particle 27

4.1 Solutes and their proporties 47

4.2 Prpoporties of Carborandum 48

4.3 Carbon size fraction and diameters using area of the particle 51

4.4 Carbon size fractions and diameters using perimeter of the particle 52

4.5 Impeller speeds for different size fractions for batch studies 57

4.6 Fixed bed operating conditions 60

6.1 The isotherm constants A, B, and for phenol and PCP 75

6.2 Operating conditions for batch studies for phenol adsorpticn 77

6.3 Operating conditions for batch studies for PCP adsorption 78

6.4 External mass transfer coefficients and intraparticle diffusion coefficients for phenol adsorption for single adsorbent sizes 84

6.5 Values for film transfer coefficient corrected for impeller speeds for phenol solute 85

6.6 Values for film transfer coefficient corrected for impeller speeds for PCP solute 88

6.7 External mass transfer coefficients and intraparticle diffusion coefficients for PCP adsorption for single adsorbent sizes 89

6.8 Weights taken for mixture of sizes for batch tests for phenol adsorption 91

6.9 Weights taken for mixture of sizes for batch tests for PCP adsorption 92

6.10 Operating conditions for batch studies for mixture of sizes for phenol adsorption 93

6.11 Operating conditions for batch studies for mixture of sizes for PCP adsorption .. 94

6.12 Average particle diameters for mixtures and their effects on mass transfer coefficients and surface diffusion coefficients estimated from batch reactor studies for phenol adsorption 102

6.13 Average particle diameters for mixtures and their effects on mass transfer coefficients and surface diffusion coefficients estimated from batch reactor studies for PCP adsorption 107

6.14 Operating conditions for fixed bed for phenol adsorption 109

6.15 Percent deviations between experimental and predicted breakthrough profiles for phenol adsorption 116

6.16 Operating conditions for fixed bed for PCP adsorption 117

6.17 Percent deviations between experimental and predicted breakthrough profiles for PCP adsorption 121

6.18 Weights taken for mixture of sizes for column studies using phenol as solute 123

6.19 Weights taken for mixture of sizes for column studies using PCP as solute 124

6.20 Fixed bed operating conditions for mixture of sizes for phenol adsorption 125

6.21 Percent deviations between experimental and predicted breakthrough curves for phenol adsorption 129

6.22 Fixed bed operating conditions for mixture of sizes for PCP adsorption 130

6.23 Percent deviations between experimental and predicted breakthrough curves for PCP adsorption 134

6.24 Prediction of equilibrium data for multisolutes using extension of the three parameter equation 136

6.25 Prediction of equilibrium data for multisolutes using the IAS model 137

6.26 Operating conditions for multisolute rate studies 142

6.27 Percent deviations between experimental and predicted data for Sauter mean for multisolute rate studies 143

LIST OF FIGURES

		Page
4.1	Schematic set up for batch studies	56
4.2	Schematic set up for fixed bed studies	59
6.1	Adsorption isotherm for phenol at 25 deg. C	72
6.2	Adsorption isotherm for PCP at 25 deg. C	73
6.3	Adaorption rate for phenol for carbon sizes #12-#14 and #14-#16	81
6.4	Adsorption rate for phenol for carbon sizes #16-#18, #18-#20, and #20-#25	82
6.5	Adsorption rate for phenol for carbon sizes #25-#30 and #30-#35	83
6.6	Adsorption rate for PCP for carbon sizes #12-#14, #18-#20, #20-#25 and #30-#35	87
6.7	Adsorption rate for phenol for Mix no. 1 ..	95
6.8	Adsorption rate for phenol for Mix no. 2 ..	96
6.9	Adsorption rate for phenol for Mix no. 3 ..	97
6.10	Adsorption rate for phenol for Mix no. 4 ..	98
6.11	Adsorption rate for phenol for Mix no's 5 and 6	99
6.12	Adsorption rate for phenol for Mix no. 7 ..	100
6.13	Adsorption rate for PCP for Mix no. 1	104
6.14	Adsorption rate for PCP for Mix no. 2	105
6.15	Adsorption rate for PCP for Mix no. 3	106
6.16	Breakthrough curve for phenol adsorption for carbon size #12-#14	110
6.17	Breakthrough curve for phenol adsorption for csrbon size #14-#16	111

6.18 Breakthrough curve for phenol adsorption for carbon size #16-#18 112

6.19 Breakthrough curve for phenol adsorption for carbon size #18-#20 113

6.20 Breakthrough curve for phenol adsorption for carbon size #20-#25 114

6.21 Breakthrough curve for phenol adsorption for carbon size #30-#35 115

6.22 Breakthrough curve for PCP adsorption for carbon size #12-#14 119

6.23 Breakthrough curves for PCP adsorption for carbon sizes #18-#20, #20-#25 and #30-#35 120

6.24 Breakthrough curve for phenol adsorption for Mix no. 1 126

6.25 Breakthrough curve for phenol adsorption for Mix no's 2 and 3 127

6.26 Breakthrough curve for phenol adsorption for Mix no. 4 128

6.27 Breakthrough curve for PCP adsorption for Mix no. 1 131

6.28 Breakthrough curve for PCP adsorption for Mix no's 2 and 3 132

6.29 Adsorption rate for multicomponent adsorption for carbon size #12-#14 140

6.30 Adsorption rate for multicomponent adsorption for carbon size #18-#20 141

6.31 Adsorption rate for multicomponent adsorption for mixture of carbon sizes 145

6.32 Breakthrough curve for multicomponent adsorption for carbon size #12-#14 146

6.33 Breakthrough curve for multicomponent adsorption for carbon size #18-#20 147

6.34 Breakthrough curve for multicomponent adsorption for carbon size #30-#35 148

6.35 Breakthrough curve for multicomponent adsorption for mixture fo carbon sizes 149

Notations

a_1	Coefficient determined by nonlinear curve fitting method.	
a_2	Coefficient determined by nonlinear curve fitting method.	
a_3	Coefficient determined by nonlinear curve fitting method.	
a_4	Coefficient determined by nonlinear curve fitting method.	
A	Three parameter isotherm constant.	
B	Three parameter isotherm constant.	
B	Breadth of the tank.	
C	Solute concentration in the liquid phase	M/L^3
C	Concentration of total organic carbon.	
C_0	The initial concentration of solute in in the solution.	M/L^3
C_1	Solution concentration of solute one.	M/L^3
C_2	Solution concentration of solute two.	M/L^3
C_1^0	Solution concentration of species one as single solute at spreading pressure pi.	M/L^3
C_2^0	Solution concentration of species two as single solute at spreading pressure pi.	M/L^3

C_{b0}	Initial concentration of solute in the liquid phase.	M/L^3
C_{b1}	Concentration of solute in the liquid phase at a particular time.	M/L^3
C_e	Final concentration of solute in the solution	M/L^3
C_n	Total organic carbon resistant to adsorption.	
C_o	Initial concentration of total organic carbon during isotherm tests	
C_s	Saturation constant of solute.	M/L^3
d_1	Diameter of upper sieve.	L
d_2	Diameter of lower sieve.	L
D_L	Diffusivity of the solute	L^2/T
dM	Differential change in sample mass.	
D_{pi}	Diameter of adsorbent particle.	L
D_s	Surface diffusivity	L^2/T
D_{LM}	Length mean diameter	L
D_{gm}	Geometric mean diameter	L

D_{SM}	Sauter mean diameter	L
J_d	Mass transfer factor	
k_f	Film transfer coefficient	L/T
L_b	Bed length	L
m	Flakiness	L/L
M	Molecular weight of the solute	M
n	Elongation	L/L
n	Parameter in Freundlich isotherm	
N_{Sc}	Schmidts number	
N_{Re}	Reynolds number	
pi	Arithmetic constant.	
p_r	Prismoidal ratio.	
q	Surface concentration of solute	M/M
q_1	Surface concentration of solute 1	M/M
q_2	Surface concentration of solute 2	M/M
q_1^0	Surface concentration of species 1 as single solute at spreading pressure pi.	M/M

q_2^0	Surface concentration of species 2 as single solute at spreading pressure pi.	M/M
q_e	Surface concentration in equilibrium with the C_0	M/M
q_T	Total surface concentration.	M/M
Q^0	The number of moles of solute at the adsorbed phase.	M/M
r	Radial distance	L
R	Radius of the adsorbent	L
t	Time	T
u	Superficial velocity	L/T
V	Volume of the solution	L
W	Weight of the adsorbent	M
z	Axial distance	L
z_1	Surface mole fraction of specise 1	
α_a	Area ratio.	
α_e	Volume shape coefficient of the equidimensional particle.	
$\alpha_{s,a}$	Surface shape coefficient of the particle.	
$\alpha_{v,a}$	Volume shape coefficient of the particle.	
β	Three parameter isotherm constant.	

ϵ_b	Porosity of the bed.
ϵ_p	Intraparticle porosity.
η_j	Interaction terms.
μ	Solution viscosity.
ψ_v	Shape factor for volume.

Chapter 1

INTRODUCTION

1.1 Discussion of problem

Water is one of the materials required to sustain life and has long been suspected of being the source of many of the illnesses of man. It was not until a little over 100 years ago that definite proof of disease transmission through water was established. For many years following the major consideration was to produce adequate supplies that were hygenically safe. The public has been more exacting in its demands as time has passed and today water engineers are expected to produce finished waters that are free of color, turbidity, taste, odor, harmful metal ions and organic compounds.

It has long been known that all natural bodies of water have the ability to oxidize organic matter, provided that the organic loading rate is kept within the limits of oxygen resources in water. Owing to the wide use of pesticides and the use of chemicals by various industries there is a great deal of organic contamination in surface and ground waters. Most of these organic compounds have adverse influence on aquatic and human life.

Every organic contaminant cannot be regulated. Hence the EPA / Environmental Protection Agency / decided to regulate

these compounds based on the following considerations:-

1) Physical volume produced yearly

2) Physical and chemical properties

3) Estimated human exposure

4) Toxicological suspicion and opinion

5) Public interest

6) Significance to society

Based on the above criteria EPA issued a list of pollutants which are called priority pollutants. In this list there are 128 compounds of which 14 are metals and 114 are organic compounds. Of these 114 organic compounds 11 are phenolic compounds.

Phenolic compounds are of growing concern as water pollutants. Some phenols have very low taste and odor thresholds (eg.2 $\mu g/L$ for 2-chlorophenol) whereas others are highly persistent and toxic eg. pentachloro-phenol (PCP) Buikema et. al (1979) reviewed the occurence and biological effects of phenolic compounds in aquatic ecosystems. More than 90% of phenols are produced by industrial synthesis, but some phenolic compounds are natural products. Phenols are used for example, for wood preserving or as chemical intermediates for dye manufacturing. Natural phenols are formed in aquatic and terrestrial vegetation and can be released as pollutants by the pulp and paper industry.

Bueikma et.al (1979), Van Hall (1979) have studied the occurences of phenolic chemicals in various types of industrial wastewaters. Hexachlorophene and PCP have been

investigated in sewage and water by Butler et al. (1930). Dietz and Trand have determined large number of phenols, especially chlorinated derivatives in domestic sewage effluents, various wastewaters and surface waters.

Chlorinated phenols, otherwise known as chlorophenols, are readily soluble in water. Most of these chlorophenols are carcinogenic in nature and they produce sicknesses such as depression of the central nervous system, increase in weight of the liver and kidney, gastrointestinal problems etc. Some of the industries that have chlorophenols in their wastewaters are textile, ink, metal finishing, steam electric, leather tanning and finishing, petroleum and paint industries.

Owing to the health problems exhibited by organic compounds on life and since they impart taste and odor to waters, their removal from waters and wastewaters is a must.

1.2 Methods of Removal

There are two methods by means of which organic compounds are removed from waters : 1) Aeration, and 2) Adsorption.

Aeration or adsorption can be used to remove volatile organic compounds, but organic compounds with high solubility can be removed from waters by adsorption quite effectively.

1.2.1 Aeration

Aeration is usually done by passing air under pressure

through a body of water. As the air bubbles up to the surface it removes the volatile organic compounds present in the water and discharges it into the atmosphere. However with aeration it is not possible to remove volatile organic compounds present in water to low concentrations.

1.2.2 Adsorption

Adsorption is defined as the tendency exhibited by all solids to condense upon their surface a layer of any gas or liquid with which they are in contact. Activated carbon is used extensively for adsorptive purposes because of its termendous surface area in relation to its mass. The total surface area represented by the walls of its pores is in the range of 900-1300 square meters per gram of carbon.

Nearly every organic material capable of being carbonized is a possible candidate for the production of activated carbon. Among the most common are wood, coal, nutshells and petroleum residues.

Activation

Activation is a physical change wherein the surface of the carbon is tremendously increased by the removal of hydrocarbons from the carbon structure. There are several methods available for the activation of charcoal. The most widely employed are treatment of the carbonaceous material with oxidizing and purging gases such as air, steam or carbon dioxide and the carbonization of raw material in the presence

of chemical agents such as zinc chloride or phosphoric acid.

1.3 Parameters that influence Adsorption

There are several parameters which influence adsorption:-

1) Temperature

2) pH

3) Nature of adsorbate

4) Particle size

Generally, adsorption capacity increases when temperature decreases or when pH increases. Adsorption depends also on the molecular weight, solubility, and the concentration of the adsorbate. As the adsorbent particle size decreases the, rate of adsorption is generally higher.

Granular activated carbon adsorption is an effective unit process for the removal of synthetic organic chemicals, trihalomethanes and other organic halides from drinking water. The performance of adsorption systems is affected by the transport properties of the solutes in the solid and fluid phases and also by equilibrium adsorption capacity. The presence of other organic solutes or background organic chemicals may retard or speed up the adsorption rates and equilibria. The particle diameter, shape and size distribution can affect these parameters.

1.4 Objectives of the study :-

1) To study from batch studies if external mass transfer rate and intraparticle diffussion rate varies with particle size.

2) To assess the performance of a fixed bed model to predict break-through curves from column studies.

3) To develop a procedure to calculate a mean diameter for a particle size distribution and corresponding mean transport coefficients for use in batch and fixed bed adsorption models.

Chapter 2

Estimation of Particle Size

There are several industrial activities in which though the quantities are small, powdered materials fulfill an essential function in a manufacturing process. The useful applications of powdered materials thus include many of the raw materials used in civil engineering, chemical and mining industries, pigments and countless other industries. Another aspect concerning materials in a state of fine division, is the harmful effect of atmospheric and industrial dusts, mine dusts, smoke and grits from boilers and furnaces.

Development of the methods of sizing is the job of a physicist or a chemist, but it is the engineer who finally has to adapt the results to practical problems. There are several sophisticated instruments recently developed for size analysis. Precision methods of control now adopted for modern industrial manufacturing processes have created a need for methods of particle size analysis to a high degree.

2.1 Methods of sizing

The practical methods of size analysis thus comprise:

1) Microscopial measurment

2) Sedimentation

3) Sieving

When the powdered materials used in industry extend over

a range of particle size that is beyond the scope of analysis by any one of the above methods particle shape and equivalent diameters must be taken into consideration.

2.1.1 Microscopial measurment

The unique feature of microscopial measurment is that the particles are measured individually, instead of being grouped statiscally by some process of classification. Thus the weight of material examined is inevitably small, though if there is great variation in size, the number of particles involved to ensure a representative count may be very large. The same difficulties exist in an even more aggravated form with the electron microscope.

The lower limit of particle size that can be resolved by the microscope using visible light is of the order of 0.2 microns. The lower limit that can be resolved using ultra-violet light is 0.03 microns (Harold Heywood, 1947).

2.1.2 Sedimentation

Sedimentation is the most frequently used process for the size analysis of particles below the sieving range.

If the particles are initially distributed uniformly in a column of fluid at rest, after the lapse of a certain time there will be a density gradient or variation in concentration along the height of the column. Determination of this density gradient after a suitable time of sedimentation enables the proportion by weight of the various

sizes of particle to be calculated. The variation in particle concertation may be determined in either of the two following ways:

1) By measuring the amount of material that has settled below the depth h, where h is the height of the sedimentation column above the sampling level. This method has been designated " cumulative ".

2) By measuring at suitable intervals of time the concentration at a particular depth h below the surface. This method has been designated " incremental ".

Cumulative methods are rarely adopted nowadays because the curve relating mean concentration and time of settlement must be differentiated graphically in order to obtain the size analysis curve of weight undersize against particle diameter. In the incremental method hydrometers are made use of in determining the concentration at a given depth periodically. Errors result due to the settling of particles on the shoulder of the bulb and also due to the disturbance of the suspension when the hydrometer is constantly removed and re-inserted. Moreover this process is time consuming.

2.1.3 Sieving

Sieving is probably the easiest and certainly the most popular method of size analysis but it is restricted to powders having the greater proportion coarser than 50 microns. For finer powders the method is not generaly used because of the high cost of producing sieves with uniform

small apertures.

A sieve is an open container, usually cylindrical having definitely spaced and uniform openings in the base. The openings are square when wire mesh is used and circular when the openings are formed by punching holes in a metal plate. By stacking the sieves in order of descending aperture size and placing the powder on the top sieve and agitating, the powder gets classified into fractions. A closed pan, a reciever, is placed at the bottom of the stack to collect the fines and a lid is placed on top to prevent loss of powder. Agitation may be either manual or mechanical, but mechanical is invariably chosen. Results are usually expressed in the form of a cumulative undersize percentage distribution in terms of the nominal apertures of the sieve.

2.1.3.1 Types of sieves

A variety of sieve aperture ranges are currently used, the most popular being the 1) German Standard, 2) A.S.T.M. standard E11-61, 3) American Tyler series A.F.N.O.R., 4) the Institute of Mining Standard, and 6) the British Standard. In all our studies sieving was done using the U. S. standard mesh size sieves which had square openings.

2.1.3.2 Sieving errors

The apertures of a sieve may be regarded as a series of gauges which reject or pass particles as they are presented at the aperture. The probability that a particle will present itself at an aperture depeds on the following factors:

1) The particle size distribution of the powder.

2) The number of particles on the sieve.

3) The physical properties of the particles (eg., surface).

4) The method of shaking the sieve.

5) The dimension and shape of the particle.

6) The geometry of the sieving surface.

Wether or not the particle will pass the sieve when it is presented at the sieving surface will then depend upon its dimension and the angle at which it is presented.

The size distribution given by a sieving operation depends also on following variables:

1) Duration of sieving.

2) Variation of sieve aperture.

3) Wear.

4) Errors of observation and experiment.

5) Errors of sampling.

6) Effect of different equipment and operation.

In all our studies sieving was conducted for 10 minutes making sure that all the sieves were cleaned well to remove particles of carbon which may have stuck in between the meshes. Wet sieving was conducted when particles less than 75 microns were needed for isotherm studies.

2.2 Particle shape and eqivalent diameters.

Many powdered materials used in industry extend over a range of particle size that is beyond the scope of analysis

by any one method. for example sieving may be necessary for the coarse particles, followed by sedimentation or microscopial measurement for subsieve particles. The equivalent diameters corresponding to these various processes are only equal in the case of spheres, and the relationship for materials such as mineral particles will be affected by particle shape.

Definition of particle shape as applied to a number of particles are statistical, for in any normal powder there exists a wide variety of shapes ranging from flakes to elongated particles and including some particles that are equi-dimensional. The numerical values of shape coefficients depend on the characteristic dimension chosen to represent the particle size. It is also necessary to distinguish between the effects of geometrical shape, i.e. the closeness with which the particle approaches the shape of one of the geometrical solids, such as sphere, cube, tetrahedron, etc., and the proportions of the particle, i.e., length, breadth and thickness.

Precise definition of the terms length, breadth, thickness is important. If the particle is assumed to be resting on a plane in the position of greatest stability, the the breadth is the minimum distance between two parallel lines tangent to the profile of the particle when viewed perpendicularly to the above plane. The length is defined as the maximum distance between two parallel lines tangent to the outline as defined above and perpendicular to the lines

defining the breadth. Thickness is the distance between the two planes parallel to the plane defining the greatest stability and tangent to the surface of the particle (Allen, 1974).

If the length, breadth and thickness are represented by L, B and T, then the flakiness and elongation of the particle can be defined by the following ratios :

Flakiness, $m = B/T$

Elongation, $n = L/B$

If we consider a particle to be circumscribed by a rectangular parallelpiped of dimensions L*B*T, then the projected area of the particle, A, can be represented by

$A = (PI/4) * dp^2 = \alpha_a BL$ ------- (1)

where α_a is the area ratio.

The volume V of the particle can be representd by

$V = \alpha_{v,a} dp^3 = \alpha_a BL p_r T$ ------- (2)

where

p_r is the prismoidal ratio and is equal to T/3

and $\alpha_{v,a}$ is volume shape coefficient.

Heywood (1947) classified particles into tetrahedal, prismoidal, subangular, and rounded. From his studies he came up with values of α_a and p_r which are shown in table 2.1.

Combining equations 1 and 2 the volume shape coefficient

$\alpha_{v,a}$ can be directly given by the following equation

$$\alpha_{v,a} = \frac{\pi^{3/2}}{8} \frac{p_r}{m\sqrt{\alpha_a n}}$$

When the particle becomes equidimensional, ie. when L=B=T and n=m=1 then the volume shape coefficient of the equidimensional particle is given by

$$\alpha_e = \frac{\pi^{3/2}}{8} \frac{p_r}{\sqrt{\alpha_a}}$$

where α_e is the volume shape coefficient of the equidimensional particle.

Hence

$$\alpha_{v,a} = \alpha_e/(m\sqrt{n})$$

Hence we see that shape can be given as a combination of the relative proportions L, B, and T and the geometrical form it falls into. As a result of this we see that there exists a method of seperating the effects of geometrical shape and relative proportions of the particle.

Surface of a particle can be given by

$$S = \alpha_{s,a} dp^2$$

where $\alpha_{s,a}$ is the surface shape coefficient of the particle.

Heywood developed a relationship for $\alpha_{s,a}$ from experiments which is given by

$$\alpha_{s,a} = 1.57 + C\left(\frac{\alpha_{e,a}}{m}\right)^{4/3}\left(\frac{n+1}{n}\right)$$

where C depends on the geometrical form of the particle and is a constant. Table 2.2 shows the values of C and $\alpha_{e,a}$ for various geometrical shapes and irregular forms of the particles.

2.3 Particle size distribution

The granular activated carbon was sieved through a series of U.S. standard sieves ranging from sieve no. 12 to sieve no. 40. Eight different size fractions where collected. The particle size distribution of the carbon supplied by the manufacturer based on weight is shown in Table 2.3.

Examination of the particles using optical scanning techniques indicate these particles are generally not spherical. Particle size and shape have a significant impact on the estimated transport coefficients used in adsorption models. Particle size and shape modification have also been shown to improve performances in fixed and fluidized beds using molecular sieve adsorbents and catalyst particles (Moharir et. al., 1980).

Activated carbon samples were examined using a Quantimet 720-23A- programmable and computerized image analyser. This equipment uses a high resolution low noise video scanning system, and is connected to a PDP-11 minicomputer for data

Table 2.1 Values for α and p_r for various shapes

Shape group		α_a	Pr
Angular	Tetrahedral	0.5 - 0.8	0.4 - 0.53
	Prismoidal	0.5 - 0.9	0.53 - 0.9
Sub-angular		0.65 - 0.85	0.55 - 0.8
Rounded		0.72 - 0.82	0.62 - 0.75

Table 2.2 Values of α_{ea} and C for various geometrical forms and also for irregular particles.

Shape group		α_{ea}	C
Geometrical forms			
Tetrahedral		0.328	4.36
cubical		0.696	2.55
spherical		0.524	1.86
Approximate forms			
Angular	Tetrahedral	0.38	3.3
	Prismoidal	0.47	3.0
subangular		0.51	2.6
rounded		0.54	2.1

Table 2.3 Particle size distribution in the given carbon.

Sieve size	Percent fraction
#12-#14	9.4
#14-#16	21.0
#16-#18	17.6
#18-#20	20.0
#20-#25	14.5
#25-#30	9.8
#30-#35	4.6
remaining	3.1

processing. Parameters measured using this instrument include particle area, perimeter and aspect ratio. These parameters for individual particles, were combined for a size fraction to generate mean particle diameters.

Quantimet image analysis is a recognized tool for direct and quantitative assessment of macro and micro objects. Quantimet-720 system was used to perform rapid and reliable analysis of coal particle samples categorized individually according to their projected area, equivalent diameters, perimeter, circularity, shape factor and aspect ratio.

Quantimet-720 utilizes a cathode ray tube vidicon. The optical images results in the formation of a matching image made up of electrical charges varying with image brightness. The charged image is scanned by an electron beam to produce an output video signal.

Conditions under which the images were digitized had to be carefully controlled. Electronic digitizing equipment have to be set to establish optimal conditions for detection. The video image of the sample is transmitted and displayed on the TV monitor. The several modules process the digitized information. Assuming proper detection, the digitized image or the detected image is a good approximation for the shape and area of the object.

The output of measurements is in the form of distribution graphs of above mentioned shape factors. Mean,

median, standard deviations of the given group were automatically calculated.

Errors could be caused by particles touching one another and this was noticed, especially in small particles. To remove this error those particles which stuck to one another were not measured. In each field a number of adsorbent particles were grouped to produce an image that filled the size of the screen. The results of Quantimet-720 measurements were plotted on log-probability paper as percent cumulative by weight less than the stated size against diameter. The particle size distribution of the sieve sizes in the range of #12-#14 to #30-#35 are shown in the appendix. The particle size distribution shown in the appendix is in the form of log-normal distribution. From these plots it is seen that for any particular size fraction there are particles with varying diameters. Table 2.4 gives the mean area of the particle, mean perimeter of the particle, mean bulkiness and mean aspect ratio of the particles.

From the table we see that the mean aspect ratio is almost equal to the mean bulkiness of the particle. It was also seen that the mean aspect ratio of the particles for each size fraction almost remained a constant at 1.3.

2.4 Determination of particle diameters

The average diameter of the particles was determined in three different ways. They are as follows :-

1) Geometric mean diameter (Dg_m).

Table 2.4 Mean properties of particles for individual size fraction based on Quantimet analysis.

Sieve size	Mean area of particle (mm^2)	Mean perimeter of particle (mm)	Mean bulkiness $\frac{(per^2)}{4*pi*Area}$	Mean aspect ratio len/br	Number of particles
#12-#14	2.27	6.07	1.29	1.3	109
#14-#16	1.7	5.25	1.29	1.25	229
#16-#18	1.01	3.9	1.20	1.29	321
#18-#20	0.824	3.5	1.18	1.25	284
#20-#25	0.622	3.18	1.29	1.3	281
#25-#30	0.45	2.6	1.20	1.26	378
#30-#35	0.28	2.05	1.19	1.28	439

2) Length mean diameter (D_{lm}).

3) Sauter mean diameter (D_{sm}).

In all our studies a known weight of carbon was used. Hence the diameters had to be evaluated based on mass. The following paragraphs discusses the different diameters and the process of converting diameters represented by number fractions into weight fractions.

1) Geometric mean diameter :- The geometric mean diameter of the carbon particle was found by finding the geometric mean of the upper and lower sieves ie.

$$D_{gm} = (d_1 * d_2)^{0.5}$$

2) Length mean diameter :- The length mean diameter is represented in terms of number distribution by the following equation : (Foust et al., 1956)

$$\sum_{i=1}^{K} \frac{D_{pi}\phi(D_{pi})\Delta D_{pi}}{\sigma'} \quad \text{where } \sigma' = \sum_{i=1}^{k} \phi(D_{pi})\Delta D_{pi}$$

but

$$\frac{dM}{\Delta D_{pi}} = \phi_m(D_{pi}) \text{ - - - - - - - - } (A)$$

The left hand side is the differential change in sample mass for a differential change in particle dimensions for discrete intervals.

$$\frac{\Delta n}{D_{pi}} = \phi(D_{pi}) \text{ - - - - - - - } (B)$$

where the left hand side is the number of particles in that dimension class.

$$\phi(D_{pi}) = \frac{\phi_m(D_{pi})}{\rho \psi_v D_{pi}^3} \text{ - - - - - - - } (C)$$

where the dinominator term is the mass of individual particles and ψ_v is the shape factor for volume.

Hence the length mean diameter in terms of mass reduces to

$$\frac{\sum_{i=1}^{K} \frac{D_{pi}\phi_m(D_{pi})\Delta D_{pi}}{\rho \psi_v D_{pi}^3}}{\sum_{i=1}^{K} \frac{\phi_m(D_{pi})\Delta D_{pi}}{\rho \psi_v D_{pi}^3}} = \frac{\frac{1}{W}\sum_{i=1}^{K} D_{pi}\phi_m(D_{pi})\Delta D_{pi}}{\frac{1}{W}\sum_{i=1}^{K} \phi_m(D_{pi})\Delta D_{pi}}$$

where W is the total mass of carbon taken. The dinominator reduces to one and so the equation reduces to

$$D_{LM} = \sum_{i=1}^{K} \Delta x_i \, \Delta D_{pi}$$

where Δx_i is the weight fraction.

3) Sauter mean diameter :- The sauter mean diameter is otherwise called the volume surface mean and can be represented in terms of number distribution by the following equation :

$$\frac{\sum_{i=1}^{K} D_{pi}^{3}\,\phi(D_{pi})\,\Delta D_{pi}}{\sum_{i=1}^{K} D_{pi}^{2}\,\phi(D_{pi})\,\Delta D_{pi}}$$

using equations A, B, and C from the previous page we can represent this equation in terms of mass

$$\frac{\sum_{i=1}^{K} \dfrac{D_{pi}^{3}\,\phi_m(D_{pi})\,\Delta D_{pi}}{\rho\,\psi_v\,D_{pi}^{3}}}{\sum_{i=1}^{K} \dfrac{D_{pi}^{2}\,\phi_m(D_{pi})\,\Delta D_{pi}}{\rho\,\psi_v\,D_{pi}^{3}}}$$

$$\Longrightarrow \frac{1}{\sum_{i=1}^{K} \dfrac{\Delta x_i}{D_{pi}}}$$

Table 2.5 gives the formulas for the conversion from number to mass or vice versa. Tables 2.6 and 2.7 give the sieve size fraction and their different diameters based on quantimet measurments with respect to area of the particle and perimeter of the particle respectively.

From the tables we see that the Sauter mean diameters based on perimeter of the particle had the largest value. Sauter mean diameters for both area and perimeter of the particle have largest diameters in their respective classes. The Sauter mean diameter is a function of the volume and the surface area of the particle. Moreover in any particular size range, particle shapes vary significantly. This results in particles with various linear dimensions. The presence of irregularly shaped particles that are extremely long or flat may result in particles with sizes larger than the upper sieve size and smaller than the lower sieve size. In comparison to the Sauter mean diameter the geometric mean diameter is just a function of the dimensions of the mesh size. This could possibly be a reason why the Sauter mean diameters are much larger than the geometric mean diameters.

Table 2.5 Mean diameters based on number and mass of particles

	Based on number	Based on mass
Geometric mean diameter	$(d_1 * d_2)^{0.5}$	$(d_1 * d_2)^{0.5}$
Length mean diameter	$\dfrac{D_{pi}\,\phi(D_{pi})\,\Delta D_{pi}}{\sigma'}$	$\sum_{i=1}^{k} \Delta x_i \,\Delta D_{pi}$
Sauter mean diameter	$\dfrac{D_{pi}^{3}\,\phi(D_{pi})\,\Delta D_{pi}}{D_{pi}^{2}\,\phi(D_{pi})\,\Delta D_{pi}}$	$\dfrac{1}{\sum_{i=1}^{k} \dfrac{\Delta x_i}{D_{pi}}}$

Table 2.6 Carbon size fraction and diameters using area of the particle.

Size fraction	Geometric mean diameter microns	Length mean diameter microns	Sauter mean diameter microns
#12-#14	1540.0	1710.0	1752.0
#14-#16	1295.0	1504.0	1556.0
#16-#18	1091.0	1122.0	1157.0
#18-#20	917.0	1045.0	1075.0
#20-#25	772.0	888.0	923.0
#25-#30	647.0	769.0	782.0
#30-#35	543.0	638.0	645.0

Table 2.7 Carbon size fractions and diameters using perimeter of the particle.

Sieve size	Geometric mean diameter microns	Length mean diameter microns	Sauter mean diameter microns
#12-#14	1540.0	1920.0	1965.0
#14-#16	1295.0	1665.0	1710.0
#16-#18	1091.0	1255.0	1297.0
#18-#20	917.0	1148.0	1184.0
#20-#25	772.0	1010.0	1067.0
#25-#30	647.0	840.0	867.0
#30-#35	543.0	655.0	686.0

Chapter 3

Review of Related Literature

Now that the particle diameters in terms of weight have been estimated it is necessary to see which of the diameters could predict batch and column adsorption best.

3.1. Isotherms

An adsorption isotherm is an expression of the equilibrium at constant temperature, between the concentration of a species on the adsorbent surface and the concentration in bulk solution. In simpler terms, isotherm indicates the maximum amount of solute a particular type of adsorbent can adsorb. Isotherms can be classified as to whether they describe the adsorption of a single solute or mixture of solutes and if it is monolayer adsorption or multilayer adsorption.

3.1.1. Single solute monolayer adsorption

The two simplest isotherm equations for describing the adsorption of a single species are the irreversible (rectangular) isotherm and the linear isotherm and they are represented by the following equations :

$$q = K_r \text{ -------- rectangular isotherm}$$

$$q = K_1 C \text{ ------- linear isotherm}$$

where q is the surface concentration and C is the

concentration of solute in the liquid phase.

Unfortunately neither equation is generally adequate in characterizing the adsorption of organics from aqueous solution onto activated carbon. The equilibrium data of a very strongly adsorbing species may in some cases be approximated by the irreversible isotherm. The linear isotherm is most likely to be valid at low concertations.

Two linear models, the Freundlich isotherm and the Langmuir isotherm have been frequently employed to describe equilibrium. They are represented by the following equations

$$q = KC^n \text{ --------- Freundlich isotherm}$$

$$q = QbC/(1 + bC) \text{ -- Langmuir isotherm}$$

The Freundlich isotherm was originally developed empirically. The Langmuir isotherm was theoretically derived on the assumptions of a monolayer as maximum adsorption, a constant energy of adsorption, and no migration of solute in the plane of the surface. It predicts a saturation surface concentration, q , for high solution concentrations and it reduces to the linear form at low concentrations.

In case of adsorption by activated carbon in aqueous systems, neither Freundlich nor Langmuir equations may describe the data satisfactorily over a range of concentrations. Therefore, an empirical equation with three parameters has been proposed (Redlich and Peterson, 1959; Radke and Prausnitz, 1972; and Mathews and Weber, 1977). The

equation is of the form

$$q = AC/(1 + BC^{\beta}) \qquad \beta \leq 1$$

At high concentrations this equation becomes Freundlich and at low concentrations it becomes linear and when $\beta = 1$ it becomes Langmuir isotherm. The three parameters A, B, β can be determined by statistical fit of the equation to the experimental data.

Another three parameter model recently presented by Jossens et al. (1978) is

$$C = (q/H)\exp(Fq^{p})$$

or

$$\ln C = \ln q - \ln H + \overset{F}{\cancel{K}}q_e^{p}$$

This equation expresses solution concentration as a function of surface concentration. p is a constant such that $0 < p < 1$ and is related to the distribution of energy sites on the surface. H and F are functions of temperature only and are constants.

Another type of isotherm expressing solution concentration as a function of surface concentration is one suggested by VanVliet and Weber (1979,1980). The equation is as follows:

$$C = a_1 q (a_2 q^{a_3} + a_4)$$

a_1, a_2, a_3, a_4 are coefficients determined by a nonlinear

curve fitting method to minimize the sum of squares of residuals between experimental and predicted values.

Sweeny et al. (1982), suggested a different approach for evaluating adsorption isotherm parameters. It assumes the amount of adsorbent as the independent variable and final concentration as the dependent variable. The equation is given as follows:

$$C^2+(1/b-C_O-C_n+q^OX)C+C_OC_n-C_O/b-Q^OC_nX = 0$$

For Langmuir isotherm

$$(C-C_O)(C-C_n)^{-1/n} + K_fX = 0$$

For Freundlich isotherm

where

b = parameter in the Langmuir equation

C = concentration of total organic carbon

C_n = total organic carbon resistant to adsorption

C_o = initial concentration of total organic carbon during isotherm tests

k_f = parameter in the Freundlich equation

n = parameter in the Freundlich equation

X = concentration of activated carbon

In our studies isotherm experimental data was fitted by the three parameter isotherm equation as proposed by Mathews and Weber,(1975).

3.1.2 Single solute multilayer adsorption

The Brunauer, Emmet, Teller (BET) model represents

isotherms reflecting multilayer adsorption. The BET model assumes that a number of layers of adsorbate molecules form at the surface and that the Langmuir equation applies to each layer. A further assumption of the BET model is that a given layer need not be completed prior to the initiation of subsequent layers. The BET isotherm reduces to the Langmuir model when the limit of adsorption is a monolayer. The BET model equation is represented as follows:

$$q_e = BCQ^o/((C_s-C)(1+(B-1)(C/C_s))$$

where C_s is the saturation concentration of solute, C is the measured concentration in solution at equilibrium, Q^o is the number of moles of solute at the adsorbed phase per unit weight of adsorbent in forming a complete monolayer on the surface, q_e is the number of moles of solute adsobed per unit weight at concentration C, and B is the constant of the energy of interaction with the surface. This equation can also be put in the linear form as follows :

$$C/((C_s-C)q_e) = 1/(BQ^o)+(B-1/(BQ^o))(C/C_s)$$

3.1.3 Multisolute equilibrium models

The Langmuir model of competitive adsorption is as follows:

$$q_i=((Q_i b_i C_i)/(1+\sum_{j=1}^{k} b_j C_j))$$

This was first derived by Butler and Ockrent and the

assumptions were based on the Langmuir model for single solute systems. The surface concentration q_i of adsorbate i is expressed as a function of the solute concentrations of all k species in the mixture. The constants in the equation are obtained from single solute systems.

Schay et al. (1957) modified the Langmuir competitive equation to improve its description of equilibrium data. The model is as follows :

$$q_i = Q_i b_i (C_i/\eta_i)/(1+\sum_{j=1}^{k} b_j C_j/\eta_j)$$

The interaction terms η_j are evaluated by correlating the model to multisolute experimental data.

Jain and Snoeynik (1973) introduced a bisolute model which is a modification of the Langmuir and is to be applied to those systems where Q_1 is not equal to Q_2. The equation is as follows :

$$q_1 = \frac{(Q_1-Q_2)b_1C_1}{1+b_1C_1} + \frac{Q_2 b_1 C_1}{1+b_1C_1+b_2C_2}$$

$$q_2 = \frac{Q_2 b_2 C_2}{1+b_1C_1+b_2C_2}$$

It is a semicompetitive model where the quantity of sites corresponding to $Q_1 - Q_2$ (where $Q_1 > Q_2$) are assumed to be due to either chemical specificity or molecular exclusions, receptive only to solute 1 whereas the solutes compete for the remaining sites corresponding to Q_2.

Mathews (1975) extended the three-parameter isotherm to

multisolute adsorption by forwarding the following equation :

$$q_i = \frac{\beta_i C_i}{1 + \sum_{j=1}^{k} a_j C_j^{\alpha_j}}$$

The constants are evaluated from single solute systems that are described by the three-parameter isotherm. He proposed another equation by applying the correlation procedure of Schay et al. (1957)

$$q_i = \frac{\beta_i \left(C_i / n_i \right)}{1 + \sum_{j=1}^{k} a_j \left(C_j / n_j \right)^{\alpha_j}}$$

Fritz and Schlunder (1974) have proposed a general empirical multisolute model :

$$q_i = \frac{a_{io} C_i^{b_{io}}}{E_i + \sum_{j=1}^{k} a_{ij} C_j^{b_{ij}}}$$

For certain values of the constants , the model reduces to the Langmuir competitive model or Mathew's multisolute extension of the three-parameter isotherm. Some of the model constants need to be obtained from multisolute data.

The ideal adsorbed solution (IAS) model has been derived from thermodynamics by Radke and Prausnitz (1972). It predicts multisolute equilibrium using single-solute

isotherms and is not restricted to any specific type of isotherm. The assumptions in the model are :

1) The adsorbent is thermodynamically inert

2) The available surface area is identical for all solutes

3) The liquid soluton is dilute

4) The adsorbed phase forms an ideal solution

The working equations are as follows :

$$q_T = q_1 + q_2 \qquad (1)$$

$$z_1 = q_1/q_T \qquad (2)$$

$$\frac{\pi A_d}{R' T_p} = \int_0^{C_1^\circ} \frac{q_1^\circ}{C_1^\circ}\, dC_1^\circ = \int_0^{C_2^\circ} \frac{q_2^\circ}{C_2^\circ}\, dC_2^\circ \quad \text{-----} \; (3)$$

$$1/q_T = Z_1/q_1^\circ + (1 - Z_1)/q_2^\circ \qquad (4)$$

$$C_1^\circ = f(q_1^\circ) \qquad (5)$$

$$C_2^\circ = f(q_2^\circ) \qquad (6)$$

$$C_1 = C_1^\circ z_1 \qquad (7)$$

$$C_2 = C_2^\circ (1-z_1) \qquad (8)$$

where

q_1° is the pure component adsorption for solute one, and

q_2° is the pure component adsorption for solute two

$$q_1^\circ = aC_1^\circ/(1 + BC_1^\beta) \qquad (9)$$

$$q_2^\circ = aC_2^\circ/(1 + BC_2^\beta) \qquad (10)$$

The values of a, B, and β are determined from single solute isotherm studies. The values for C_1^0 and C_2^0 can be solved simultaenously by substituting the equations 9 and 10 into the equations 3 and 4. From equations 7 and 8 the solution concentration C_1 and C_2 can be calculated and using the values for C_1 and C_2, q_1 and q_2 can be determined.

There are several possible drawbacks to the IAS model. Single-solute data are required at very low concentrations for the accurate calculation of spreading pressure. Considerable computational effort is required to solve the simultaneous equations, especially if the spreading pressure integration (equation 3) cannot be accomplished analytically. Finally, the assumptions of an ideal adsorbed phase may fail at high surface loadings, leading to poor predictions.

3.2 Adsorption kinetics

Adsorption kinetics involve determining the rate of adsorption on the adsorbent. The rate of adsorption is determined by one or more diffusional steps. The steps are as follows :

1) Mass transfer from solution phase to the external surfaces of the adsorbent through the liquid film surrounding the particle and is known as film transfer; 2) Transport of the liquid within the particle and is known as intraparticle diffuion; 3) adsorption reaction at the surface.

The intraparticle diffusion can be further divided into pore and surface diffussion. Pore diffussion is when the solute is transferred to the centre of the particle by the liquid within the pores and surface diffusion is when the solute is transferred to the centre of the particle by moving along the surface of the adsorbent and can be said to be a result of the concentration gradient within the individual adsorbent particle. The slowest of the three steps is the rate limiting step. The reaction step is usually very fast and is neglected as the rate limiting step.

3.2.1 Single solute batch kinetics modeling

Several models have been developed taking into account one or more different rate processes. There have also been attempts to simplify these rate processes by taking into consideration different assumptions. They are as follows :
1) An overall or effective reaction rate expression - (Thomas, 1944; Hiester and Vermeulen, 1952; Keinath and Weber, 1968). 2) A linear or quadratic driving force approximation for intraparticle diffusion (Glueckauf and Coates, 1947; Vermeulen, 1953; Vassiliou and Dranoff, 1962; Hall et al. 1966; Cooney and Strusi, 1972; Hsieh et al. 1977) 3) Film transfer as the only rate controlling factor - (Gariepy and Zwiebel, 1971; Zwiebel et al. 1972; Kyte, 1973; Keinath, 1977)

Weber and Rumer (1965) have proposed a model

considering pore diffusion, cylindrical psrticle shape and Langmuir isotherm for adsorption of benzenesulfonates on actvated carbon. Snoeyink and Weber (1968) proposed a similar model but having spherical particles.

Suzuki and Kawazoe (1974) proposed a model which considered surface diffusion as the rate controlling step. The diffusivities were found for fifteen different organics and correlated to the ratio of the boiling point of the solute to the sdsorption temperatures.

Neretnieks (1967) has presented and solved equations for pore surface and combined diffusion along with film transfer considerations. The isotherms used were of Freundlich and Langmuir forms.

Digiano and Weber (1973) have considered film resistance, pore diffusion and Langmuir isotherm in their infinite batch model to describe data for p-nitrophenol and 2,4-dinitrophenol with activated carbon. Infinite batch system is one in which a boundary condition of constant concentration of solute in solution is implied. It was found that the anionic forms of the solute did not diffuse as rapidly ss in their neutrsl forms.

Mathews and Weber (1977) developed the homogenous solid phase diffusion model with the three parameter isotherm and succesfully predicted adsorption for four solutes exhibiting widely different adsorption equilibrium and rate characteristics.

3.2.2 Single solute kinetics for fixed beds

Several models have been developed using the rate process described earlier to predict breakthrough profiles of fixed beds.

Morton and Murril (1967), Stuart and Camp (1973) have used fixed bed models accounting for film and surface diffusion and a nonlinear isotherm. The experimental data fitted well to the model. A similar model but with axial dispersion was used by Colwell and Dranoff (1969) and it was seen that the experimental data fitted the model well.

In 1970 Wheeler and Middleman proposed a model which incorporated three types of resistances. Intraparticle transport was described by surface diffusion and the surface reaction was assumed to obey Michaelis-Menton kinetics. Particle to fluid convective mass transfer was also considered.

Peel and Benedeck (1980) have developed a model based on the knowledge of the internal structure of the activated carbon. Here the carbon particle is divided into two regions, micropores and macropores. In the macropores relatively rapid diffusion and adsorption takes place and the rest of it takes place in the micropores till equilibrium is reached. This model, however did not show any significant change in the model predictions.

Weber and Pirbazari (1982) studied the adsorption charachteristics of benzene, p-dichlorobenzene, carbon

tetrachloride, dieldrin, and two PCB's in water. They used the Michigan Adsorption Design and Application Model (MADAM) for data synthesis to simulate and predict how carbon beds perform in removing compounds under water treatment conditions.

3.2.3 Single solute fixed bed models with two or more adsorbents.

Many researchers have tried to use different adsorbents rather than one adsorbent. Smith et al. (1959) studied the adsorption of 2,4-dichlorophenol with four different types of activated carbon. They tried to correlate kinetics to the carbon charachteristics like, pore size distribution and surface area. A relationship was apparaent between adsorption rate and micropores which were less than 250 Å radius.

Suzuki and Kawazoe (1974) have proposed a model for the adsorption of 2-dodecyl benzene sulfonate on four different types of activated carbon, assuming a rectangular isotherm.

Westermark (1975) modeled four carbons. The water used was treated by sedimentation, biological oxidation and coagulation with alum. It was further filtered to remove suspended matter. The contaminants were measured in terms of COD. The experimental data was corrected for nonadsorbable and extremely adsorbable compounds by varying the values of the isotherm constants in the linear isotherms, and the pore diffusivity.

Holzel et al. (1979) found a fairly linear relationship

between the surface diffusivities for p-nitrophenol and the pore volume of the activated carbons. The p-nitrophenol exhibited a higher diffusivity in a carbon with larger pore volume.

Van Vliet and Weber (1979) used two activated carbons and eight synthetic (carbonaceous and polymeric) adsorbents to study the adsorption of p-chlorophenol and p-toluene sulfonate. The adsorbents differed widely in capacity, film transfer coefficients and surface diffusivity values. Film transfer coefficients for synthetic adsorbents could not be estimated accurately by using literature values. They therefore incorporated particle shape and surface topography factor in film transfer coefficients.

Lee et al. (1980), have developed a model to predict adsorption of humic substances on different carbons. The model predicted correctly the fixed bed performance by using film transfer coefficients and surface diffusivities independent of fixed bed experimental data. They also found that alum coagulation before adsorption increased service time of all carbons.

3.2.4 Multisolute Modelling for Batch Systems

Mathews (1975) has applied the homogenous solid phase diffusion model for single solute and multisolute adsorption in a finite batch reactor. The three parameter isotherm of Radke and Prausnitz was extended for a bisolute system using

bisolute equilibrium data. Film transfer coefficients and surface diffusivities were estimated by a parameter search technique to fit single solute rate data and these values were used to predict bisolute batch reactor data. Runs with a mixture of phenol and p-toulene sulphonate were well predicted but data fron phenol and p-bromophenol were not so well predicted. The mixture of phenol and dodecyl benzene sulphonate was poorly predicted and was thought to be due to the interaction between the solutes. A change in film transfer coefficients but the same diffusivities gave better predictions.

Liapis and Rippin (1978) proposed a model with general equations describing multisolute adsorption in a finite batch reactor. The equations included film and intraparticle resistance. Intraparticle resistance was due to the pore, surface or combined diffusion. Numerical solutions of bisolute adsorption with pore or surface diffusion were given in the case of independendtly diffusing solutes. A solute could be assumed to diffuse into the adsorbent either independent of the concentration or with dependence on other solutes. Experimental data for 2-butanol and t-amyl alcohol adsorbed on activated carbon were tested against the predictions of the model. The single solute dats was described by the Freundlich isotherm, while bisolute data was described by the five parameter equation of Fritz and Schlunder (1980).Film transfer coefficients were calculated from literature and surface diffusivities were estimated by

trial and error. Both models described the adsorption model well and they also found that pore diffusivity happened to decrease with increasing starting concentration.

Adsorption of several phenolic compounds on activated carbon was tested by Fritz et. al(1980) to develop their model for single solute and bisolute systems. Freundlich isotherms were used for single solute data but IAS theory or Fritz-Schlunder equations were used for bisolute data. Both film and intrparticle transport were used in this model. They found that for low concentrations of the order of 10^{-4} M, a simple film resistance model predicted the data well and for high concentrations intraparticle transport had to be taken into consideration. Deviations in the predictions from experimental data were thought to be due to the diffusional interaction between solutes.

3.2.5 Multisolute Modelling for Fixed Beds

Crittenden (1976) and Crittenden and Weber (1978) have studied single solute and bisolute adsorption of the same solutes and adsorbent as used by Mathews (1975). They used homogeneous solid diffusion model including film resistance. Influent concentrations were varied 20%. The surface diffusivities were calculated from single solute batch studies, while film transfer coefficients were estimated from literature. The model predictions were good for single solute data but not for bisolute fixed bed experiments. The

discrepancies observed were thought to be due to experimental data scatter, poor equilibrium description or failure of the assumption of independent diffusion of the solutes.

Liapis and Rippin (1978) have proposed another fixed bed model which includes film resistance, pore diffusion and axial dispersion. The model incorporates diffusivities from batch experiments and predictions for two alcohols were found to be in good agreement with the experimental results. The model, however, failed to describe the overshoot of the weaker species. Also, increase in bed length was observed to induce a larger displacement of this species.

Crittenden et. al (1980), studied the adsorption of p-nitrophenol and p-bromophenol on a duolite A-7 resin with a model that incorporated homogenous solid diffusion and film transfer. Film transfer coefficients were estimated from literature. The equilibrium data was described by Langmuir competitive isotherm. The surface diffusivities were calculated by fitting the model to experimental fixed bed data for simultaneous feeding of two solutes. Good agreement was observed between predictions of the model and the experimental bed run data for sequential feeding of two solutes.

Famularo et al (1980), have developed a micro/macro shell model representing diffusion through an adsorbent having a bimodal pore size distribution. An adsorbent particle was divided into two regions, a spherical core with micropores enclosed by an annular shell with macropores. A

linear driving force was assumed to be the driving force for the transport through each region. Film resistance was also incorporated. Kinetic parameters were determined for phenol and p-nitrophenol with carbon as adsorbents, by single solute batch tests and isotherms were previously determined.

Thacker et. al (1981), have studied adsorption of 3,5-dimethyl phenol and Rhodamine 6G on four different activated carbons. One carbon was pretreated with aqueous chlorine to evaluate the effect of chlorine pretreatment on adsorption. The film transfer and homogenous surface diffusion were the mass transfer steps incorporated into the model. The single solute data were fitted by the Freundlich and Myers isotherms whereas the bisolute data was fitted by the IAS model. The model predicted well for single and bisolute bed studies of adsorption, desorption and sustained step changes in the influent concentration.

Yen and Singer (1984) applied the IAS model with a modified calculation to test ten sets of binary and ternary phenolic mixtures. The Langmuir competitive model was used for comparison. Here they found that the IAS model gave better predictions than the Langmuir competitive model in all cases of study.

Chapter 4

EXPERIMENTAL MATERIALS AND METHODS

4.1 Materials

4.1.1 Solutes

The solutes used in the study were phenol and parachlorophenol. The properties of both solutes are shown in the table 4.1. Both the solutes were obtained in the crystallised form from J.T.Baker Chemical Co; (Phillipsburg, NJ). Phenol has a water solubility of 82 gm/l whereas parachlorophenol has a solubility of 2.70 gm/l.

For all experiments stock solutions were initially prepared and in no experiment were the crystals directly introduced into the reactors. All solutions were made up using tap water that was passed through a three foot carbon column to remove organics and other adsorbables present in the water. The water passing through this carbon column was used for equilibrium experiments, batch studies and column experiments.

4.1.2 Adsorbent

The adsorbent used was activated carbon (Carborandum) supplied by CECA Inc., Pryor, Oklahoma. The properties of the carbon used are listed in table 4.2.

Table 4.1 Solutes and their proporties.

	Phenol	PCP
Supplier	J.T. Baker Chm. Company	J.T. Baker Chm. Company
Reagent grade	Baker TM	Baker TM
Formula		
Molecular Weight	94.1	128.56
pK_a		
Solubility in water per litre	82gm /L	2.70gm /L 27.0
Diffusivity @ 25 deg. C. in cm^2/sec	$1.04*10^{-5}$	$9.9*10^{-6}$

Table 4.2 Proporties of the adsorbent.

Manufacturer	CECA Inc., Pryor, Okhlahoma
U.S. Mesh size	12/40
Raw material	Bituminus coal
Physical Proporties	
Surface area, m^2/gm	1000-1100
Apparent density, gm /cc	0.47
Particle density wetted in water, gms/cc	0.60
Effective size, mm	1.9 or less

4.2 Methods

4.2.1 Analytical Methods

Solution concentrations of phenol and parachlorophenol were analyzed by ultraviolet light absorption spectrophotometry with a Baush and Lomb spectronic 710 spectrophotometer. Initially, tests were made to find the maximum wavelengths of absorption for phenol and parachlorophenol. Once these were established, several solutions of different concentrations for phenol and parachlorophenol were prepared and these solutions were used to obtain the calibration charts for each solute independently at its wavelength of maximum absorbance. Phenol was analysed at a wavelength of 268 nM and parachlorophenol at a wavelength of 279 nM.

In the case of the bisolute system Friedel's method (1951) was made use of to compute individual concentrations. This method is based on the assumption that absorbance measured in a mixture is the sum of the absorbance of each compound at that wavelength. Equations developed at each wavelength is as follows:

$$A_{268} = \epsilon_{phenol1} C_{phenol} + \epsilon_{PCP1} C_{PCP}$$

$$A_{279} = \epsilon_{PCP2} C_{PCP} + \epsilon_{phenol2} C_{phenol}$$

where

A_{268}, A_{279} = Total absorbance at 268 nM and 279 nM

C_{PCP}, C_{Phenol} = Concentration of p-chlorophenol and

phenol respectively.

$\epsilon_{phenol1}$, ϵ_{pcp1} = Molar absorptivities of pheonol and p-chlorophenol at wavelength 268 nM

$\epsilon_{phenol2}$, ϵ_{pcp2} = Molar absorptivities of phenol and p-chlorophenol at wavelength 279 nM

From the above set of equations we see that the only unknowns are C_{pcp} and C_{phenol} and since there were two equations these concentrations were established.

4.2.2 Analysis of particle diameters.

This has already been discussed in chapter two and table 4.3 and table 4.4 lists the the diameters of the particles based on the area and perimeter of the particle respectively.

4.3 Experimental Methods

4.3.1 Equilibrium Experiments

Equilibrium experiments were conducted to determine the capacity of carbon at various solution concentrations. This was determined by the standard bottle-point method. This method consists of allowing a solution of known initial concentration to come into contact with different amounts of carbon doses until equilibrium is reached. The carbon used for these experiments were the ones passing through 75μm and retained on the 53μm sieve. This carbon was obtained by wet sieving. The carbon obtained was then placed in glass

Table 4.3 Carbon size fraction and diameters using area of the particle.

Size fraction	Geometric mean diameter microns	Length mean diameter microns	Sauter mean diameter microns
#12-#14	1540.0	1710.0	1752.0
#14-#16	1295.0	1504.0	1556.0
#16-#18	1091.0	1122.0	1157.0
#18-#20	917.0	1045.0	1075.0
#20-#25	772.0	888.0	923.0
#25-#30	647.0	769.0	782.0
#30-#35	543.0	638.0	645.0

Table 4.4 Carbon size fractions and diameters using perimeter of the particle.

Sieve size	Geometric mean diameter microns	Length mean diameter microns	Sauter mean diameter microns
#12-#14	1540.0	1920.0	1965.0
#14-#16	1295.0	1665.0	1710.0
#16-#18	1091.0	1255.0	1297.0
#18-#20	917.0	1148.0	1184.0
#20-#25	772.0	1010.0	1067.0
#25-#30	647.0	840.0	867.0
#30-#35	543.0	655.0	686.0

beakers and dried at a temperature of 120 deg.C. To test if the carbon was totally free of all moisture, a sample of the carbon was set aside in the heater and when the weight of this carbon did not differ from two consecutive readings taken on two consecutive days it was presumed that the carbon was free of moisture. It took five days for the carbon to reach this state.

Different amounts of carbon were then added carefully to marked bottles with teflon seal caps. To each bottle 100 ml of solution of known concentration was added. The pH of the water used to make up the solution was 7. This was done by initially filling up a jar of 4 liter capacity with tap water. One thousand mL of tap water was then filled into a beaker and the pH of this water was measured while the water was being stirred. The pH of the water varied from day to day studies but remained between 8.5 and 8.7. Depending on the pH of the water a certain quantity of 3.6N sulphuric acid was introduced into the water in the beaker by using a burette until the pH reached 7. From this the amount of sulphuric acid needed to lower the pH of the water in the jar was established. This water was then made use of to make up the solutions. Once the solutions were introduced into the bottles, the bottles were then tightly closed and sealed to make sure that they were air tight. The bottles were then placed in an incubator shaker (Labline Instruments 111). Since all experiments were to be conducted at 25 deg.C care was taken to see that the temperature in the incubator was 25

deg.C. The shaker was set in such a way that the carbon particles were suspended and no carbon stuck to the sides of the bottles. Three bottles of solution with no carbon were kept aside in the incubator shaker to see if the glass adsorbed any of the solutes or if there was any change due to biological reaction. Three bottles of solution of the same concentration and the same weight of carbon were set aside to see when equilibrium was reached. Both phenol and parachlorophenol reached equilibrium after three days.

Once equilibrium was reached, the samples were filtered. The filtrate was then analyzed for the remaining concentration.

The surface concentration q_e in equilibrium with the solution concentration was then computed using the following set of equations

$$q_e = (C_o - C_e)\frac{V}{W}$$

where,

q_e = surface concentration in mmoles/gm or mg/gm

C_o = initial concentration in mmoles/L or mg/L

C_e = final concentration in mmoles/L or mg/L

V = volume of the solution in L (liters)

W = weight of adsorbent in gm

4.3.2 Batch Experiments

The carbon for batch experiments was obtained by sieving

the desired fractions. Each size fraction was washed thoroughly with deionized water to remove fines. The samples were then dried in an oven at 120 deg.C until constant weight was attained. The carbon was then stored in glass bottles and placed in an incubator.

Experiments were conducted in a rectangular plexiglass vessel with internal dimensions LxBxH of 34x30x35 cm. The schematic setup of the batch experiment is as shown in Figure 4.1. For all the experiments 24 litres of solution of known concentration was made. The water in the vessel was stirred by a four bladed impeller. The temperature was maintained at 25 deg.C from the beginning and until the end of the experiment. Before the experiment could be run the pH of the water in the vessel was maintained at 7. This was done by using the same approach used for isotherm studies, and by making use of 3.6N sulphuric acid.

Once this was set up a known weight of carbon was added. The speed of the impeller was maintained at a speed of 800 rpm for particles in the range of 12-14 to 18-20, and at a speed of 700 rpm for particles in the range of 20-25 to 30-35. The lower speed could not be used for the larger sizes because the particles were not completely suspended. Table 4-5 shows the size fraction and the impeller speed used for the different size fractions. The same impeller speeds were used for both phenol and parachlorophenol experiments. In the case of mixture of size fractions even if one of the sizes fell in

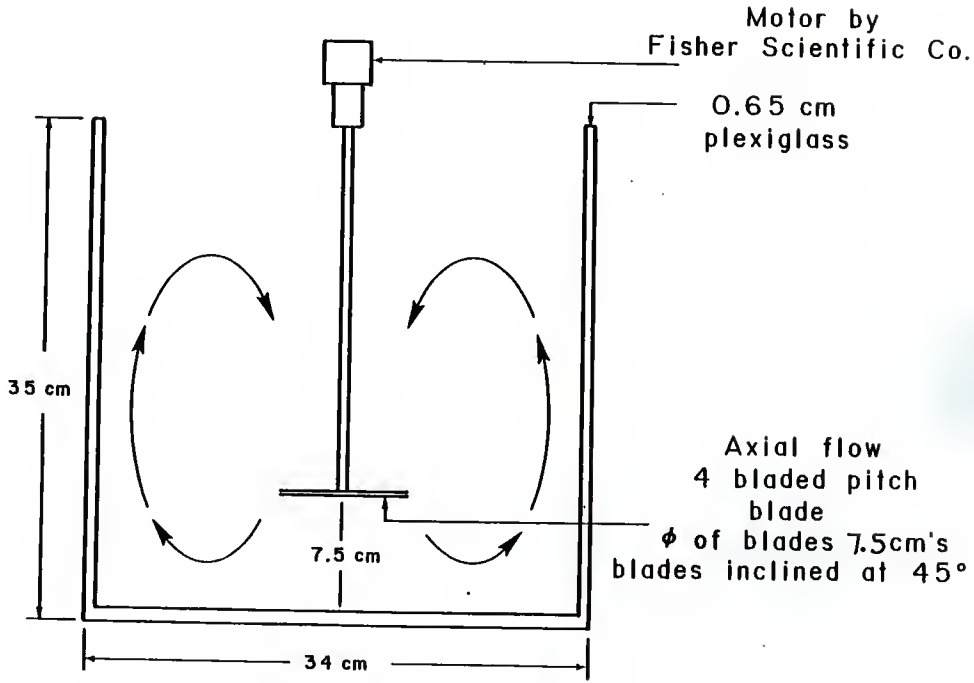

Fig. 4.1. Schematic setup for rate studies.

Table 4.5 Impeller speeds for different size fractions for batch studies.

Sieve size	Impeller speeds
#12-#14	800
#14-#16	800
#16-#18	800
#18-#20	800
#20-#25	700
#25-#30	700
#30-#35	700

the higher impeller rpm range the higher impeller speed was used for the experiment.

After the addition of carbon readings were taken at intervals of every minute for ten minutes and then readings were taken every fifteen or twenty minutes for four hours. The sample was collected using a clean pipette with a teflon filter attached so that no carbon entered the sample. The graphs of C/C_O were then plotted against time.

4.3.3 Fixed bed experiments

The experimental set up for the fixed bed experiments are as shown in the Figure 4.2. Two sizes of columns were used. For the range of particles 12-14 to 18-20 the column with a diameter of 5.08 cm was used, and for the particles in the range of 20-25 to 30-35 the column with a diameter of 3.1 cm was used. Table 4-6 shows the operating conditions for fixed bed experiments for both phenol and parachlorophenol. In the case of a mixture of sizes even if one of the carbon size fractions fell in the range of the bigger column diameter then the operating conditons for the column with the bigger diameter was used.

The carbon in both the columns was supported using a brass wire mesh. The carbon for fixed bed studies was prepared by sieving different size fractions and washing each size fraction thoroughly in deionized water to remove fines. This carbon was then dried in an oven at 120 deg. C for sufficient time till constant weight was attained. The dried

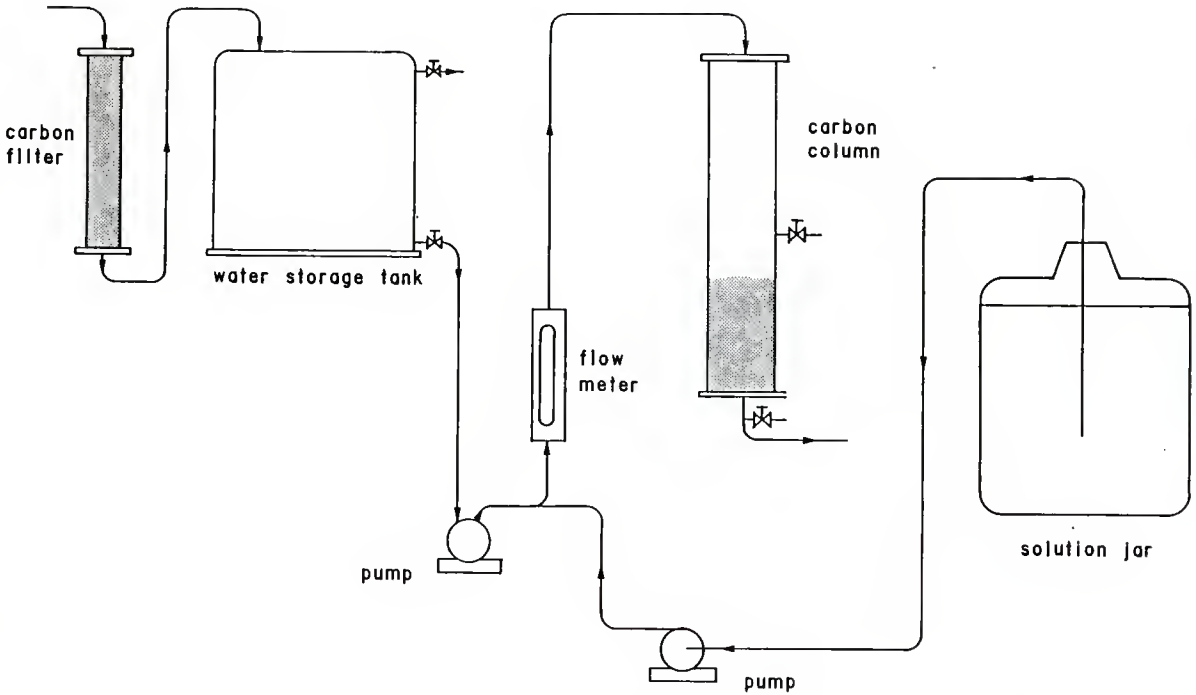

Fig. 4.2 Schematic setup for column studies

Table 4.6 Fixed bed operating conditions

Sieve size fraction	Column diameter	Flowrate	Hydraulic loading rate
	cms	ml/min	m/min
#12-#14	5.08	500	0.247
#14-#16	5.08	500	0.247
#16-#18	5.08	500	0.247
#18-#20	5.08	500	0.247
#20-#25	3.1	125	0.166
#25-#30	3.1	125	0.166
#30-#35	3.1	125	0.166

samples were then stored in glass jars in an incubstor at constant temperature.

The column was fed with tap water from a tank in which constant head was maintained by overflow. The water collected into this tank initially passed through a three foot carbon column. Two different dimeter of columns were used depending upon the size range of the particle. For the smaller diameter column two variable flow pumps were manipulated to force the water as well as the concentrated solution into the column at a total flowrate of 125 mL/min. The flowrate of the solution was 12.5 mL/min. For the bigger column a variable flow master flex pump was used along with one variable flow pump to force the water as well as the solution into the column at a flow rate of 500 mL/min. The flowrate of the solution in this case was 50 ml/min. The solution was stored in a jar of 20 liter capacity. The solution was maintained in the jar at a concentration 10 times higher than what was required in the experiment and the flow from the jar was adjusted so as to have proper dilution to the desired concentration in the system.

Predetermined amount of carbon was introduced into the column. In case a mixture of sizes was used then the largest size was introduced first followed by the next smaller size and so on so that the bed was completely stratified according to size. Water was then passed through the column for about half an hour and the walls of the column were gently tapped to remove all the entrapped air.

Before the column could be operated the temperature in the constant head tank was maintained at a temperature of about 30 deg. C so that when this water mixed with the solution from the jar the temperature of the water entering the column was exactly 25 deg. C. Once again the pH was maintained at 7. For this the solution in the jar was made up with tap water maintained at pH 7. For all column runs the flowrate of water from the tank was 9 times higher than that from the solution jar. The pH of the water in the tank was measured and the amount of 3.6N sulphuric acid required to bring down the pH to 7 was also noted. Since the flowrate from the tank was 9 times higher than that from the solution jar, nine times more acid was to be addded in the solution jar to maintain the pH of the water entering the column at 7. This procedure was adopted for maintaining the pH at 7 in the column.

The column was operated almost sixteen hours after the initial setup, i.e. until the column was almost 95% saturated. Effluent readings were taken at intervals of an hour and were analyzed for effluent concentrations. The nondimensional values of C/C_O were then plotted against time.

Chapter 5

Kinetic Model

Film transfer, surface diffusion and pore diffusion are important rate controlling steps in adsorption phenomenon. Depending upon the conditions, one of these or a combination of these will control the rate of adsorption. Pore and surface diffusion are two parallel processes. Besides these, the equilibrium relatiohship is also important and the isotherm shape has been found to influence the shape of the breakthrough curve (Chakravorti and Weber, 1974).

5.1 Model Equations

Assumptions

The following assumptions were made to determine the equations for a finite batch model as well as a fixed bed model.

1) The rate of adsorption is diffusion limited, ie., local equilibrium prevails at the external surface of the adsorbent.

2) Liquid diffusion resistance occurs at the external surface and can be described as film transfer.

3) The adsorbent particle is a homogenous solid.

4) The particle is spherically shaped.

5) Plug flow occurs in the fixed bed.

5.1.1 Finite Batch Reactor

A finite batch adsorber is composed of a finite volume of solution in which the adsorbent particles are rapidly agitated. The finite batch adsorber model for a single solute consists of the following set of equations:

1) The mass balance equation on the adsorbent particle is given as

$$\epsilon_p \frac{\partial c}{\partial t} + \frac{\partial q}{\partial t} = \frac{D_s}{r^2} \frac{\partial}{\partial r}\left(r^2 \frac{\partial q}{\partial r}\right) + \frac{D_p}{r^2} \frac{\partial}{\partial r}\left(r \frac{\partial c}{\partial r}\right)$$

The first term on the left hand side of the equation gives the rate of accumulation of solute into the fluid in the pores and the second term gives the rate of accumulation on the surface of the particle. The first term on the right hand side of the equation gives the rate of homogenous solid diffusion while the second term is the rate of pore diffusion. If homogenous solid diffusion is considered important and the fluid phase accumulation term is neglected, and since surface concenteration is greater when compared to concentration in pore fluid for small values of ϵ_p, the equation reduces to

$$\frac{\partial q}{\partial t} = \frac{D_s}{r^2} \frac{\partial}{\partial r}\left(r^2 \frac{\partial q}{\partial r}\right)$$

This equation was developed by Rosen in 1952. The film

transfer can be taken into account in the diffusion model by applying appropriate boundary conditions. In the homogenous solid diffusion this condition is obtained by equating the rate of mass transfer through the surface film to the rate of change of average concentration of the particle and is expressed as

$$R^2 k_f \frac{(C-C_s)}{\rho} = \frac{\partial}{\partial t}\int_0^R q r^2 \partial r \qquad @\, t \geq 0,\ r = R$$

The initial and boundary conditions are

$$@\ t = 0,\ 0 \leq r \leq R\ ;\ q = 0$$

$$@\ t \geq 0,\ r = 0;\ \frac{\partial q}{\partial r} = 0$$

$$@\ r = R,\ C_s = f(q_s)$$

5.1.2 Fixed Bed Model

The following equations apply for adsorption in a single solute fixed bed adsorber:

$$\partial q/\partial t = \frac{D_s}{r^2}\frac{\partial}{\partial r}\left(r^2 \frac{\partial q}{\partial r}\right) \qquad (1)$$

$$@\ t = 0;\ 0 \leq r \leq R\ :\ q = 0 \qquad (2)$$

$$@\ t \geq 0,\ r = 0\ :\ \partial q/\partial r = 0 \qquad (3)$$

$$@\ t \geq 0,\ r = R:\ R^2 k_f (C - C_s)/\rho = \partial/\partial t \int_0^R q r^2 dr \qquad (4)$$

$$@\ r = R\ :\ C_s = f(q_s) \qquad (5)$$

$$\partial C/\partial t = \left(-V\, \partial C/\partial z - 3(1-\varepsilon_b)/\varepsilon_b R\right) k_f (C - C_s) \qquad (6)$$

$$@\ t = 0,\ 0 \leq z \leq L_b\ :\ C = 0 \qquad (7)$$

$$@\ t \geq 0,\ z = 0\ :\ C = C_o \qquad (8)$$

Equations 1 to 5 give the rate of accumulation of solute on the surface of the adsorbent particle through homogenous solid diffusion. D_s is the solid phase diffusion coefficient. The radial distance from the centre of the adsorbent particle is r. The surface concentration is q. Equation 2 states that the initial condition that at time t=0 the surface concentration at any radial distance inside the particle is zero. Equation 3 implies that at any time greater than zero, the concentration gradient at the centre of the particle is zero. The radius of the particle is R. Equation 4 gives the mass balance equation on the adsorbent particle. The rate of mass transfer through surface film is equal to the rate at which the average concenteration of the particle changes. The film transfer coefficient is k_f, C_s is the solution concentration at the external surface of the particle and ρ is the apparent density of the particle. Equation 5 is the isotherm relation between the surface concentration and solution of the solute with q_s as the surface concentration at the external surface of the particle. Equations 6, 7, and 8 apply to fixed bed conditions. Equation 6 gives the mass balance of the solute at any point in the bed. The rate of change in concentration of the solute is equal to the sum of the convective change in concentration inside the bed and the rate of mass transfer through the film to the solid surface. Here, V is the superstitial velocity in the fixed bed. ϵ_b is

the porosity of the bed and Z is the axial distance inside the bed. Equation 7 is initial condition to the bed at time t=0, when solution concentration inside the bed is zero. Equation 8 implies that at any time greater than zero, the solution concentration at the entrance to the bed is equal to the initial concentration. L_b and C_o are length of the bed and initial solution concentration, respectively.

5.2 Solution of the Model

Generally, in the case of a nonlinear isotherm, the differential equations in the adsorbent model are solved using numerical methods. Solutions can be obtained using finite difference, orthogonal collacation, or finite element methods. The present model uses orthogonal collaction method to solve the differential equations numerically.

In the collocation method the solution of the differential equations is approximated by a trial function. This trial function has constants and/or functions such that when this trial solution is substituted into the differential equation the residual is forced to zero at the collocation points. Orthogonal collocation is a special case of collocation method, in that, the trial functions are a set of orthogonal polynomials and the collocation points are the roots of these polynomials.

By the use of collocation points the partial differential equations are reduced to first order ordinary differential equations. These ordinary differential equations

are solved by a computer subroutine program developed by Gear (Gear, 1976; Hindmarsh, 1974). This subroutine utilizes the Adams predictor-corrector method for numerical integration of the ordinary differential equations.

The program was modified by Mathews and Kulkarni (1983) and treated the whole bed as a series of small beds containing one particular size of carbon.

As the first bed becomes saturated, effluent from this bed becomes influent for the next bed at respective times. The series of effluent becomes influent to the next bed until the last layer, the effluent of which is the final effluent of the whole bed.

In the original program single solute equilibrium constants were determined by fitting a Freundlich isotherm equation to the equilibrium data. The curved portion of the data near small concentrations was represented by a linear isotherm. However when this was done there were some portions on the isotherm which could not be represented by a linear fit. This resulted in erroneous predictions. Hence the program was modified by Mathews (1984) so that equilibrium can be represented by the three parameter isotherm requirements.

There are several input data requirements for the program. These are 1)weight of carbon 2)length of the bed 3)radius of the adsorbent particle 4)molecular weight of the solute 5)influent concentration 6)isotherm constants

7)collocation constants 8)intrapaticle diffusion coefficient and 9)external mass transfer coefficient.

The intraparticle diffusion coefficient was established from batch studies. The external mass transfer coefficient was established using a method suggested by Dwiwedi and Upadhyay(1977). The set of equations used to determine the external mass transfer coefficient are as follows:

$$\epsilon J_d = 1.1068\, N_{Re}^{-0.72} \qquad \text{for } N_{Re} \leq 10$$

$$\epsilon J_d = 0.4548\, N_{Re}^{-0.4069} \qquad \text{for } N_{Re} > 10$$

$$J_d = (k_f/u)\, N_{Sc}^{2/3}$$

where

ϵ = porosity of the bed

J_d = mass transfer factor

N_{Re} = Reynolds number (DpG/μ)

k_f = film transfer coefficient

u = superficial fluid velocity (G/ρ)

N_{Sc} = Schmidts number ($U/(\rho D_L)$)

here D_L is the molecular diffusivity and was determined from the equation of Wilke and Chang (1955), which was given by

$$D_L = T \times 10^{-7} (M)^{0.5} / (\mu (V_o)^{1/3})$$

where

T = absolute temperature in deg. K

M = molecular weight of the solvent

μ = solution viscosity in centipoise

V_o = molal volume of the solute at normal boiling point

Chapter 6

Results and Discussion

6.1 Equilibrium studies

6.1.1 Single solute isotherm studies for phenol and PCP

Two isotherm experiments were conducted, one for phenol and the other for p-chlorophenol. The temperature for both the experiments were maintained at 25 deg. C and the pH was maintained at 7. Tap water was used to make up the solutions. This water initially passed through a carbon column, three feet in height to and was used to remove organics and other adsorbables present in tap water.

The isotherm data was represented by the three parameter isotherm equation shown below

$$q = AC/(1 + BC^{\beta}) \qquad \text{for } \beta < 1$$

This equation was used for describing the data for both phenol and p-chlorophenol. The experimental and predicted points are shown in Figures 6-1 and 6-2 for phenol and p-chlorophenol, respectively. The plots are log-log plots. The estimation was done by using a non linear parameter estimation computer program (Mathews, 1975). The parameters A, B, and β are computed by using the principal axis method and minimization of the sum of squares of residuals between experimental and predicted values.

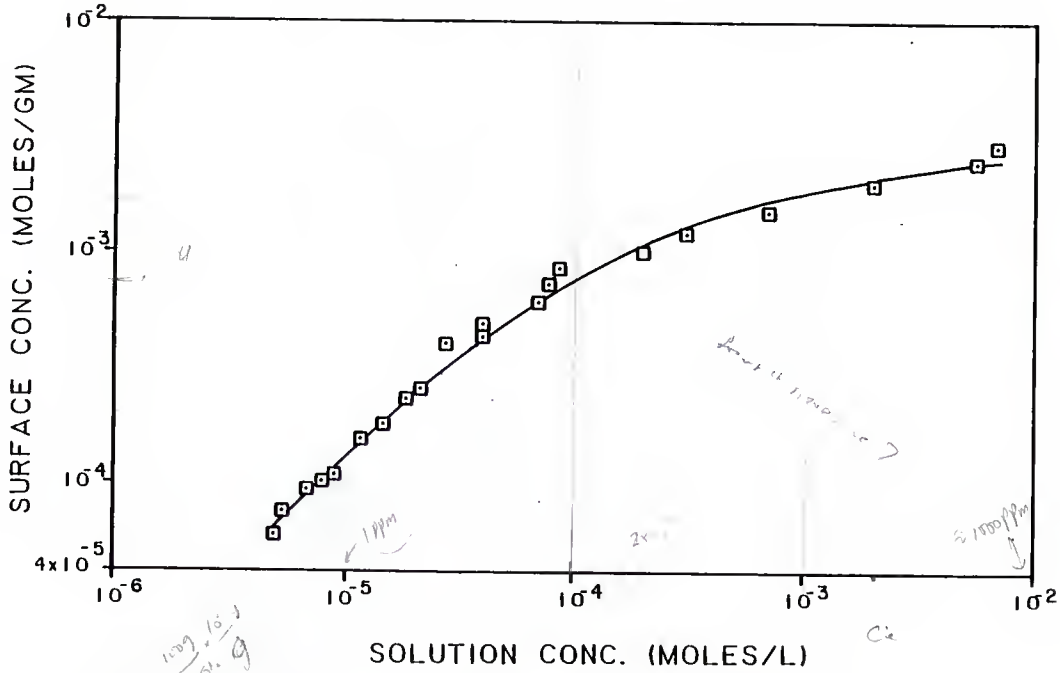

Fig. 6.1. Adsorption isotherm for phenol at 25 C.
(⊡) experimental data, (——) predicted values.

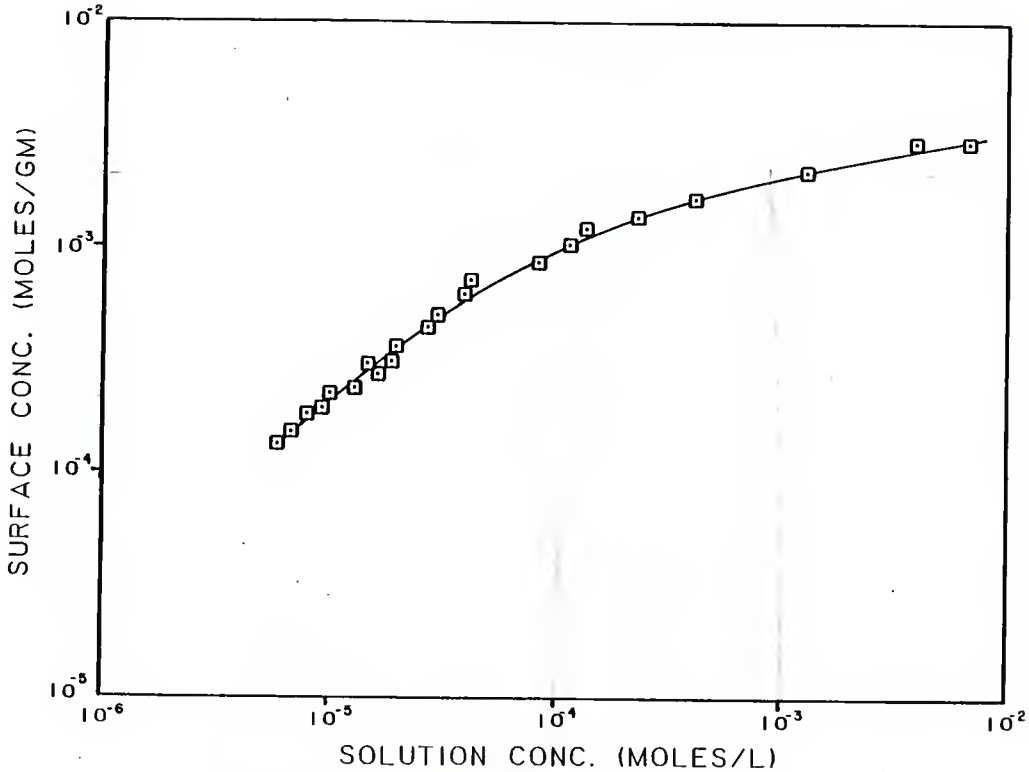

Fig. 6.2. Adsorption isotherm for PCP at 25 C.
(⊡)experimental data,(——) predicted values.

From the plots we see that the curve for the p-chlorophenol isotherm is higher than that of the phenol isotherm. That means that the rate of adsorption for p-chlorophenol is higher than that of phenol adsorption.

Table 6.1 gives the values of the A, B, and β for the solutes phenol and p-chlorophenol at 25 deg. C and pH 7.

Table 6.1. Three parameter isotherm constants for phenol and PCP

Solute	A	B	β
Phenol	15.11	7.546	0.8685
PCP	30.06	29.92	0.9466

6.2 Single solute rate studies for single adsorbent sizes

Rate studies were conducted for differnt sizes of carbon using a temperature of 25 deg. C and pH of 7. The solutes used were phenol and p-chlorophenol. Tables 6.2 and 6.3 show the operating conditions for batch studies for phenol and p-chlorophenol, respectively. The surface diffusivities and batch film transfer coefficient for the different sizes were estimated using a computer program written by Mathews (1975). The computer program needed an initial estimate for film transfer coefficient and intraparticle diffusion coefficient.

The film transfer coefficient can be calculated from initial rate data according to the formula (Mathews and Weber, 1977, Larson and Tien, 1983).

$$\ln(C_{bi} / C_{bo}) = -((3*M*K_f*t)/(ap*\rho p*V))$$

Here,

ap is the radius of the particle

C_{bi} is the concentration of the solution at a particular time

C_{bo} is the initial concentration of the solution

M is the mass of adsorbent

t is the time

ρp is the density of the particle

V is the volume of the solution

Table 6.2 Operating conditions for batch studies for phenol solute

Sieve size	Initial solution concentration (M/L)*10^4	Weight of carbon gms
#12-#14	2.515	8
#14-#16	2.461	6.5
#16-#18	2.481	8
#18-#20	2.488	8
#20-#25	2.556	8
#25-#30	2.495	6
#30-#35	2.468	6.5

Table 6.3 Operating conditions for batch studies for PCP

Sieve size	Initial solution concentration (M/L)*10^4	Weight of carbon gms
#12-#14	2.582	8
#18-#20	2.438	8
#20-#25	2.561	8
#30-#35	2.136	8

The above equation can be represented as a linear graph and holds good for the first five minutes of the experiment. However, this depends on the solute and the type of adsorbent used.

Figures 6.3 to 6.5 gives the experimental and predicted plots for batch studies for phenol solution and size fractions from #12-#14 to #30-#35. Table 6.4 gives the sieve size used, the film transfer coefficients and the intraparticle diffusion coefficients estimated from the batch rate data for phenol.

From studies conducted by Mathews and Weber for adsorption in slurry reactors (1984), they concluded that mass transfer coefficient was proportional to $N^{0.75}$, where N is the impeller speed. From our studies with 212 micron particle size we found that the mass transfer coefficient is proportional to $N^{0.80}$.

Correction for k_f is needed, especially in the case of adsorption with a mixture of adsorbent sizes. This was important in our case of study because batch studies were conducted at two different impeller speeds. The impeller speeds used were 800 rpm and 700 rpm. The equation for conversion of mass transfer from one rpm to another is given by

$$\frac{k_{f,800}}{k_{f,700}} = \left(\frac{800}{700}\right)^{0.80}$$

Tables 6.5 shows the corrected mass transfer

coefficients for the particles in the range of #20-#25 to #30-#35 for phenol. The mass transfer coefficients were converted from mass transfer coefficients at impeller speed of 700 rpm to mass transfer coefficient at 800 rpm.

It can be seen from the experiments that the calculated and estimated value of film transfer coefficient are very close and within 5% of each other. It can also be seen that as the particle size decreased to within a certain range, the film transfer coefficient increased and then remained a constant. Within the range of #12-#14 to #18-#20 the film transfer coefficient increased and within the range of #20-#25 to #30-#35 the film transfer coefficient remained a constant of almost around $7.4*10^{-3}$ cm/sec.

It was also seen that when geometric mean diameter was used the intraparticle diffusivities ranged from $3.2*10^{-8}$ cm^2/sec to $3.4*10^{-8}$ cm^2/sec. but when Sauter mean diameter was used the intraparticle diffusivities remained a constant at $3.5*10^{-8}$ cm^2/sec .

To study the above phenomenon batch studies were conducted using p-chlorophenol as the solute. Once agin it was seen that the intraparticle diffusion coefficients remained a constant at $3.7*10^{-8}$ cm^2/sec when Sauter mean diameters were used and ranged from $2.9*10^{-8}$ cm^2/sec to $3.2*10^{-8}$ cm^2/sec when geometric mean diameter was used. The film transfer coefficients were found to increase in the same range as that in the case of phenol and remained a constant

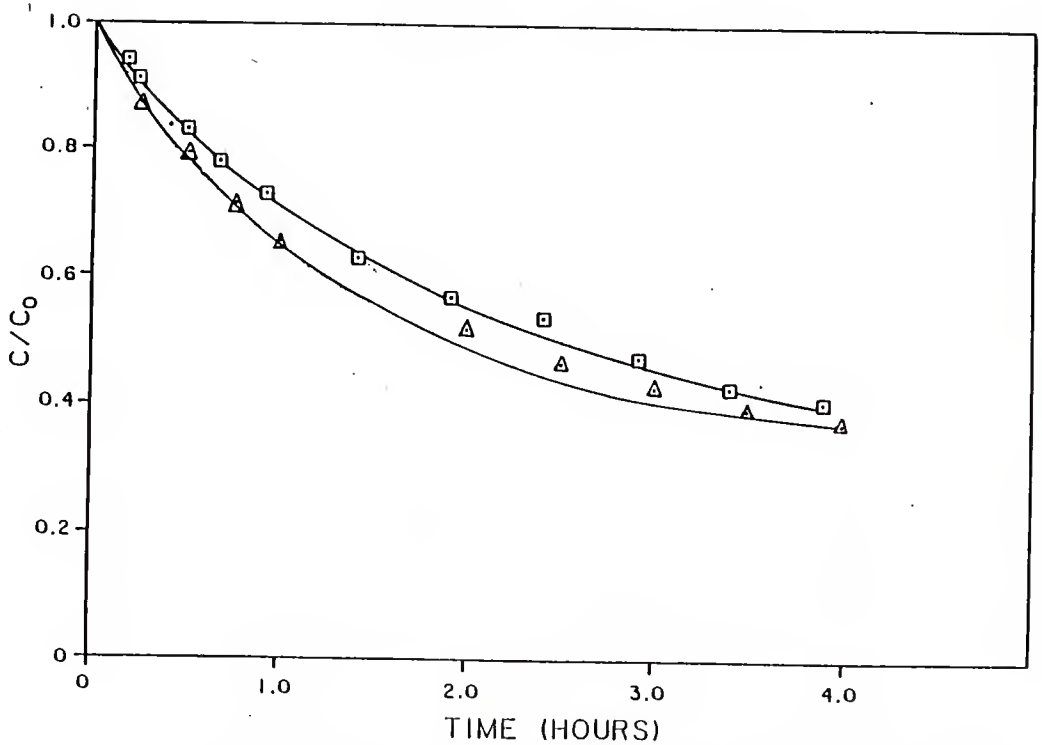

Fig. 6.3. Adsorption rate for phenol for carbon sizes #12-#14 and #14-#16. ⊡,△ are experimental data for #12-#14 and #14-#16 respectively. (—) predictions using Sauter mean diameter.

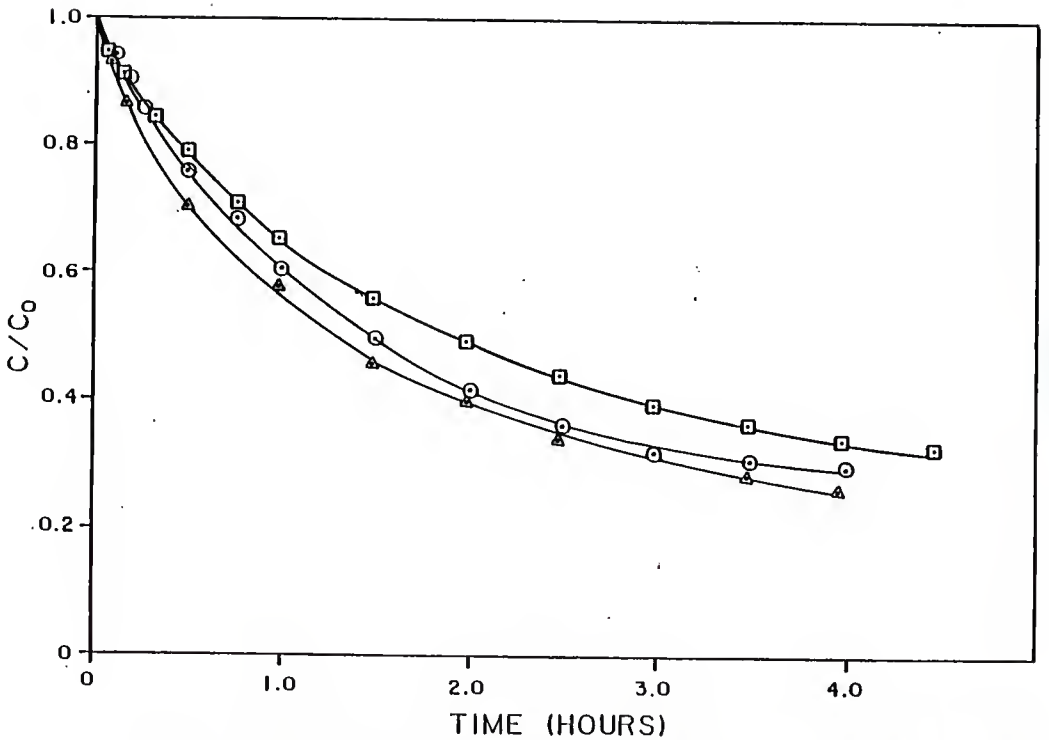

Fig. 6.4. Adsorption rate for phenol for carbon sizes #16-#18, #18-#20, #20-#25. (⊡,⊙,△) are experimental data for #16-#18, #18-#20, and #20-#25 respectively. (———) predictions using Sauter mean diameter.

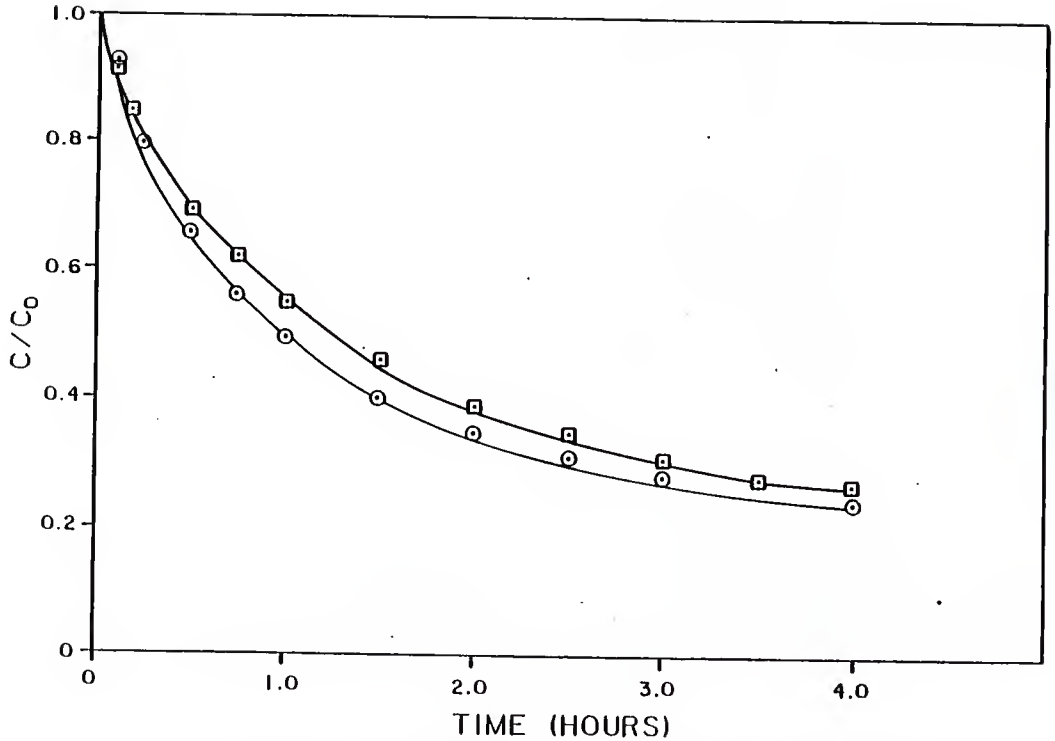

Fig. 6.5. Adsorption rate for phenol for carbon sizes #25-#30 and #30-#35. (⊡,⊙) experimental data for #25-#30 and #30-#35 respectively. (———) predictions using Sauter mean diameter.

Table 6.4 External mass transfer coefficients and intraparticle diffusion coefficients for phenol adsorption for single adsorbent sizes.

Sieve size	Geometric mean dia. microns (A)	Sauter mean dia. microns (B)	k_f based on (A) (calc) *	k_f based on (A) estimated *	D_s based on (A) estimated +	k_f based on (B) (calc) *	k_f based on (B) estimated *	D_s based on (B) estimated +
#12-#14	1544	1752	5.04	5.06	3.4	5.72	5.8	3.5
#14-#16	1294	1556	5.02	5.03	3.3	6.03	6.02	3.5
#16-#18	1091	1157	5.56	5.64	3.3	5.89	5.86	3.5
#18-#20	917	1075	6.16	6.15	3.2	7.23	7.23	3.5
#20-#25	772	923	6.27	6.26	3.2	7.51	7.49	3.5
#25-#30	647	782	6.11	6.21	3.3	7.39	7.39	3.5
#30-#35	543	645	6.31	6.23	3.2	7.49	7.42	3.5

* (cm/sec)*10^3
\+ (cm^2/sec)*10^8

Table 6.5 Values for film transfer coefficient corrected for impeller speeds for phenol solute

Sieve size	Film transfer coefficient for impeller rpm 700 based on		Corrected film transfer coefficient for impeller rpm 800 based on	
	Geometric diameter cm/sec	Sauter diameter cm/sec	Geometric diameter cm/sec	Sauter diameter cm/sec
#20-#25	$6.26*10^{-3}$	$7.49*10^{-3}$	$6.96*10^{-3}$	$8.33*10^{-3}$
#25-#30	$6.21*10^{-3}$	$7.39*10^{-3}$	$6.91*10^{-3}$	$8.22*10^{-3}$
#30-#35	$6.22*10^{-3}$	$7.42*10^{-3}$	$6.92*10^{-3}$	$8.25*10^{-3}$

at for the other range.

Figure 6.6 shows the plots of the experimental and predicted values using Sauter mean as diameter using p-chlorophenol as the solute. Table 6.6 gives the values for k_f corrected for impeller speeds for p-chlorophenol adsorption. Table 6.7 gives the sieve size used and the estimated film transfer coefficients and the intraparticle diffusion coefficients.

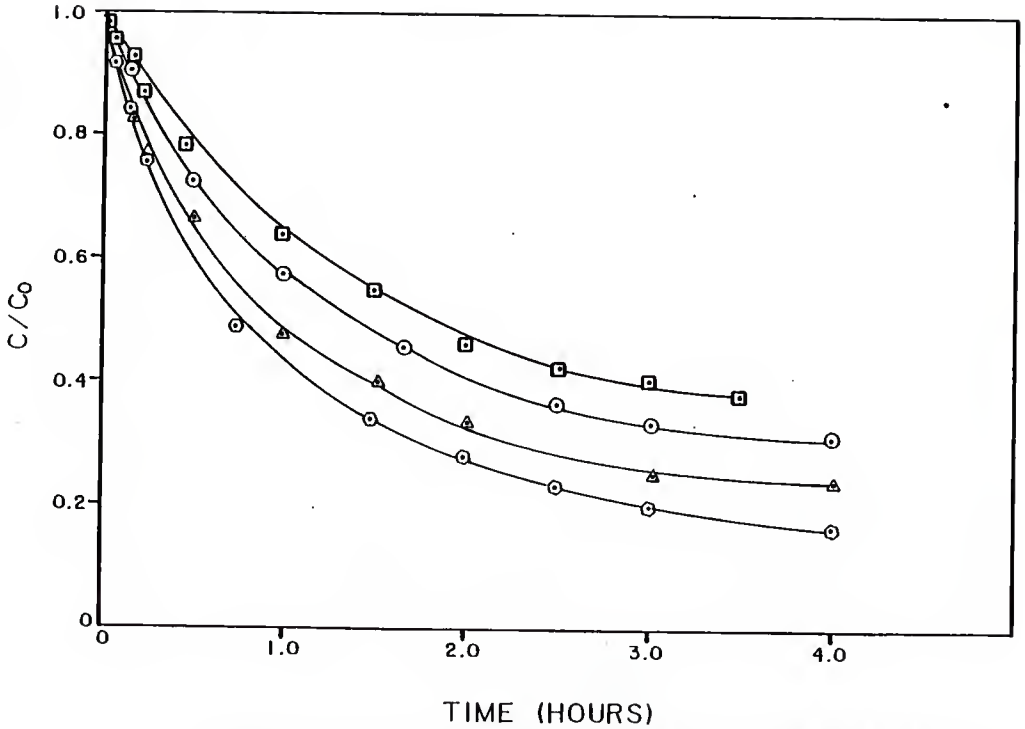

Fig. 6.6. Adsorption rate for PCP for carbon sizes #12-#14, #18-#20, #20-#25, and #30-#35. (□,○,△,⊙) esperimental data for #12-#14, #18-#20, #20-#25 and #30-#35. (———) predictions using Sauter mean diameter.

Table 6.6 Values for film transfer coefficient corrected for impeller speeds for PCP solute.

Sieve size	Film transfer coefficient for impeller rpm 700 based on		Corrected film transfer coefficient for impeller rpm 800 based on	
	Geometric diameter	Sauter diameter	Geometric diameter	Sauter diameter
	cm/sec	cm/sec	cm/sec	cm/sec
#20-#25	$9.13*10^{-3}$	$10.92*10^{-3}$	$10.17*10^{-3}$	$12.15*10^{-3}$
#30-#35	$9.20*10^{-3}$	$10.93*10^{-3}$	$10.25*10^{-3}$	$12.16*10^{-3}$

Table 6.7 External mass transfer coefficients and intraparticle diffusion coefficients for PCP adsorption for single sizes

Sieve size	Geometric mean dia. microns (A)	Sauter mean dia. microns (B)	k_f based on (A) (calc) *	k_f based on (A) estimated *	D_s based on (A) estimated +	k_f based on (B) (calc) *	k_f based on (B) estimated *	D_s based on (B) estimated +
#12-#14	1544	1752	8.033	8.033	3.1	9.117	9.117	3.7
#18-#20	917	1075	8.603	8.603	3.2	10.096	10.102	3.7
#20-#25	772	923	9.136	9.136	3.0	10.919	10.919	3.7
#30-#35	543	645	9.208	9.208	2.9	10.929	10.931	3.7

* (cm/sec)*10^3

\+ (cm^2/sec)*10^8

6.3 Single solute rate studies for mixtures of adsorbent sizes

Experiments were conducted for a mixture fo sizes to study their effects on mass transfer and intraparticle diffusion coefficients estimated from batch reactor studies. Tables 6.8 and 6.9 gives the weight of carbon taken for batch studies for a mixture of particle sizes for phenol and p-chlorophenol respectively. Tables 6.10 and 6.11 give the operating conditions for batch studies for a mixture of sizes for phenol and p-chlorophenol respectively. Figures 6.7 to 6.12 show the plots of the experimental and predicted curves using Sauter mean diameter for phenol adsorption. The model predictions were obtained using the computer program for single solute rate adsorption developed by Mathews (1975).

When experiments were conducted for a mixture of adsorbent sizes some of the individual size ranges fell in the impeller rpm range of 800 while the others fell in the range of 700 rpm. For such cases the mass transfer coefficients for the particles in the range of 700 rpm were corrected to mass transfer coefficients for 800 rpm. The mass transfer coefficient for the mixture was then calculated by multiplying the weight fraction of individual sizes present in the mixture with their respective mass transfer coefficients (corrected or uncorrected depending on the impeller speed used for the experiment) and then summing them up. The intraparticle diffusion coefficients used for

Table 6.8 Weights taken (gms) for mixture of sizes for batch studies for phenol adsorption

Mix no.	Sieve sizes ----------						
	#12-#14	#14-#16	#16-#18	#18-#20	#20-#25	#25-#30	#30-#35
1	0	0	0	0	2.667	1.06	4.28
2	0	0	0	0	4.27	2.67	1.06
3	1.28	2.24	2.24	2.24	0	0	0
4	2.24	2.24	2.24	1.28	0	0	0
5	0	1.6	1.6	1.6	1.6	0	1.6
6	0	0	0	2.56	2.56	0.32	2.56
7	1.28	1.28	1.28	1.28	1.28	0.32	1.28

Table 6.9 Weights taken (gms) for mixture of sizes for batch studies for PCP adsorption.

Mix no.	Sieve sizes ---------->			
	#12-#14	#18-#20	#20-#25	#25-#30
1	2	2	2	2
2	0	2	2	4
3	4	2	2	0

Table 6.10 Operating conditions for batch studies for mixture of sizes for phenol adsorption

Mix no.	Initial solution concentration (M)*10^3	Weight of carbon gms
1	2.563	8.00
2	2.522	8.00
3	2.584	8.00
4	2.536	8.00
5	2.386	8.00
6	2.447	8.00
7	2.638	8.00

Table 6.11 Operating conditions for batch studies for mixture of sizes for PCP adsorption.

Mix no.	Initial solution concentration (M)*10^3	Weight of carbon gms
1	2.383	8.00
2	2.585	8.00
3	2.432	8.00

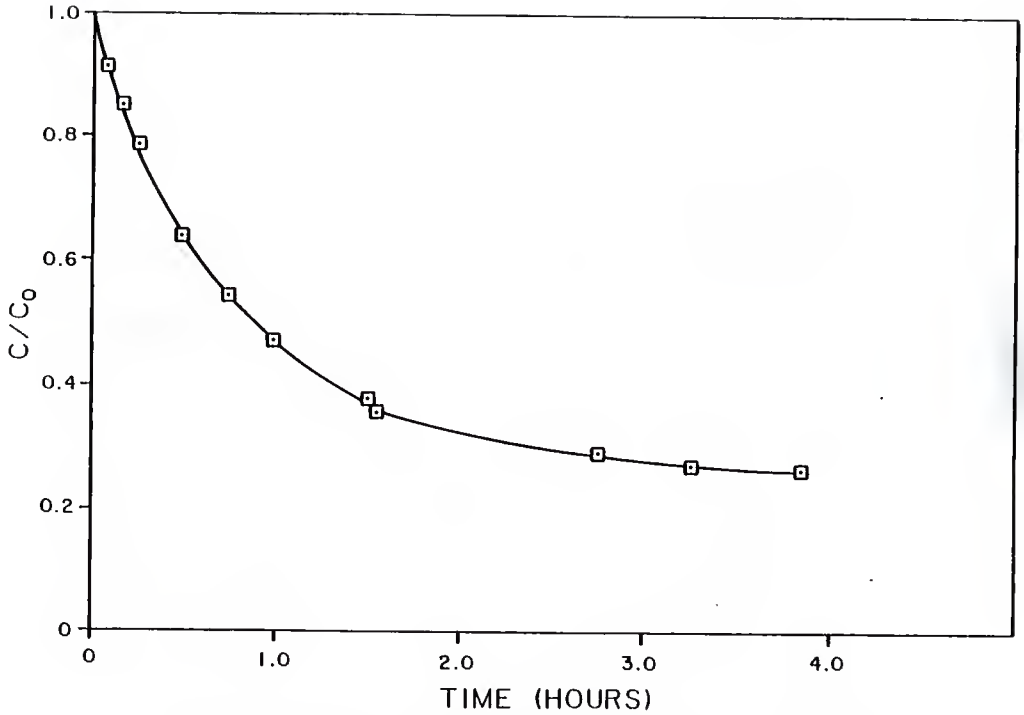

Fig. 6.7. Adsorption rate for phenol for Mix no. 1. (⊡) experimental data, (———) prediction using Sauter mean diameter.

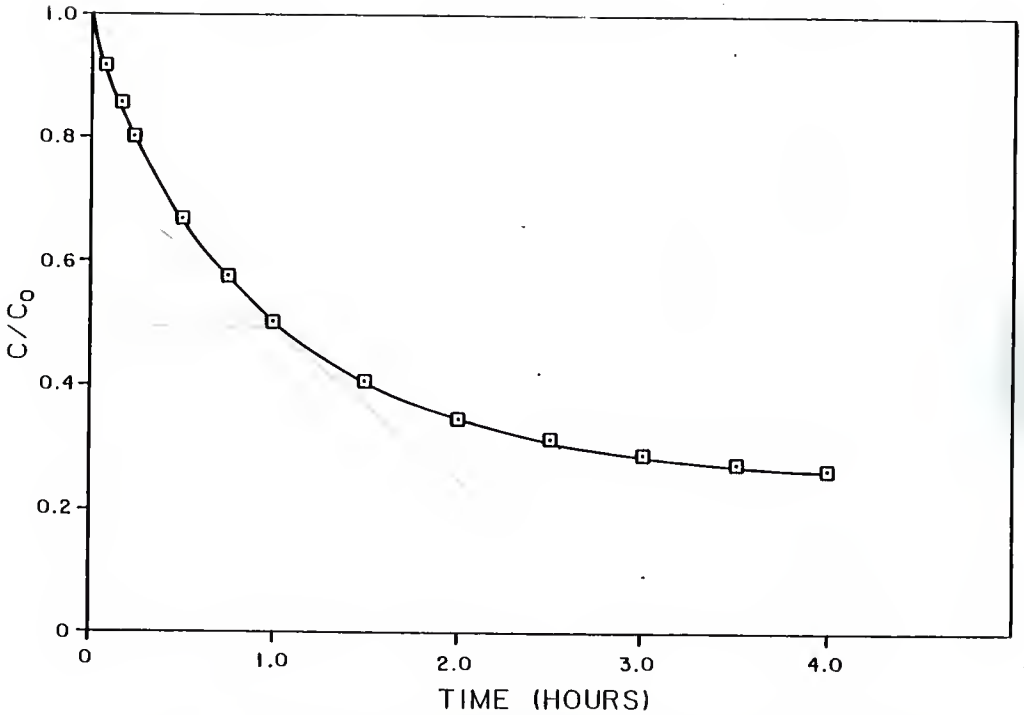

Fig. 6.8. Adsorption rate for phenol for Mix no. 2. (⊡) experimental data, (———) predictions using Sauter mean diameter.

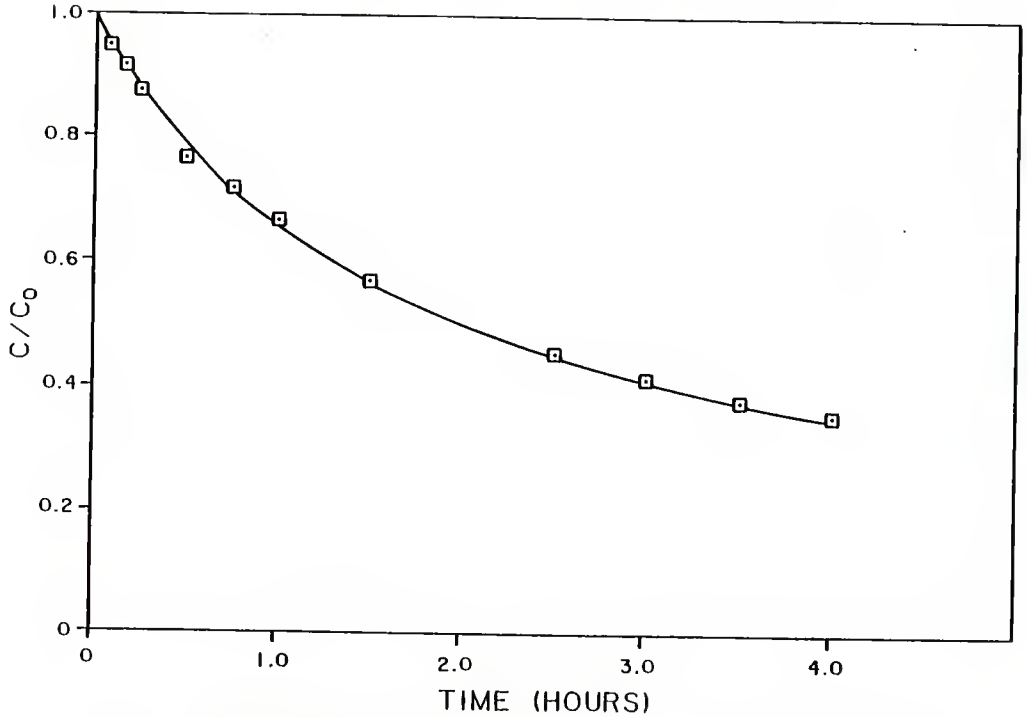

Fig. 6.9. Adsorption rate for phenol for Mix no. 3. (⊡) experimental data, (———) predictions using Sauter mean diameter.

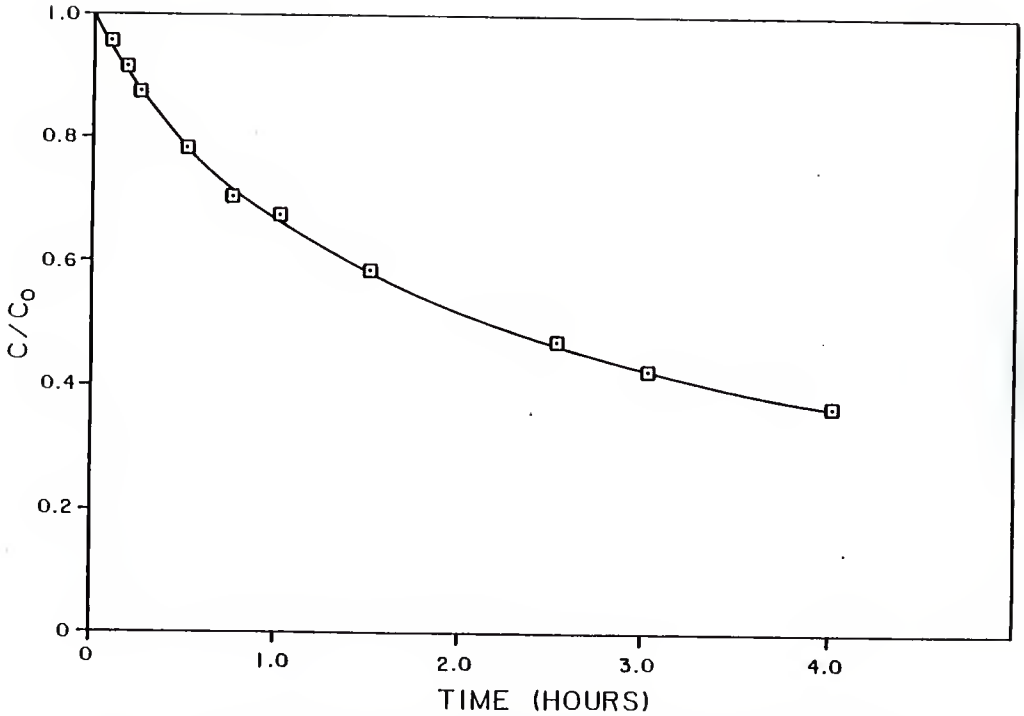

Fig. 6.10. Adsorption rate for phenol for Mix no. 4. (⊡) experimental data, (———) predictions using Sauter mean diameter.

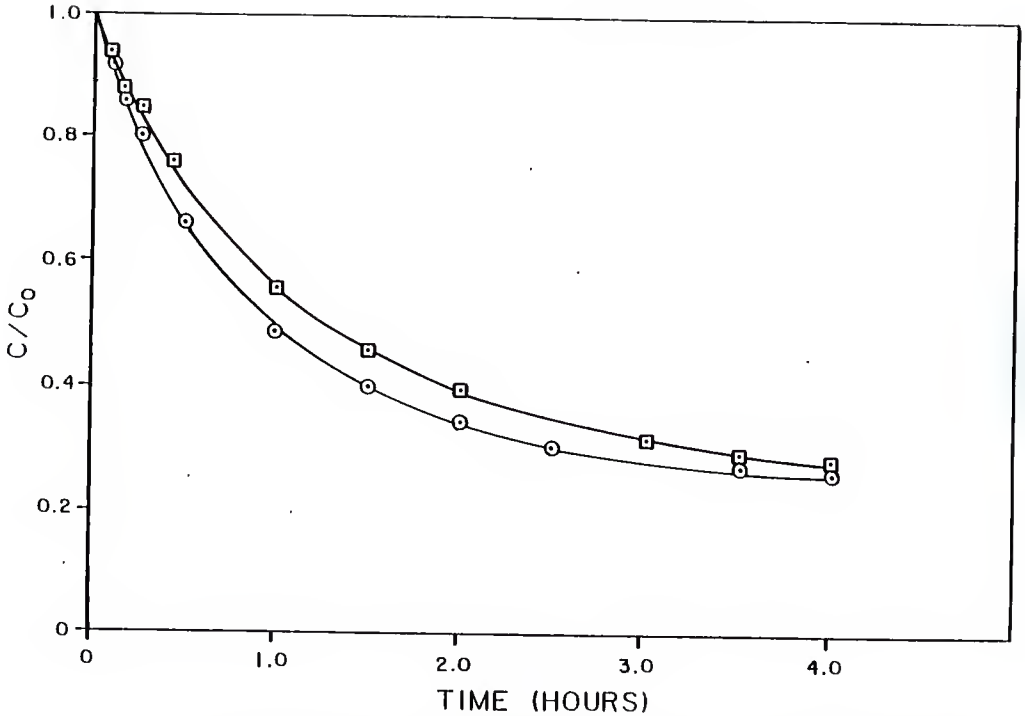

Fig. 6.11. Adsorption rate for phenol for Mix no. 5 and 6. (⊡ , ⊙) experimental data for Mix no. 5 and 6 respectively. (———) predictions using Sauter mean diameter.

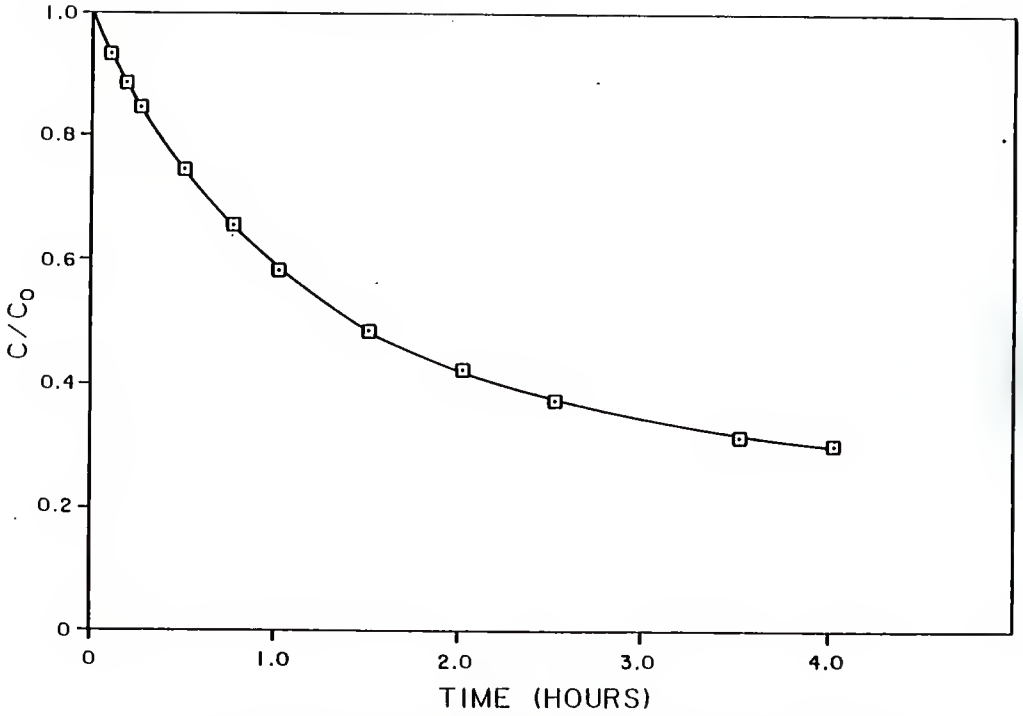

Fig. 6.12. Adsorption rate for phenol for Mix no. 7. (⊡) experimental data, (———) predictions using Sauter mean diameter.

geometric mean diameters were just the mean of the individual intraparticle diffusion coefficients.

Table 6.12 gives the mass transfer coefficients and intraparticle diffusion coefficients used to predict the kinetic curves when a mixture of particle sizes were used for phenol adsorption. From the Table 6.12 we see that the percent deviations for Mixtures for 1, 2, 6, and 7 were much lower than percent deviations for Mixtures 3 and 4. A possible reason why Mixtures 1 and 2 are much lower than mixtures 3 and 4 could be because the impeller speed used for mixes 1 and 2 was 700 rpm. At 700 rpm the probability of shearing of particles due to contact with the impeller blades is lower. Moreover, for the Mixtures 3 an 4 the particles were in the range of #12-#14 to #18-#20, and in this range there was a great deal of variation in the mass transfer coefficients and the method adopted by us for averaging these mass transfer coefficients might not have been very accurate.

It is also seen from Table 6.12 that the percent deviations between experimental and predicted results were much lower when Sauter mean of Sauter mean diameters were used than when Sauter mean of geometric mean diameters were used.

Batch studies were conducted for mixture of adsorbent sizes using p-chlorophenol as solute. In this case too it was seen that Sauter mean diameter of Sauter mean diameters gave better predictions, ie., the percent deviations from

Table 6.12 Average particle diameters for mixtures and their effects on mass transfer and surface diffusion coefficients estimated from batch reactor studies for phenol adsorption.

Mix no. @	Sauter mean dia. based on geometric mean of sieve size microns (A)	Sauter mean dia. based on Quantimet image analysis microns (B)	k_f based on (A) *	D_s based on (A) +	k_f based on (B) *	D_s based on (B) +	Percent deviation between experiment and predicted results using diameters (A)	(B)
1	617	735	6.421	2.8	7.778	3.5	0.624	0.1774
2	689	825	6.306	2.8	7.579	3.5	1.23	0.2146
3	1134	1292	5.62	3.3	6.275	3.5	1.846	0.532
4	1207	1369	5.41	3.3	6.095	3.5	1.477	0.966
5	845	986	5.937	3.2	7.27	3.5	1.521	0.774
6	707	839	6.687	2.9	8.147	3.5	0.6509	0.183
7	899	1048	6.043	3.0	7.073	3.5	0.6321	0.177

* (cm/sec)*10^3

\+ (cm^2/sec)*10^8

@ The impeller was operated at 700 rpm for mixture 1 and 2 and at 800 rpm for mixtures 3 to 7.

experimental and predicted were much lower when Sauter mean diameters of Sauter mean diameters were used than when Sauter mean diameters of geometric mean diameters were used. Figures 6.13 to 6.15 show the experimental and predicted curves using Sauter mean diameters for p-chlorophenol adsorption. Table 6.13 gives the results of our studies conducted for a mixture of particle sizes using p-chlorophenol as the solute. Here we see, again, that using Sauter mean of Sauter mean diameters gave better predictions than when Sauter mean diameters of geometric mean diameters.

Hence, it was concluded that Sauter mean diameters could be a better way of representing particle diameters for batch studies than geometric mean diameter of sieve sizes.

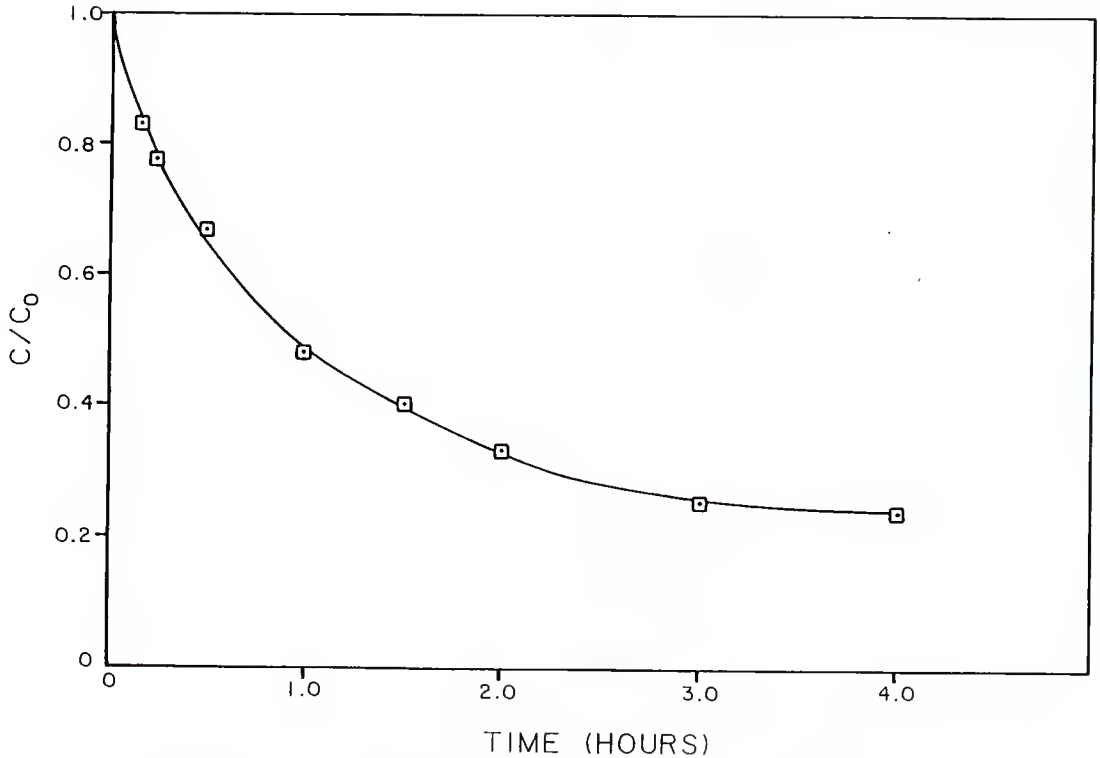

Fig. 6.13. Adsorption rate for PCP for Mix no. 1. (⊡) experimental data, (———) prediction using Sauter mean diameter.

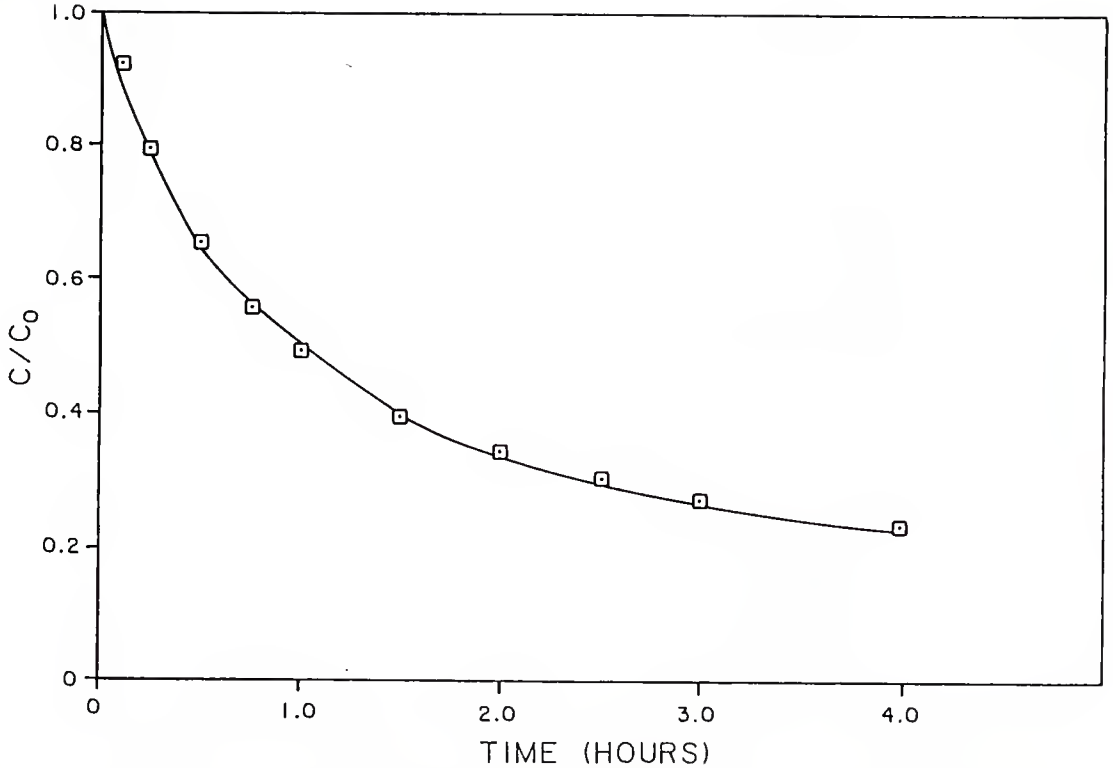

Fig. 6.14. Adsorption rate for PCP for Mix no. 2. (⊡) experimental data, (———) prediction using Sauter mean diameter.

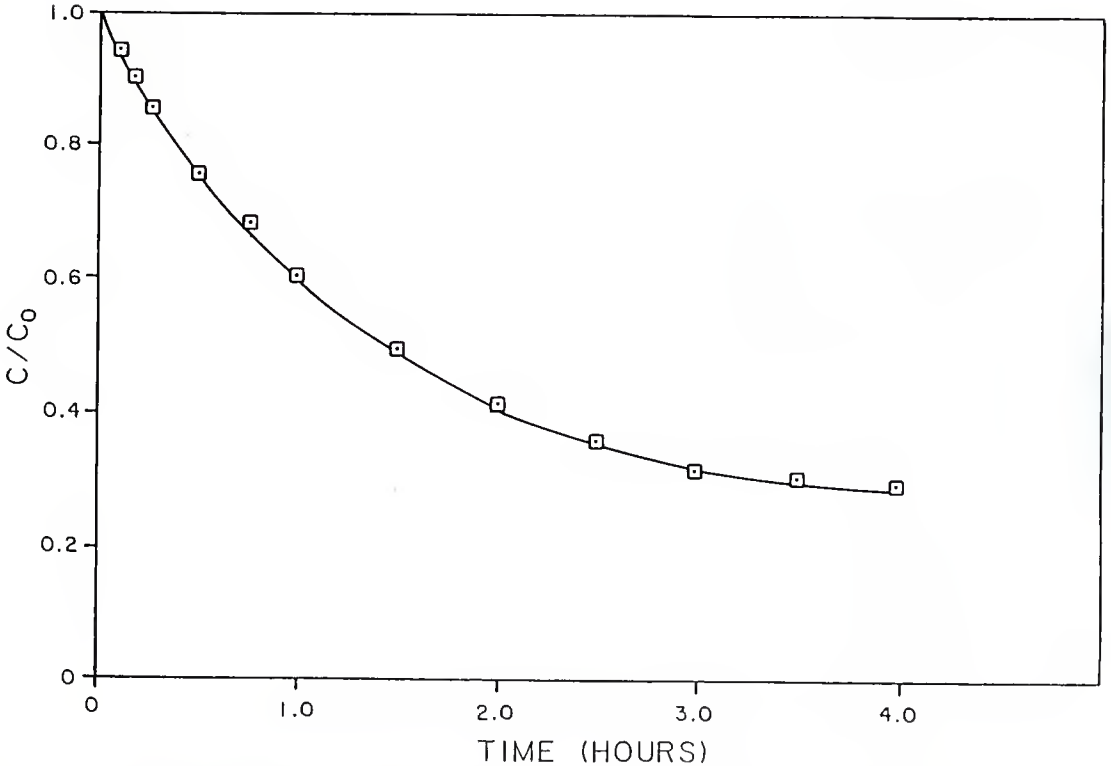

Fig. 6.15. Adsorption rate for PCP for Mix no. 3. (⊡) experimental data, (———) prediction using Sauter mean diameter.

Table 6.13 Average particle diameters for mixtuers and their effects on mass transfer and surface diffusion coefficients estimated from batch reactor studies for PCP adsorption.

Mix no.	Sauter mean dia. based on geometric mean of sieve size	Sauter mean dia. based on Quantimet image analysis	k_f based on (A)	D_s based on (A)	k_f based on (B)	D_s based on (B)	Percent deviation between experiment and predicted results using diameters	
@	microns (A)	microns (B)	*	+	*	+	(A)	(B)
1	821	967	8.745	3.05	10.267	3.7	1.563	0.601
2	659	778	9.039	3.0	10.717	3.7	0.732	0.183
3	1084	1267	8.452	3.1	9.8136	3.7	1.233	0.221

* (cm/sec)*10^3

\+ (cm^2/sec)*10^8

6.4 Single solute column studies for single sizes

The column studies were the fixed bed type and the column was operated in the downflow direction. The column was operated with solutes being phenol and p-chlorophenol and experiments were conducted to judge the efficiency of the mathematical model.

Table 6.14 gives the fixed bed operating conditions for phenol adsorption. Figures 6.16 to 6.21 give the experimental and predicted breakthrough curves for phenol with single sizes. As mentioned earlier, the intraparticle diffusion rate from batch studies were used, but the external mass transfer coefficients used were estimated using the method suggested by Divivedi and Upadhyay (1979) as discussed in chapter 5.

Table 6.15 gives the percent deviations between experimental and predicted values along with the diameters of the particles and their respective film transfer coefficients and intraparticle diffusion coefficients.

It can be seen from Table 6.15 that the predictions for the breakthrough curves are closer to the experimental data when Sauter mean diameters were used. It was also seen that there was not much of a pronounced difference from the geometric mean diameter and Sauter mean diameter predictions with respect to percent deviations from the experimental points in the case of phenol adsorption.

To test this the column experiments were conducted again, only in these cases using p-chlorophenol. Table 6.16

Table 6.14 Fixed bed operating conditions for phenol adsorption

Sieve size	Bed diameter	Bed height	Flow rate	Hydraulic loading rate	Weight of carbon
	cm	cm	ml/min	m/min	gms
#12-#14	5.08	30.9	500	0.247	250
#14-#16	5.08	30.3	500	0.247	250
#16-#18	5.08	29.9	500	0.247	250
#18-#20	5.08	29.1	500	0.247	250
#20-#25	3.1	23.2	125	0.166	75
#25-#30	3.1	22.9	125	0.166	75
#30-#35	3.1	22.8	125	0.166	75

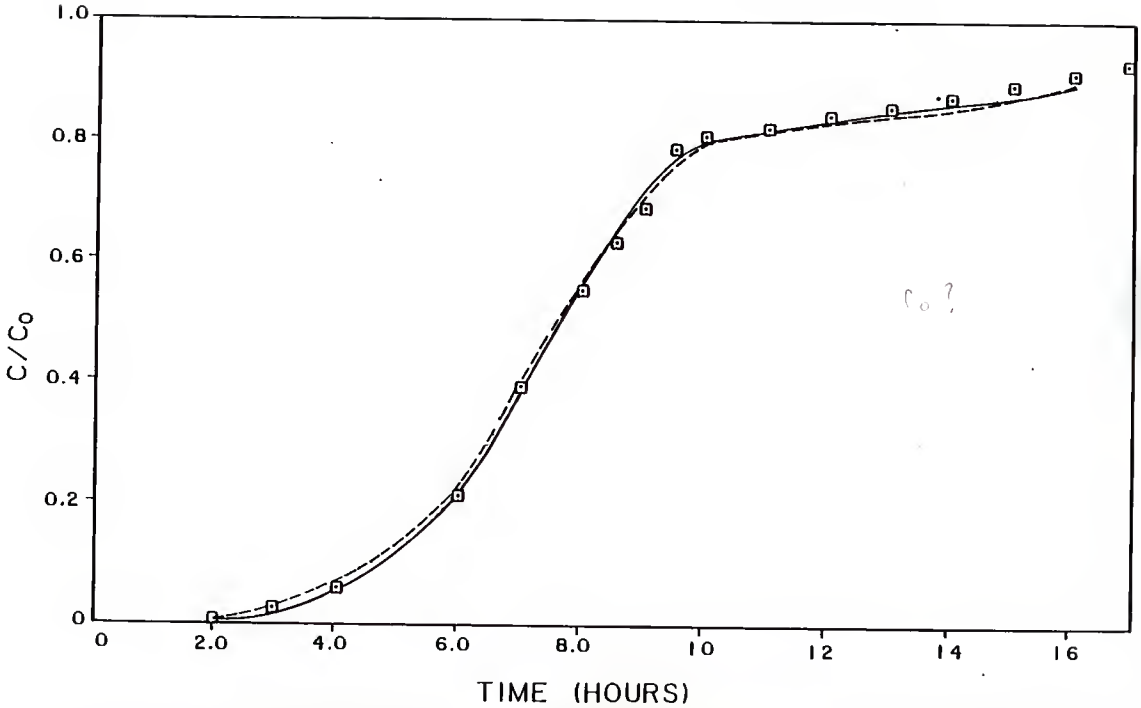

Fig. 6.16. Breakthrough curve for phenol adsorption for carbon size #12-#14. (⊡) experimental data, (-------) predictions using geometric mean diameter, (———) predictions using Sauter mean diameter

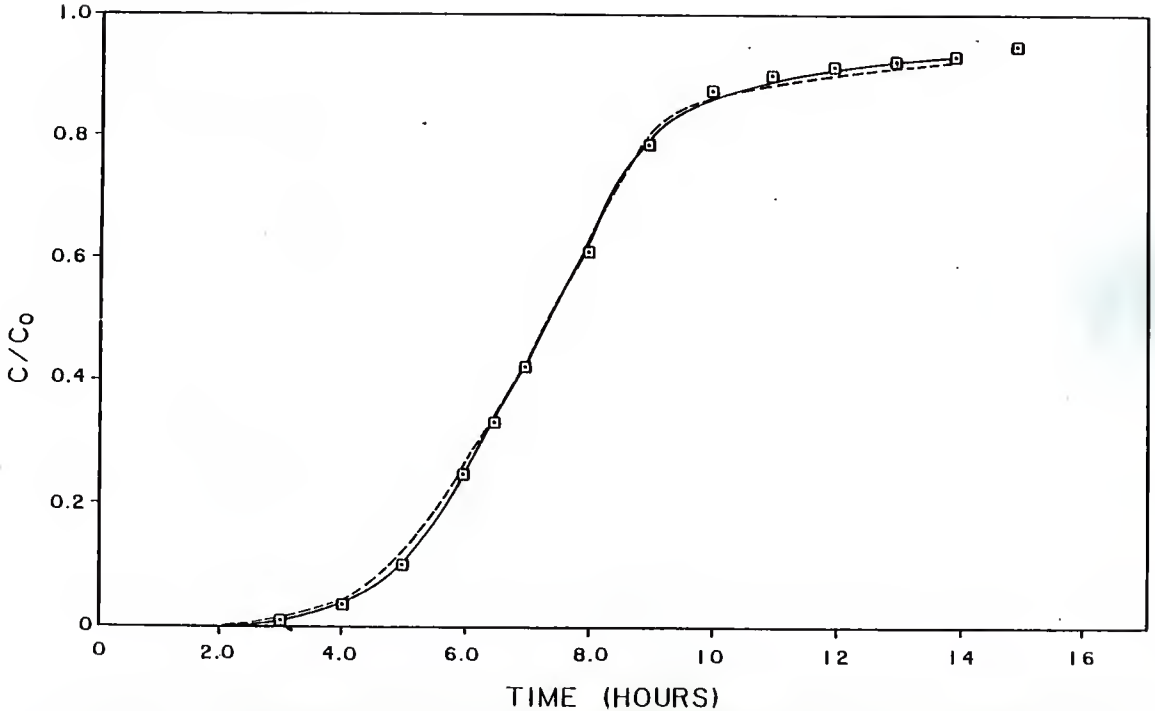

Fig. 6.17. Breakthrough curve for phenol adsorption for carbon size #14-#16. (⊡) experimental data, (-------) predictions using geometric mean diameter, (———) predictions using Sauter mean diameter.

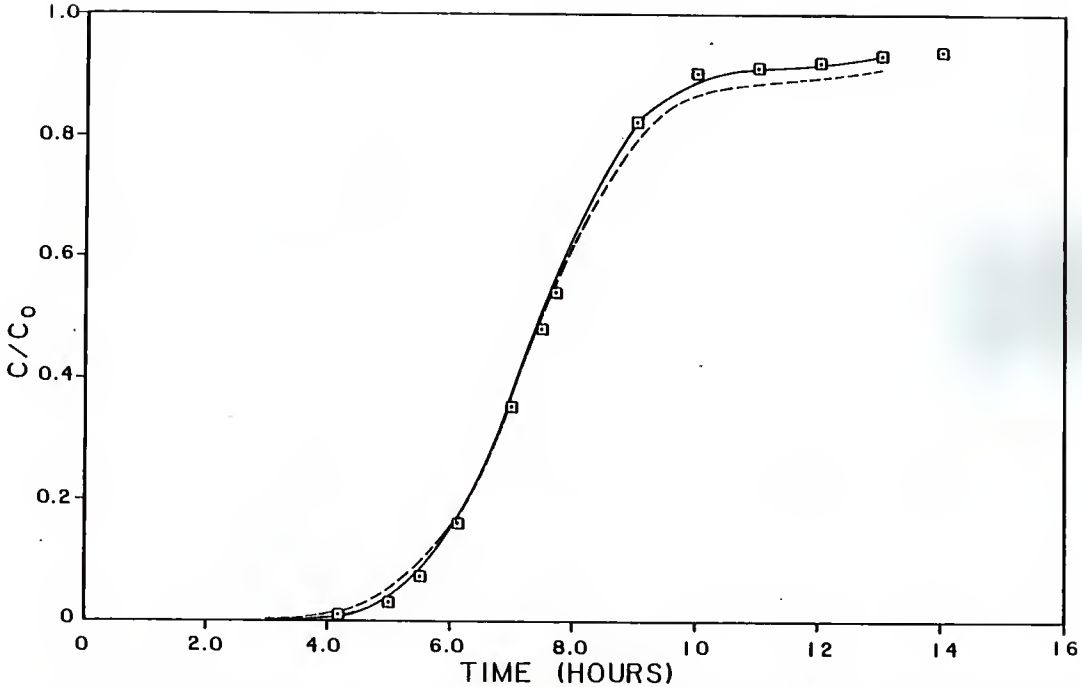

Fig. 6.18. Breakthrough curve for phenol adsorption for carbon size #16-#18. (⊡) experimental data, (-------) predictions using geometric mean diameter. (———) predictions using Sauter mean diameter.

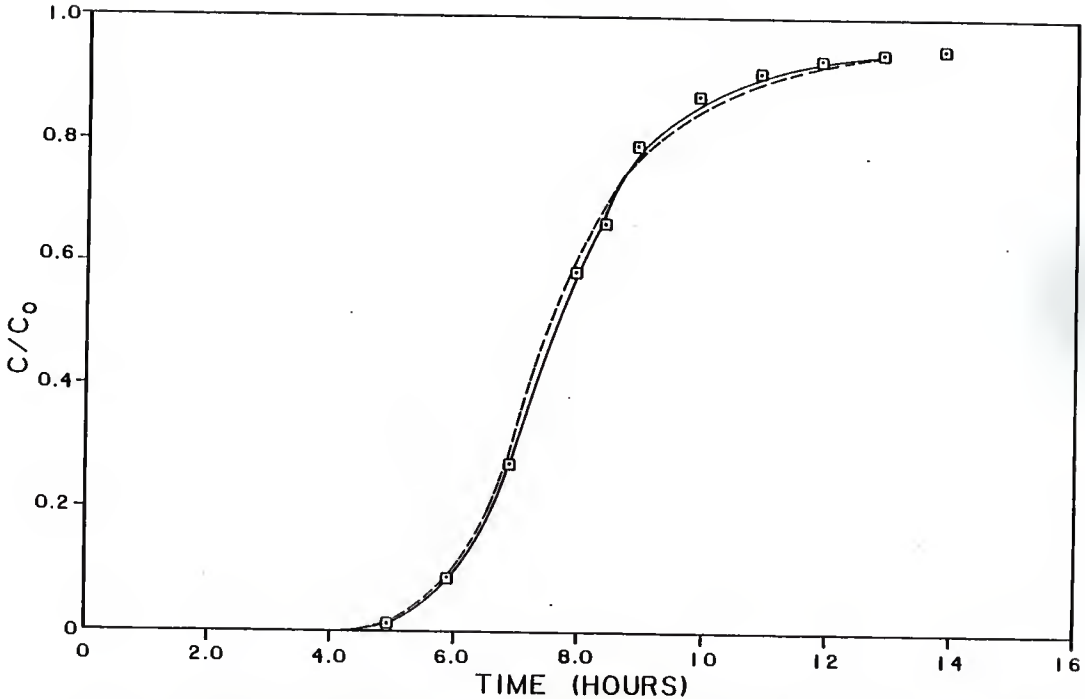

Fig. 6.19. Breakthrough curve for phenol adsorption for carbon size #18-#20. (⊡) experimental data, (-------) predictions using geometric mean diameter. (———) predictions using Sauter mean diameter.

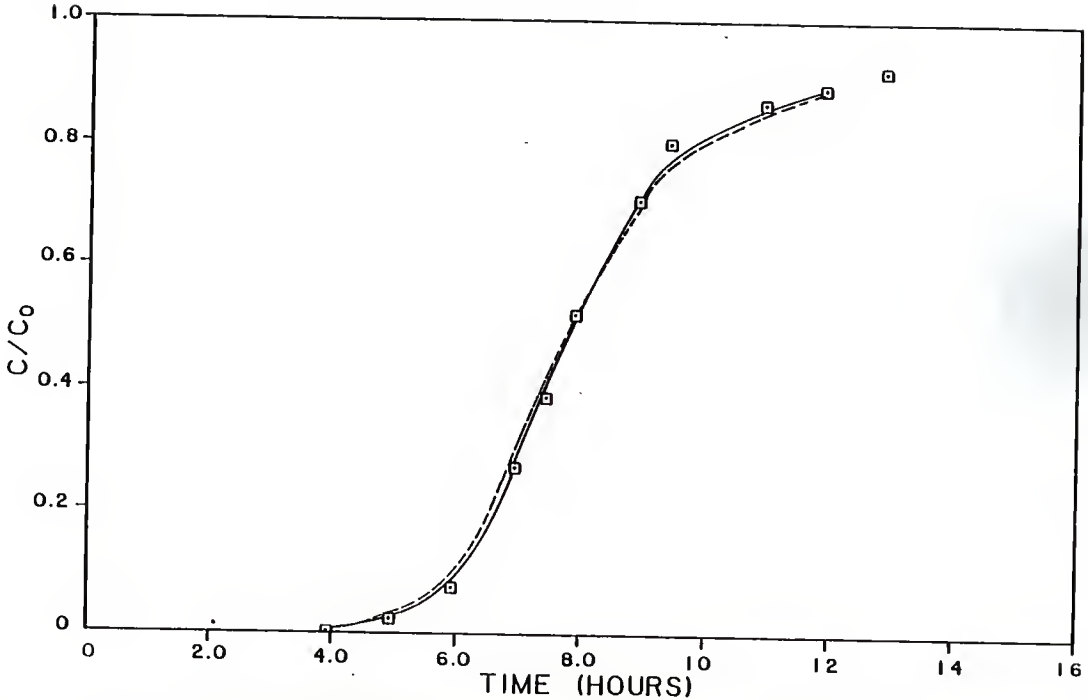

Fig. 6.20. Breakthrough curve for phenol adsorption for carbon size #20-#25. (⊡) experimental data, (-------) predictions using geometric mean diameter. (———) predictions using Sauter mean diameter.

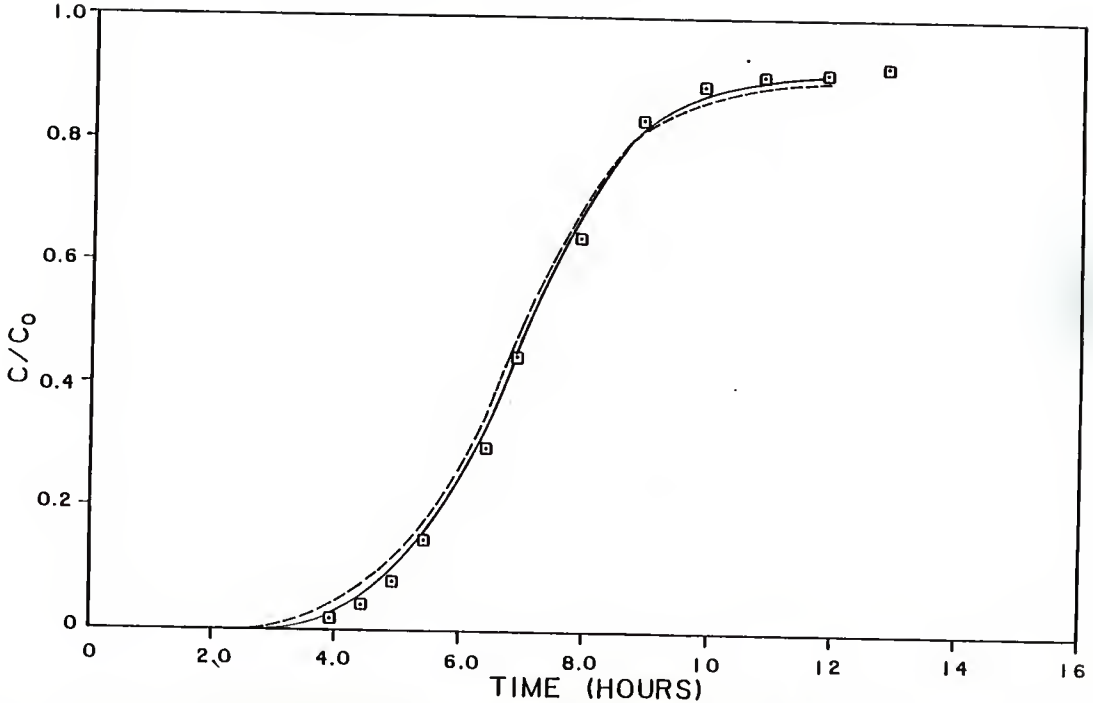

Fig. 21. Breakthrough curve for phenol adsorption for carbon size #30-#35. (⊡) experimental data, (-------) predictions using geometric mean diameter. (———), predictions, using Sauter mean diameter.

Table 6.15 Percent deviations between experimental and predicted breakthrough profiles for phenol adsorption for single sizes.

Sieve size	Geometric mean dia.	Sauter mean dia.	k_f based on (A)	D_s based on (A)	k_f based on (B)	D_s based on (B)	Percent deviations between experiment and predicted results using diameters	
	microns (A)	microns (B)	(calc) *	estimated +	(calc) *	estimated +	(A)	(B)
#12-#14	1544	1752	3.03	3.4	2.76	3.5	1.61	1.02
#14-#16	1294	1556	3.54	3.3	3.1	3.5	1.32	0.79
#16-#18	1091	1157	4.09	3.3	3.92	3.5	1.61	0.92
#18-#20	917	1075	4.85	3.2	4.32	3.5	1.53	1.05
#20-#25	772	923	5.01	3.2	4.41	3.5	1.65	1.1
#25-#30	647	782	5.8	3.3	5.06	3.5	1.45	0.92
#30-#35	543	645	6.66	3.2	5.89	3.5	1.54	1.13

* (cm/sec)*10^3

\+ (cm^2/sec)*10^8

Table 6.16 Fixed bed operating conditions for PCP adsorption

Sieve size	Bed diameter cm	Bed height cm	Flow rate ml/min	Hydraulic loading rate m/min	Weight of carbon gms
#12-#14	5.08	30.9	500	0.247	250
#18-#20	5.08	29.1	500	0.247	250
#20-#25	3.1	23.2	125	0.166	75
#30-#35	3.1	22.8	125	0.166	75

shows the fixed bed operating conditions for p-chlorophenol adsorption. Figures 6.22 and 6.23 shows the experimental and predicted breakthrough curves for p-chlorophenol. Table 6.17 shows the percent deviations for the predictions from experimental points when geometric mean diameters and Sauter mean diameters were used. It was seen once again that Sauter mean diameters gave better predictions than when geometric mean diameters were used, but, in this case, the predictions were more pronounced as opposed to that for phenol fixed bed predictions.

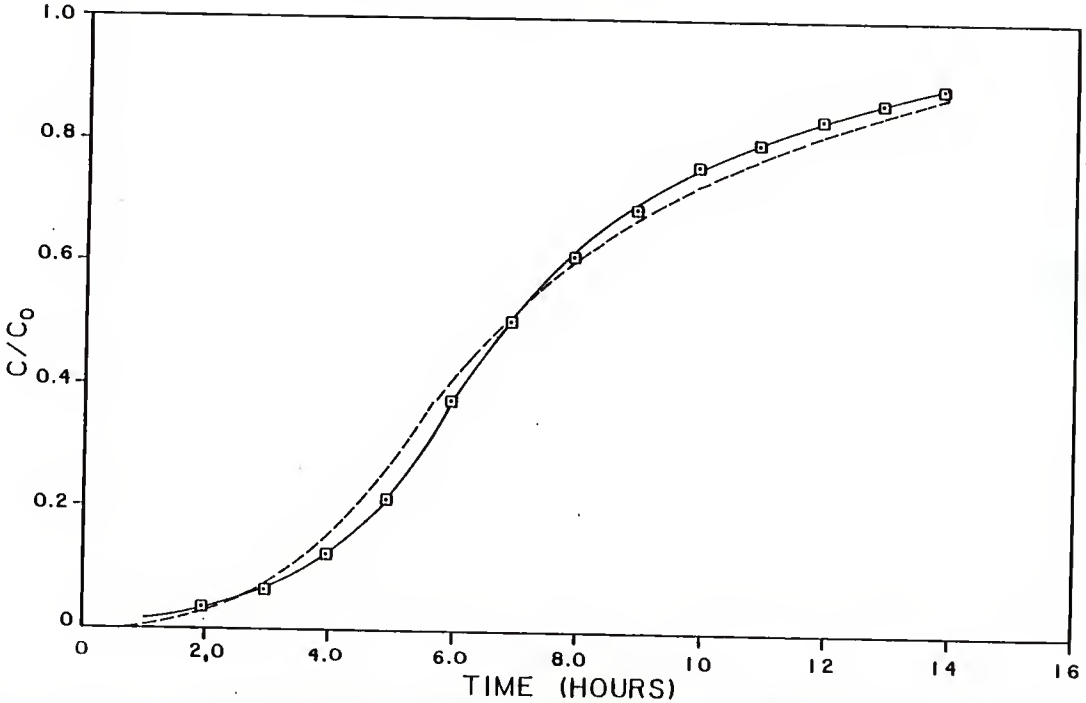

Fig. 6.22. Breakthrough curve for PCP adsorption for carbon size #12-#14. (⊡) experimental data, (-------) predictions using geometric mean diameter. (———) predictions using Sauter mean diameter.

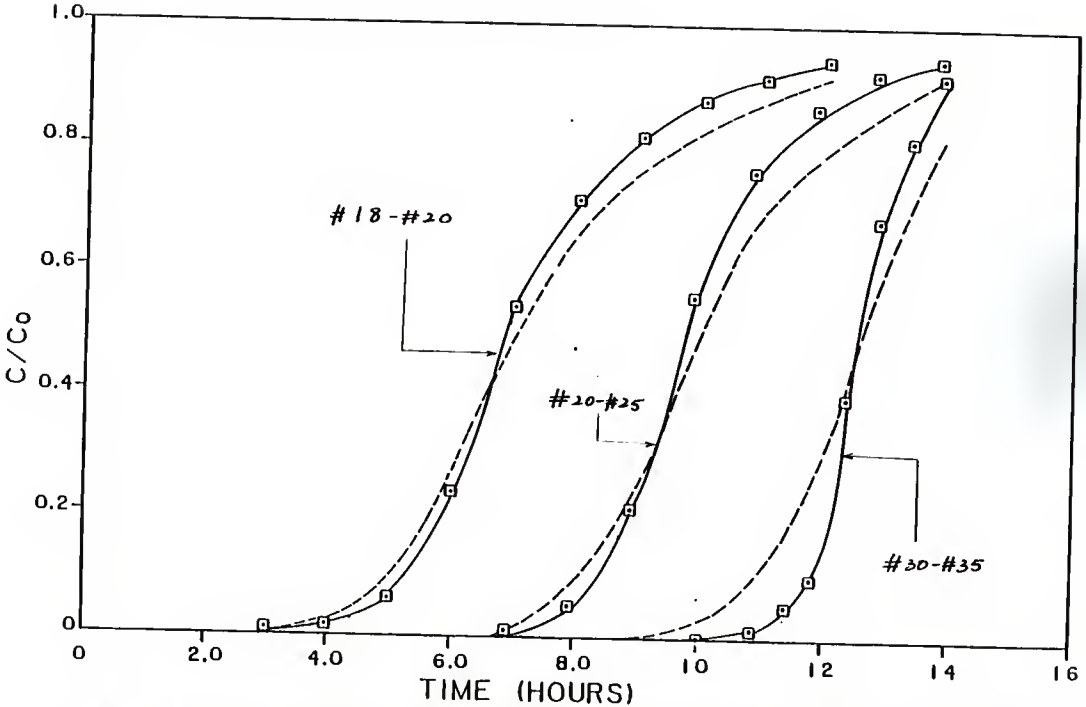

Fig. 23. Breakthrough curves for PCP adsorption for carbon sizes as indicated. (⊡) experimental data, (-------) predictions using geometric mean diameter, (———) predictions using Sauter mean diameter.

Table 6.17 Percent deviations between experimental and predicted breakthrough profiles for PCP adsorption for single sizes.

Sieve size	Geometric mean dia.	Sauter mean dia.	k_f based on (A)	D_s based on (A)	k_f based on (B)	D_s based on (B)	Percent deviations between experiment and predicted results using diameters	
	microns (A)	microns (B)	(calc) *	estimated +	(calc) *	estimated +	(A)	(B)
#12-#14	1544	1752	2.93	3.1	2.67	3.7	2.72	0.76
#18-#20	917	1075	4.68	3.2	4.17	3.7	3.01	0.84
#20-#25	772	923	4.84	3.0	4.26	3.7	3.87	1.02
#30-#35	543	645	6.45	2.9	5.68	3.7	5.13	0.89

* (cm/sec)*10^3

\+ (cm^2/sec)*10^8

6.5 Single solute column studies for mixture of carbon sizes

Column studies were conducted for mixture of carbon sizes. Tables 6.18 and 6.19 give the weights of carbon sizes taken for column studies for phenol and p-chlorophenol experiments, respectively. Table 6.20 gives fixed bed operating conditions for phenol adsorption for mixture of sizes. Figures 6.24 to 6.26 give the predictions and experimental breakthrough curves for the mixture of sizes with phenol as the solute. Table 6.21 gives the percent deviation for the predictions from the experimental and the diameters and their respective film transfer coefficient and intraparticle diffusion coefficient. In these cases the mean diameters were determined first. Then, using the equation by Upadyay and Dwiwedi (1977), the film transfer coefficients were determined. Surface diffusion coefficients were determined by taking the mean of the surface diffusion coefficients of the individual particles which were established from batch studies with single sized particles.

From the experiments it was seen that Sauter mean of the Sauter mean diameters gave better predictions than when Sauter mean of geometric mean diameters were used. This same occurrence was noticed in the case of p-chlorophenol adsorption for a mixture of sizes. Table 6.22 gives the fixed bed operating conditions for p-chlorophenol adsorption. Figures 6.27 and 6.28 give the breakthrough curves for a

Table 6.18 Weights taken (gms) for mixture of sizes for fixed bed studies for phenol adsorption.

Mix no.	Sieve sizes ---------->						
	#12-#14	#14-#16	#16-#18	#18-#20	#20-#25	#25-#30	#30-#35
1	40	70	70	70	0	0	0
2	40	40	40	40	40	10	40
3	0	0	0	0	25	10	40 ?
4	0	50	50	50	50	0	50

Table 6.19 Weights taken (gms) for mixture of sizes for fixed bed studies for PCP adsorption.

Mix no.	Sieve sizes ---------->			
	#12-#14	#18-#20	#20-#25	#30-#35
1	60	60	60	70
2	80	80	0	90
3	0	0	37.5	37.5

Table 6.20 Fixed bed operating conditions for phenol adsorption for a mixture of sizes

Mix no.	Bed diameter cm	Bed height cm	Flow rate ml/min	Hydraulic loading rate m/min	Weight of carbon gms
1	5.08	30	500	0.247	250
2	5.08	28.7	500	0.247	250
3	3.1	22.9	125	0.166	75
4	5.08	29.6	500	0.247	250

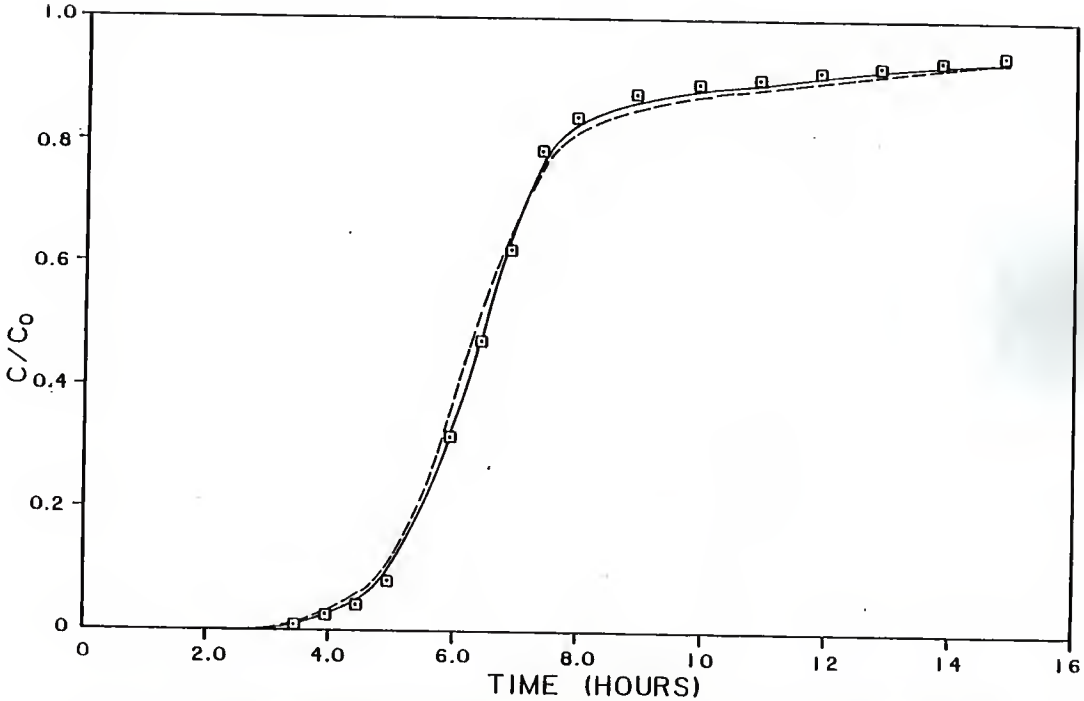

Fig. 6.24. Breakthrough curves for phenol adsorption for Mix no. 1 (⊡) experimental data, (-------) predictions using geometric mean diameter. (———) predictions using Sauter mean diameter.

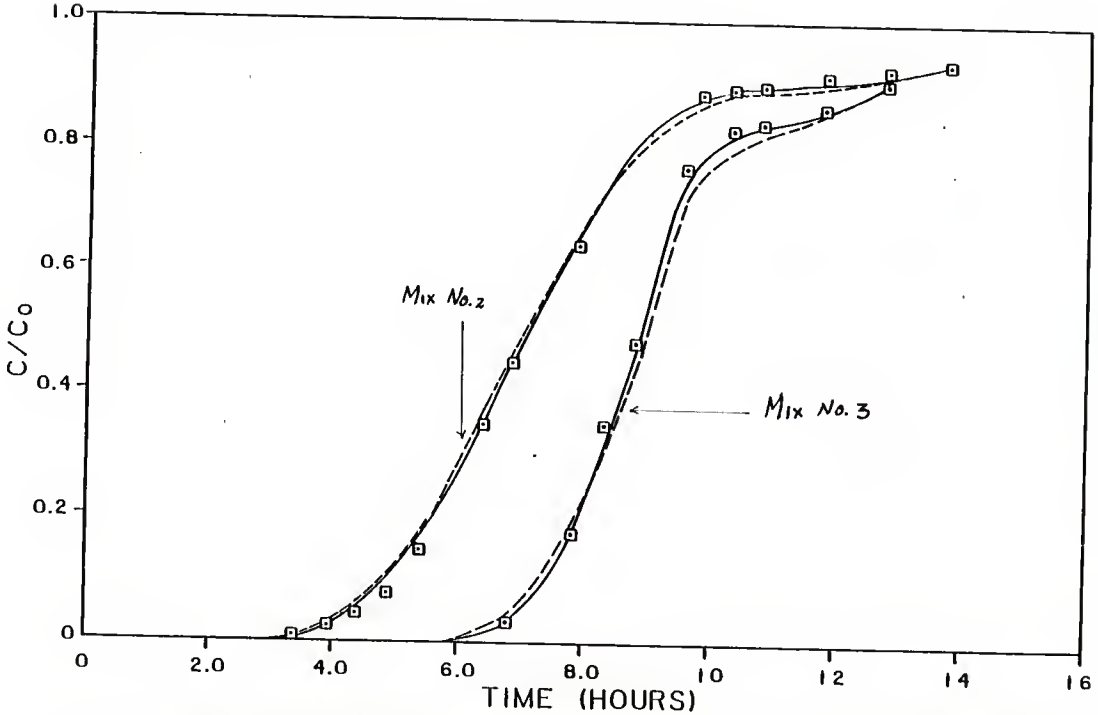

Fig. 6.25. Breakthrough curves for phenol adsorption for Mix no. 2 and 3. (⊡) experimental data, (-------) predictions using geometric mean diameter. (———) predictions using Sauter mean diameter.

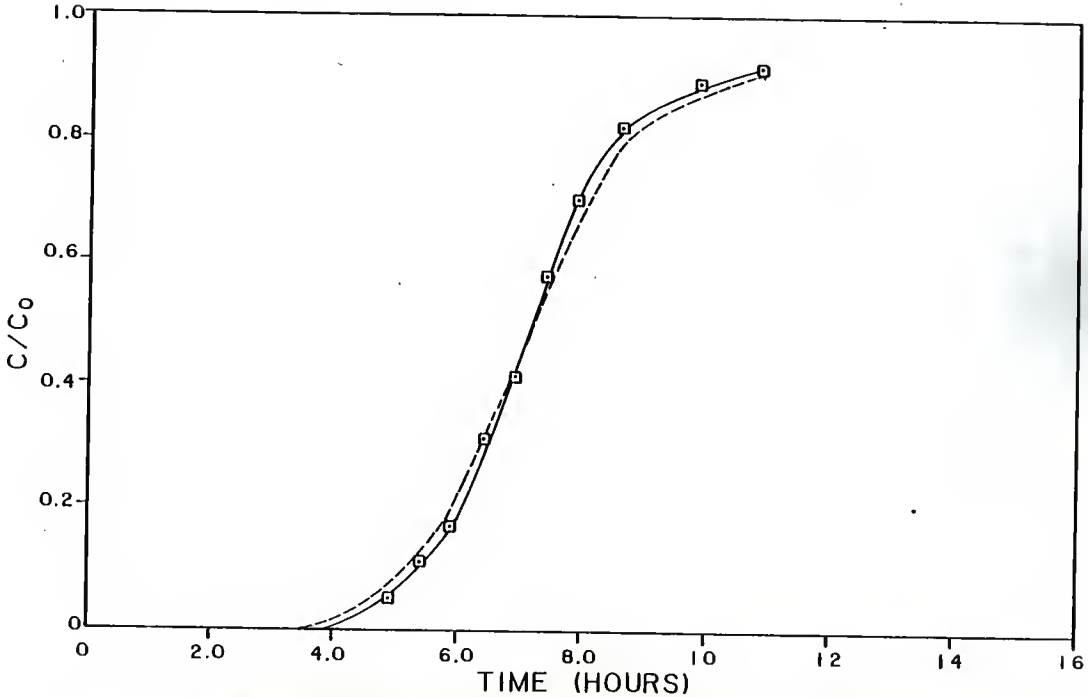

Fig. 6.26. Breakthrough curve for phenol adsorption for Mix no. 4. (⊡) experimental data, (-------) predictions using geometric mean diameter. (———) predictions using Sauter mean diameter.

Table 6.21 Percent deviations between experimental and predicted breakthrough profiles fpr phenol adsorption for mixture of sizes.

Mix no.	Geometric mean dia. micron (A)	Sauter mean dia. micron (B)	k_f bssed on (A) (calc) *	D_s based on (A) estimated +	k_f based on (B) (calc) *	D_s based on (B) estimated +	Percent devistion between experiment and predicted using diameters (A)	(B)	Percent deviation between experiment snd predicted using stratified bed model
1	1338	1392	3.95	3.31	3.59	3.5	1.62	1.09	0.50
2	795	1048	5.5	3.27	4.51	3.5	1.53	1.21	0.71
3	845	986	5.13	3.24	4.59	3.5	1.54	0.99	0.51
4	617	735	5.99	3.22	5.28	3.5	1.69	1.02	0.69

* (cm/sec)*10^3

\+ (cm^2/sec)*10^8

16/18

Table 6.22 Fixed bed operating conditions for PCP adsorption for mixture of sizes.

Mix no.	Bed diameter cm	Bed height cm	Flow rate ml/min	Hydraulic loading rate m/min	Weight of carbon gms
1	5.08	26.5	500	0.247	250
2	5.08	27.6	500	0.247	250
3	3.1	23.0	125	0.166	75

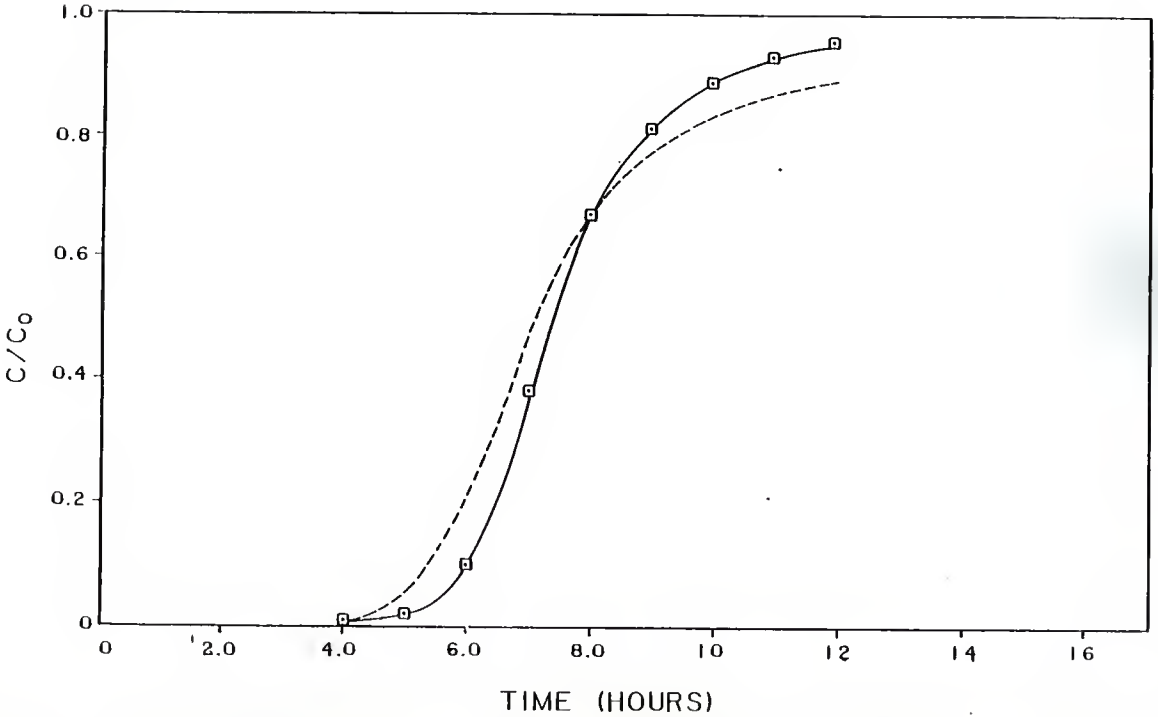

Fig. 6.27. Breakthrough curve for PCP adsorption for Mix no. 1. (⊡) experimental data, (-------) predictions using geometric mean diameter. (———) predictions using Sauter mean diameter.

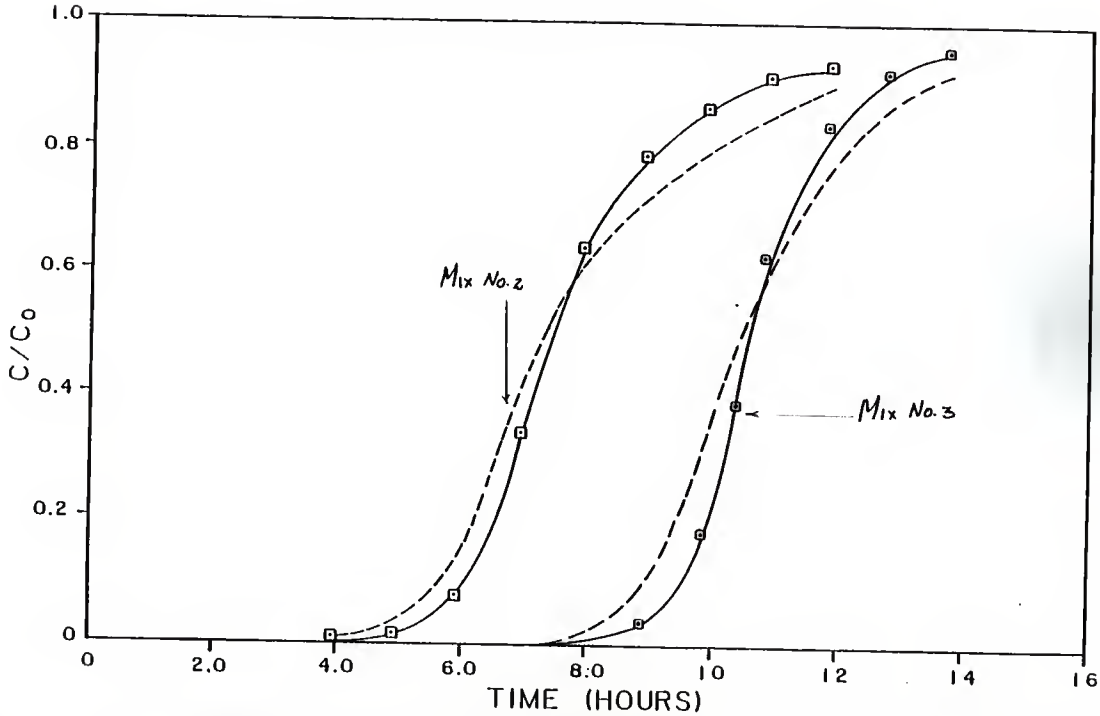

Fig. 6.28. Breakthrough curves for PCP adsorption for Mix no. 2 and 3. (⊡) experimental data, (———) predictions using Sauter mean diameter.

mixture of sizes for p-chlorphenol adsorption. Table 6.23 gives the percent deviation of predicted from experimental for mixture of sizes p-chlorophenol fixed bed operations. From the experiments it was noticed that Sauter mean diameters gave better predictions than when geometric mean diameters were used.

The computer program was also run taking into consideration a layered bed. The individual film transfer coefficients and the individual surface diffusion coefficients replaced the averaged film transfer coefficients and surface diffusion coefficients and individual particle diameters replaced averaged particle diametrs. Using this approach it is seen in Tables 6.21 and 6.23 that the percent deviations between experimental and predicted data are much closer than either Sauter mean of Sauter mean diameters or Sauter mean of geometric mean diameters.

From fixed bed studies we concluded that the Sauter mean diameters was a better way of representing particle size distribution for column studies.

Table 6.23 Percent deviations between experimental and predicted breakthrough profiles for PCP adsorption for mixture of sizes.

Mix no.	Geometric mean dia.	Sauter mean dia.	k_f based on (A)	D_s based on (A)	k_f based on (B)	D_s based on (B)	Percent deviation between experiment and predicted results using diameters		Percent deviation between experiment and predicted results using stratified bed model
	microns (A)	microns (B)	(calc) *	estimated +	(calc) *	estimated +	(A)	(B)	
1	804	948	5.11	3.05	4.53	3.7	4.91	0.91	0.43
2	820	963	4.99	3.0	4.45	3.7	4.41	1.12	0.53
3	637	759	5.64	3.0	4.98	3.7	5.33	0.93	0.44

* (cm/sec)$*10^3$

\+ (cm^2/sec)$*10^8$

6.6 Multicomponent adsorption

6.6.1 Experimental methods

Experimental procedures for multicomponent adsorption were similar to that of single solute adsorption, i.e., all the preliminary precautions taken for single solute adsorption were applicable for multicomponent adsorption. In all studies (equilibrium, batch and fixed-bed studies) the temperature was maintained at 25 deg. C and pH was maintained at 7.

6.6.2 Equilibrium studies

In multicomponent equilibrium studies, experimental data for phenol and p-chlorophenol was collected. To describe the data two multicomponent models were selected. They were

1) Mathew's model (1975) which is given as

$$q_{v_i} = A(c_i/\eta_i)/(1+B_i(c_i/\eta_i)^{\beta_i})$$

2) Prausnitz's model (IAS model).

The isotherm constants A, B, and β used for the models were obtained from single solute isotherm studies.

Recently, it has become necessary to make use of theoretical models that allow the predictions of multicomponent adsorption with less amount of experimental data. Tables 6.24 and 6.25 show the experimental and predicted values for the multicomponent studies using the models stated above. From the tables we see that both models

Table 6.24 Prediction of equilibrium data for multisolutes using extension of the three parameter equation.

C1 mM/L	C2 mM/L	Q1 experimental mM/gms	Q1 calculated mM/gms	Q2 experimental mM/gms	Q2 calculated mM/gms
1.8360	0.2190	0.219	0.186	1.662	1.055
0.7085	0.2960	0.450	0.509	1.803	1.132
0.0354	0.0134	0.310	0.274	0.530	0.492
0.0159	0.0075	0.252	0.185	0.491	0.414
3.2020	0.9961	0.616	0.573	1.006	0.848
1.1360	0.1915	0.834	0.786	0.720	0.631
0.0595	0.0033	0.593	0.664	0.199	0.176
0.0174	0.0053	0.333	0.231	0.332	0.336
0.0102	0.0058	0.249	0.140	0.320	0.377
0.4181	0.3150	1.521	1.370	0.428	0.491
1.5770	0.1239	1.422	1.201	0.501	0.454
0.4778	0.0439	1.127	0.965	0.473	0.422
0.1783	0.0295	0.881	0.620	0.536	0.489
0.1052	0.0102	0.712	0.692	0.287	0.320

Q1 stands for surface concentration of phenol solute

Q2 stands for surface concentration of PCP solute

Table 6.25 Prediction of equilibrium data for multisolute using IAS model

C1 mM/L	C2 mM/L	Q1 experimental mM/gms	Q1 calculated mM/gms	Q2 experimental mM/gms	Q2 calculated mM/gms
0.7085	0.2960	0.450	0.517	1.803	1.755
0.0354	1.3370	0.310	0.396	0.530	0.478
0.0159	0.0075	0.252	0.236	0.491	0.449
0.0595	0.0032	0.593	0.609	0.199	0.209
0.0174	0.0053	0.333	0.264	0.332	0.303
0.0102	0.0058	0.249	0.171	0.320	0.270
1.5570	0.1239	1.422	1.578	0.501	0.512
0.1052	0.0102	0.712	0.764	0.287	0.347

Q1 stands for surface concentration of phenol solute

Q2 stands for surface concentration of PCP solute.

gave good predictions for the experimental data. It was seen that Mathew's model was under predicting for high concentrations. The values of η_i for Mathew's model was 0.4679 and 0.1945. The percent deviations for phenol solute and p-chlorophenol solute was estimated using the equation as followa:

$$\%\,\text{deviation} = \left(\frac{\Sigma \left| Q_{exp,phenol} - Q_{calc,phenol} \right|}{N} + \frac{\Sigma \left| Q_{exp,PCP} - Q_{calc,PCP} \right|}{N} \right) * 100$$

Using the above equation it was seen for the Mathew's model the percent deviation between experimental and predicted values for surface adsorption was 24% whereas for the IAS model the percent deviation was 14%.

6.6.3 Batch studies

Multicomponent adsorption for batch studies were conducted. Batch experiments were conducted for two single adsorbent sizes and one mixture of adsorbent sizes. The aim in these experiments was to see how the multicomponent adsorption rate model would predict batch data. The IAS equlibrum model was incorporated into the multicomponent rate model.

Figures 6.29 and 6.30 gives the experimental and predicted values for the multicomponent adsorption rate model written by Mathews (1983). The program needed inputs for film transfer coefficients and surface diffusion coefficients. It also needed the constants of the three parameter isotherm equation. All these inputs were determined from single solute rate and equilibrium studies. The diameters used in these predictions were the Sauter mean diameter and the geometric mean diameter. Table 6.26 gives the operating conditions for batch studies for multicomponent adsorption. Table 6.27 gives the percent deviations from predicted and experimental values for multicomponent rate studies. From this table we see that Sauter mean diameters gave better predictions than when geometric mean diameters were used. It was also seen that the incorporation of the IAS model for multicomponent rate studies gave predictions which were very close to the experimental data.

Batch studies for multicomponent adsorption were

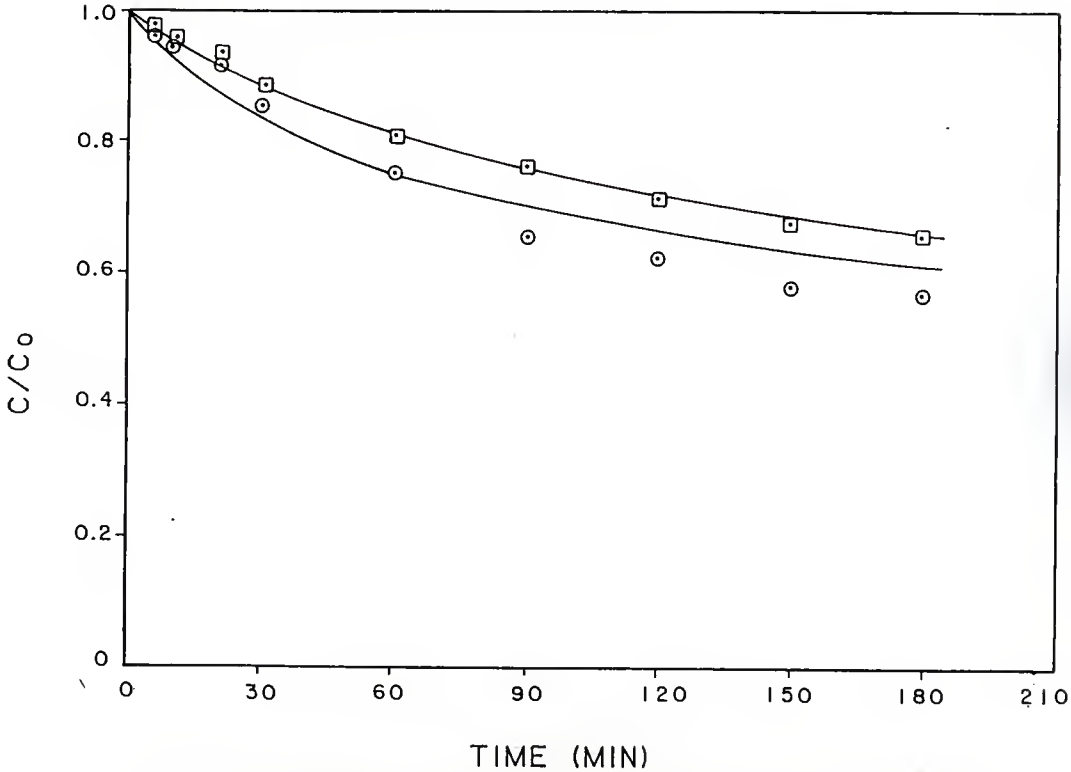

Fig. 6.29 Adsorption rate for multicomponent adsorption for carbon size #12-#14 ( ) experimental data for phenol and PCP. ( ) predictions using Sauter mean diameter.

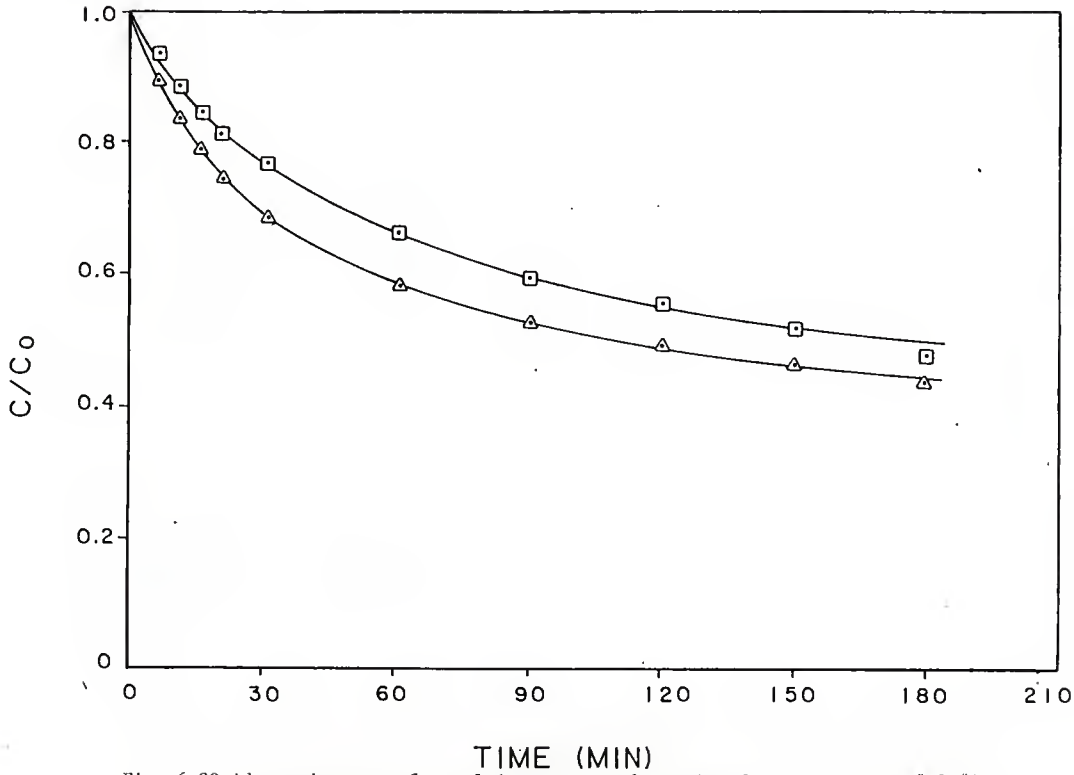

Fig. 6.30 Adsorption rate for multicomponent adsorption for carbon size #18-#20 ( ) experimental data for phenol and PCP. ( ) predictions using Sauter mean diameter.

Table 6.26 Operating condition for multicomponent rate studies.

Sieve size	Initial solution concentration.		Weight of carbon taken
	Phenol	PCP	(gm)
#12-#14	2.394	2.804	8.0065
#18-#20	2.500	2.518	8.0006
Mix 4	2.501	2.538	8.0017

Initial solution concentration is $M*10^4$

Mix 4 had 2.0002, 2.0009, 2.0001, and 2.0005 gms of sieve size #12-#14, #18-#20, #20-#25, and #30-#35 respectively.

Table 6.27 Percent deviations between experimental and predicted results for bisolute batch studies using diameters geometric and Sauter.

Sieve size	% deviation for geometric mean	% deviation for Sauter mean
#12-#14	8.23	4.1
#18-#20	7.31	0.99
Mix 4	1.27	4.29

conducted for a mixture of carbon of sizes. The film transfer coefficients and the surface diffusion coefficient were determined the same way as done in the case of single solute batch studies for a mixture of adsorbent sizes. Figure 6.31 gives the experimental and predicted data for the mixture of solutes using a mixture of adsorbents. Table 6.26 shows the percent deviation between experimental and predicted values for Sauter mean diameter and geometric mean diameter.

6.6.4 Fixed-bed studies

A total of four column studies were conducted, three for single adsorbent sizes and one for a mixture of adsorbent sizes. No predictions were conducted and the Figures 6.32 to 6.34 show the experimental values for the column runs for single adsorbent sizes.

From these plots we see that as the particle size decreased in diameter the peak values attained for phenol concentration in the effluent increased. It was also seen that C/C_o values in all of these runs exceeded 1.0. The possible reason for this could be due to the fact that p-chlorphenol is adsobed faster at the top of the column initially and phenol at the bottom of the column. As the top gets saturated p-chlorophenol moves downward displacing the adsorbed phenol back into the solution and this raised the concentration of phenol in the water.

Figure 6.35 shows the experimental data for column

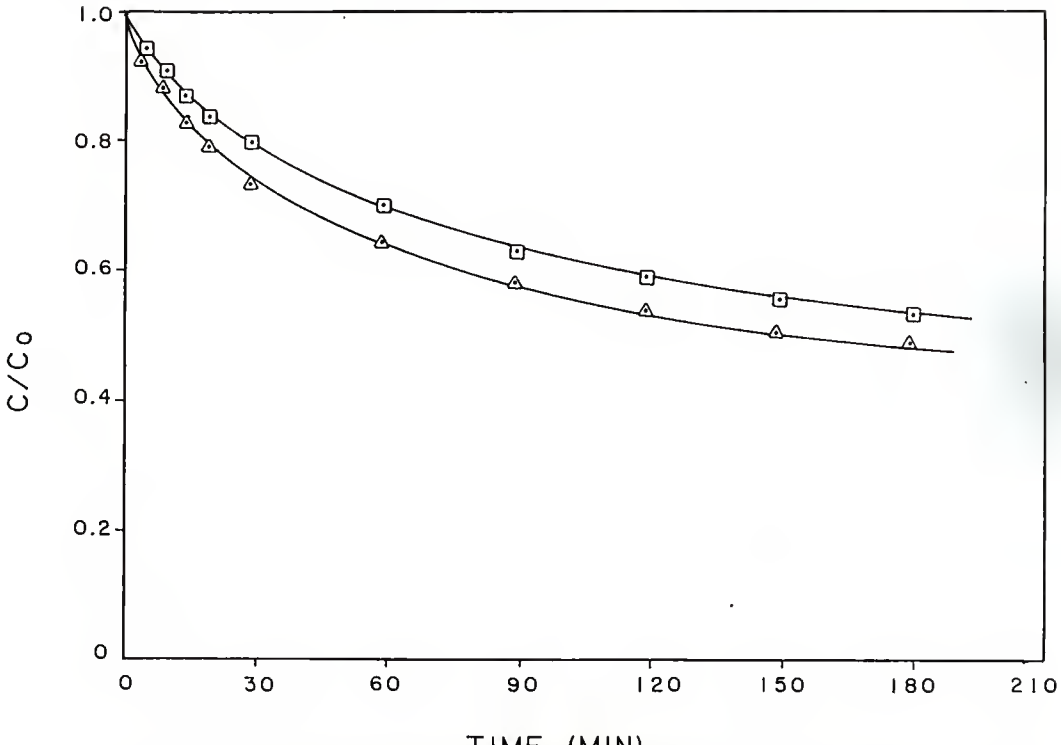

Fig. 6.31 Adsorption rate for multicomponent adsorption for Mix no. 4
( ) experimental data for phenol and PCP. ( ) predictions using Sauter mean diameter

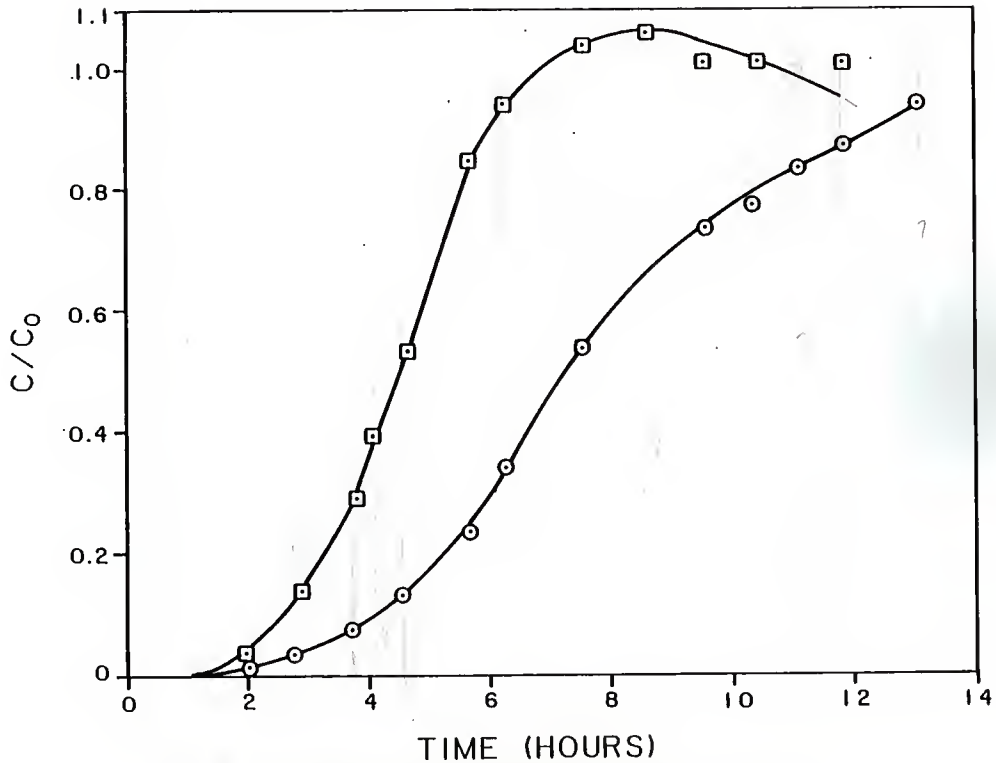

Fig. 6.32 Breakthrough curve for multicomponent adsorption for carbon size #12-#14. (⊡, ⊙) experimental data for phenol and PCP respectively

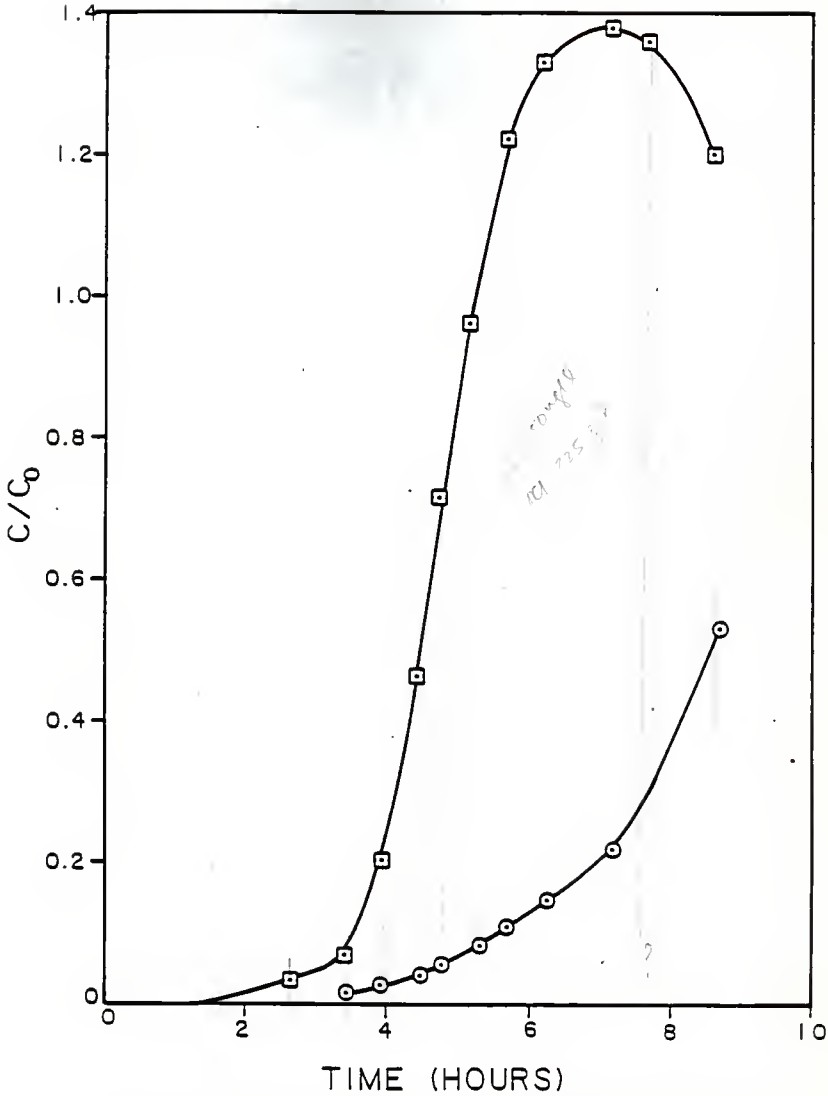

Fig. 6.33 Breakthrough curve for multicomponent adsorption for carbon size #18-#20. (⊡, ⊙) experimental and predicted data for phenol and PCP respectively

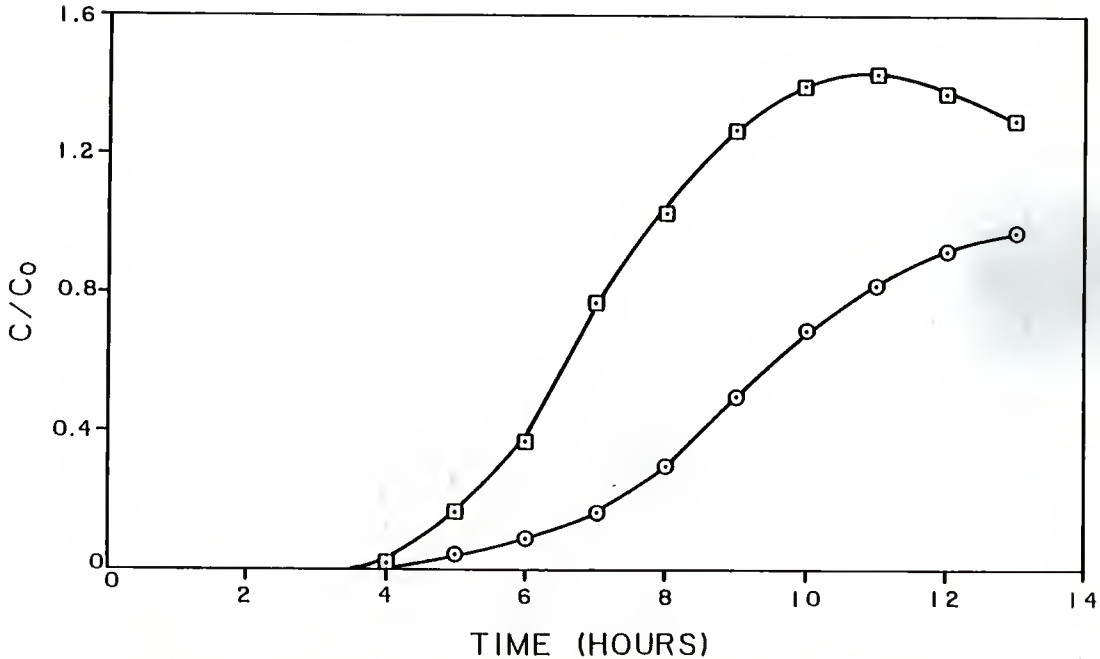

Fig. 6.34 Breakthrough curve for multicomponent adsorption for carbon size #30-#35. (⊡ , ⊙) experimental data for phenol and PCP respectively

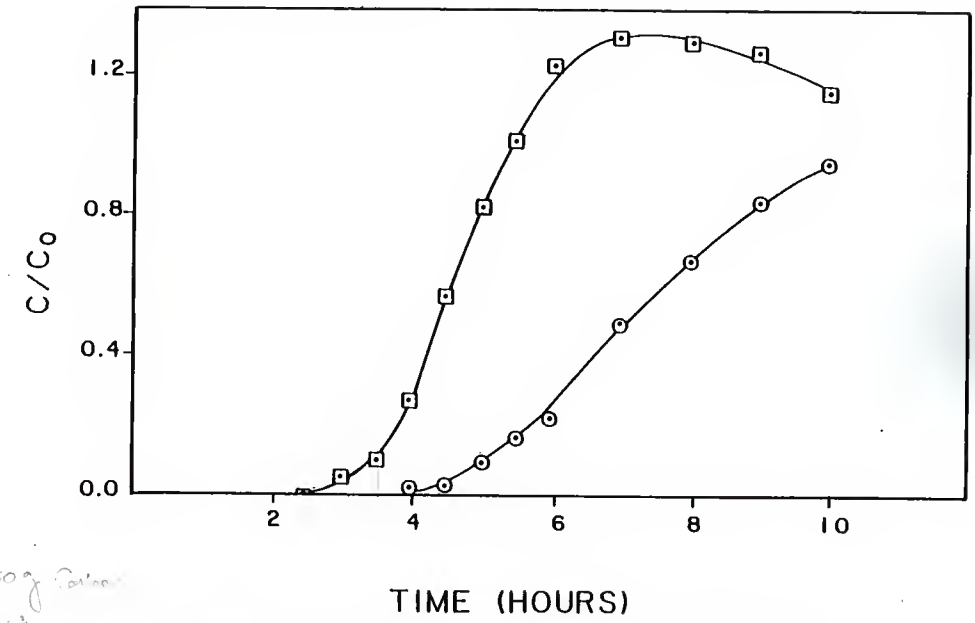

Fig. 6.35 Breakthrough curve for multicomponent adsorption for mixture of carbon sizes. (⊡, ⊙) experimental data for phenol and PCP respectively

studies for a mixture of carbon sizes. A total of 250 gms of carbon was taken. From the plot we see that the peak value attained for phenol solute in the effluent was greater than the peak value attained for single adsorbent size #12-#14, but was lower than that for #18-#20 and #30-#35. For sieve #03-#35 the weight of carbon taken was 75 gm.

The initial concentrations for the influents for sieve sizes #12-#14, #18-#20, and #30-#35 was $1.847*10^{-3}$, $1.643*10^{-3}$, and $1.900*10^{-3}$ for phenol concentrations. PCP concentrations were $1.831*10^{-3}$, $1.751*10^{-3}$, and $1.817*10^{-3}$. For mixture of sizes the initial influent concentrations was $1.832*10^{-3}$ for phenol, and for PCP it was $1.862*10^{-3}$.

Chapter 7

Summary and Conclusions

Equilibrium studies were conducted for the adsorption of two solutes 1) phenol and 2) parachlorophenol on activated carbon from water. The tests were conducted for both solutes at 25 deg. C. and the pH of the tapwater was adjusted to 7. (The water initially passed through a three foot carbon column to remove organic and other adsorbables from it. Both solutes took three days to attain equilibrium). The data were fitted by the three parameter isotherm equation which was established by Mathews and Weber (1977). It was seen that the three parameter isotherm fitted the experimental data well. In the case of p-chlorophenol the adsorption isotherm curve was higher than for phenol isotherm indicating that p-chlorophenol is more strongly adsorbed than phenol.

Batch studies were conducted for phenol and p-chlorophenol for single adsorbent sizes as well as for a mixture of carbon sizes. Two different methods of averaging the particle sizes were tried. They are the geometric mean diameters and Sauter mean diameters. For all the experiments conducted during batch studies the pH of the water was maintained at 7 and the temperature regulated to 25 deg. C.

For batch studies involving phenol and p-chlorophenol adsorption and single sizes, the film transfer coefficient

increased as particle size decreased to within the size range of 1544 microns to 917 microns. It then remained constant within the size range of 772 microns to 543 microns.

It was also seen that when Sauter mean diameter based on area was used the surface diffusion coefficient remained a constant for both phenol and p-chlorophenol at $3.5*10^{-8}$ and $3.7*10^{-8}$ cm^2/sec, respectively. Whereas, when geometric mean diameters were used the surface diffusion coefficient varied from $3.2*10^{-8}$ to $3.4*10^{-8}$ for phenol solutes and varied from $2.9*10^{-8}$ to $3.2*10^{-8}$ for p-chlorophenol solute.

In the case of batch studies for a mixture of sizes, it was seen that better predictions for the data were obtained when the Sauter mean diameters were used than when geometric mean diameters were used to average the particle size distribution. For both phenol and p-chlorophenol batch studies for a mixture of adsorbent sizes, it was seen that the predicted and experimental data were within 5% of each other.

Column studies were conducted for single adsorbent sizes as well as for a mixture of adsorbent sizes. Columns of two different diameters were used depending on the size of the adsorbent. The temperature and pH were maintained at 25 deg. C and 7, respectively. The program used to predict the breakthrough profiles was the homogenous solid phase diffusion model which was modified by Mathews (1984) so that equilibrium could be represented by the three parameter isotherm.

For column studies it was seen that when Sauter mean diameter was used, the model predictions were much closer to the experimental data than when geometric mean diameter was used. This was noticed in the case of single adsorbent sizes as well as for a mixture of adsorbent sizes. In both cases, ie., for single adsorbent sizes as well as for a mixture of adsorbent sizes the percent deviations from experimental and predicted data were within 5% of each other.

Multicomponent equilibrium studies were conducted in a similar fashion as that of the single solute equilibrium studies. Two models were used to fit the isotherm data. They were the extension of the three parameter isotherm equation established by Mathew's (1977) and the ideally adsorbed solution model (IAS model). However, the percent deviations between experimental and predicted data were lower when the IAS model was used than when Mathew's model was used. When using Mathew's model the percent deviation was 24% whereas when using the IAS model the percent deviation was 14%.

Batch studies were conducted for single as well as for a mixture of sizes. Predictions were obtained by making use of the multicomponent adsorption rate model program written by Mathew's (1983). It was seen that the use of Sauter mean diameters, based on area, gave better predictions than when geometric mean diameters were used. This was also noticed in the case of batch studies for a mixture of adsorbent sizes.

In the case of fixed-bed studies with multicomponents it

was seen that as the particle size decreased the peak value attained for phenol solute in the effluent kept increasing with time. It was also noticed that C/C_o values for phenol adsorption exceeded 1.0. The possible reason for this could be due to the fact that p-chlorophenol is adsorbed faster at the top of the column initially and phenol at the bottom of the column. As the top became saturated, p-chloroophenol moved downward displacing the adsorbed phenol back into the solution.

For fixed bed studies for multicomponent adsorption using mixture of adsorbent sizes, it was seen that the peak value attained for phenol solute in the effluent was higher than the peak value attained for multicomponent adsorption for single adsorbent size #12-#14, but was lower than that for #18-#20 or #30-#35.

APPENDIX

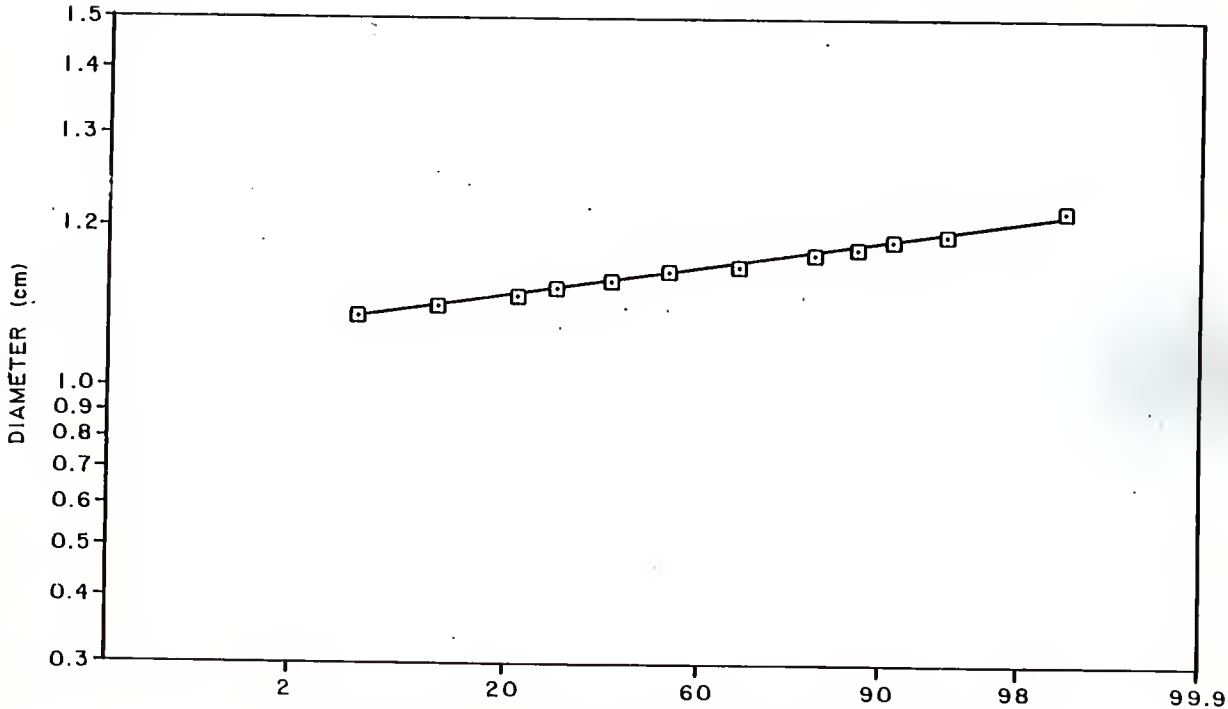

CUMULATIVE WEIGHT FRACTION WITH DIAMETER SMALLER THAN STATED for #12-#4

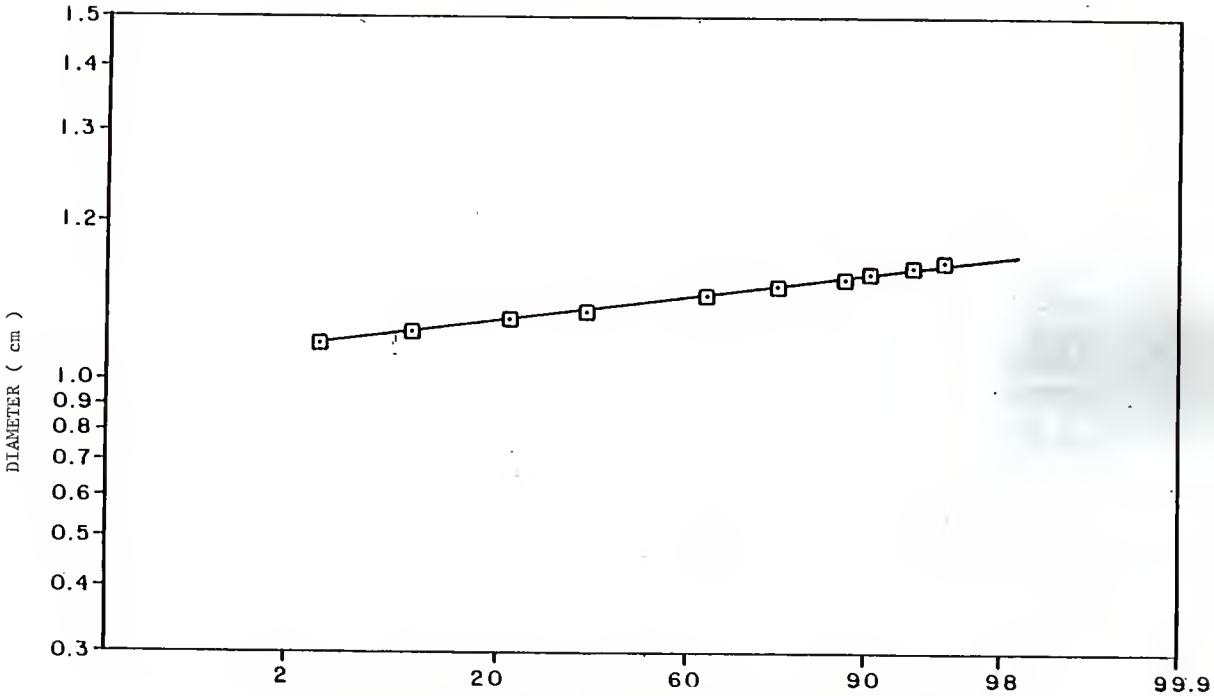

Cumulative weight fraction with diameter less than stated
for particle size #14-#16 based on the area of the particle

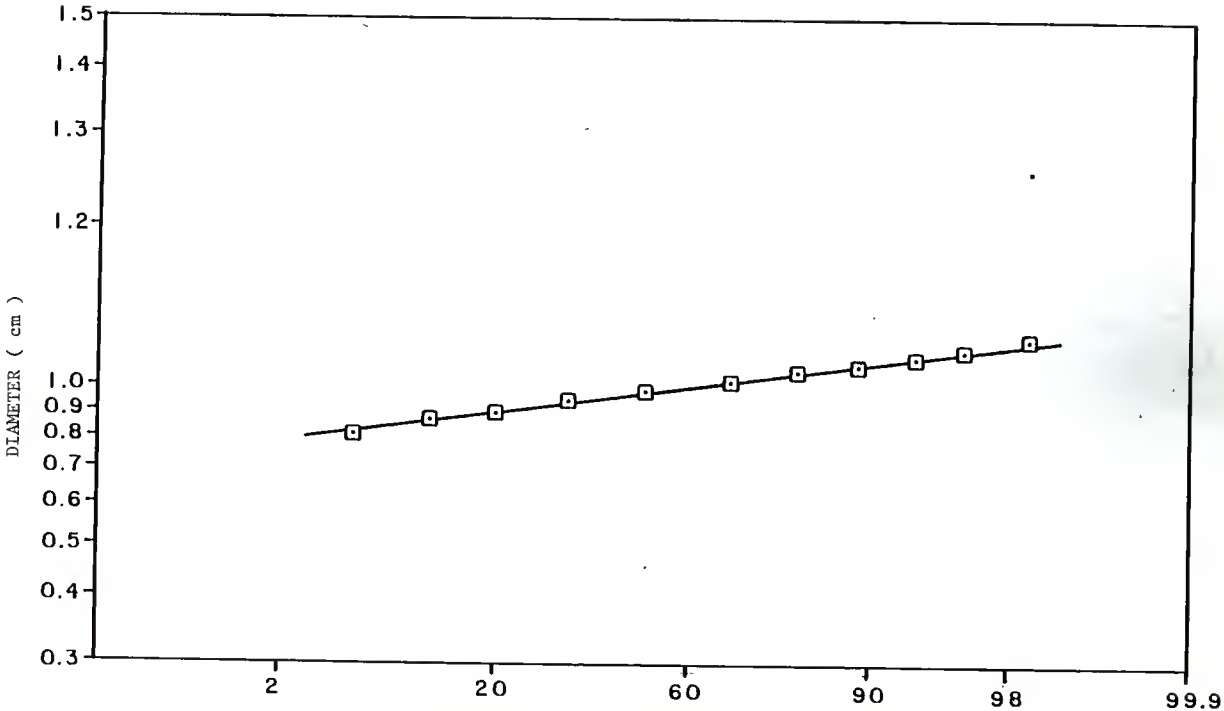

Cumulative weight fraction with diameter less than stated
for particle size #18-#20 based on the area of the particle

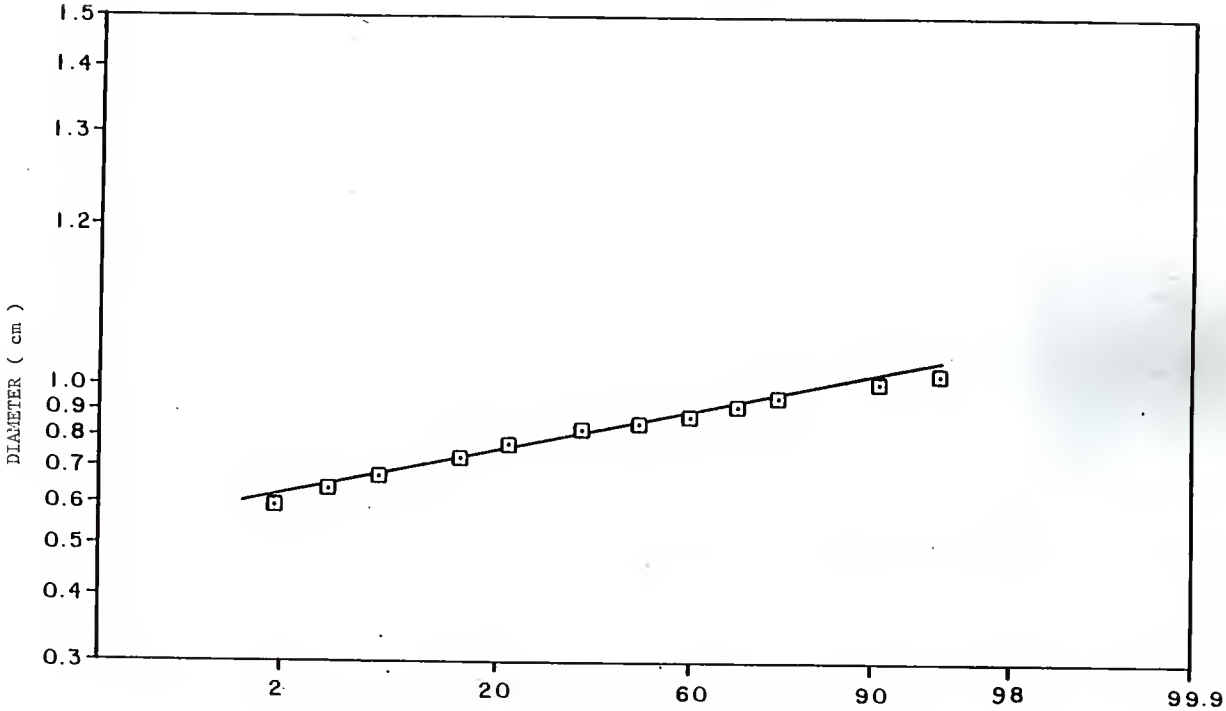

Cumulative weight fraction with diameter less than stated
for particle size #20-#25 based on area of the particle

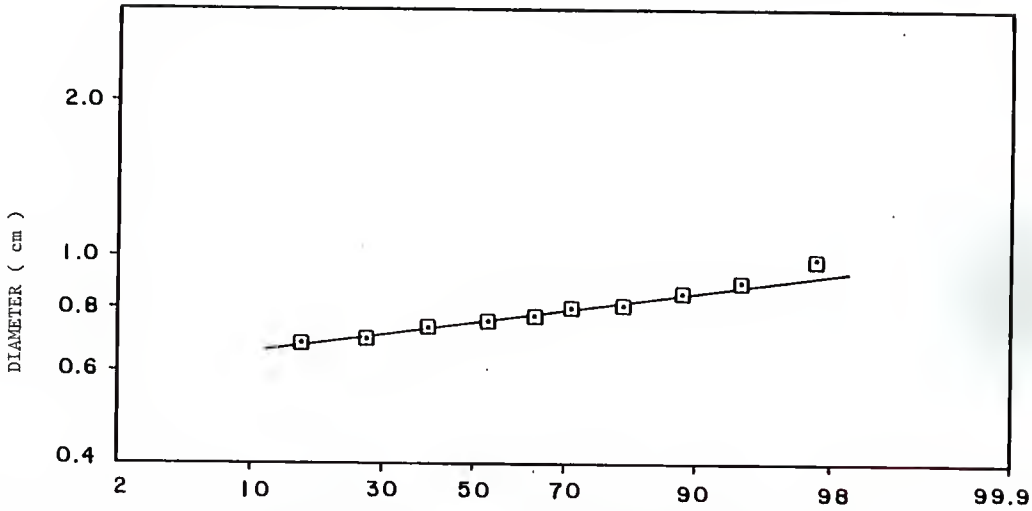

Cumulative weight fraction with diameter less than stated
for particle size #25-#30 based on area of the particle

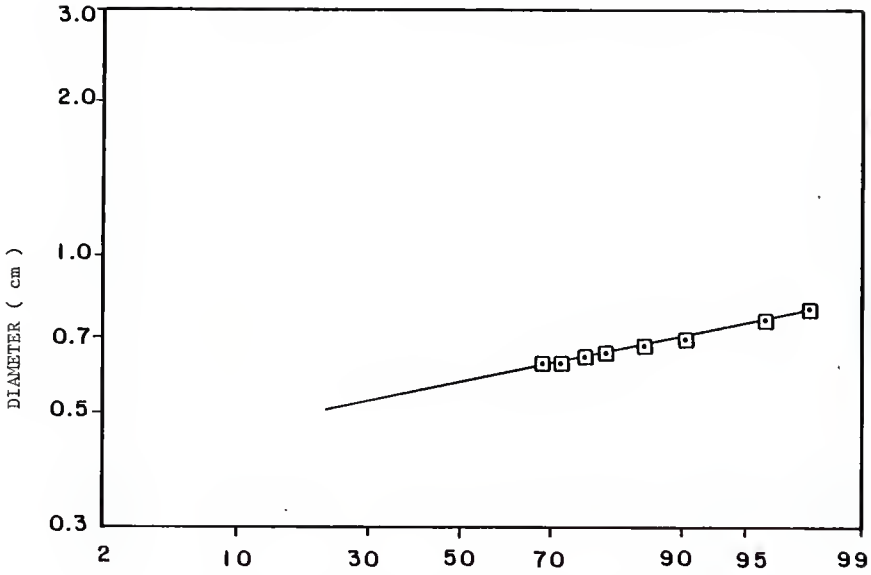

Cumulative weight fraction with diameter less than stated for particle size #30-#35 based on area of the particle

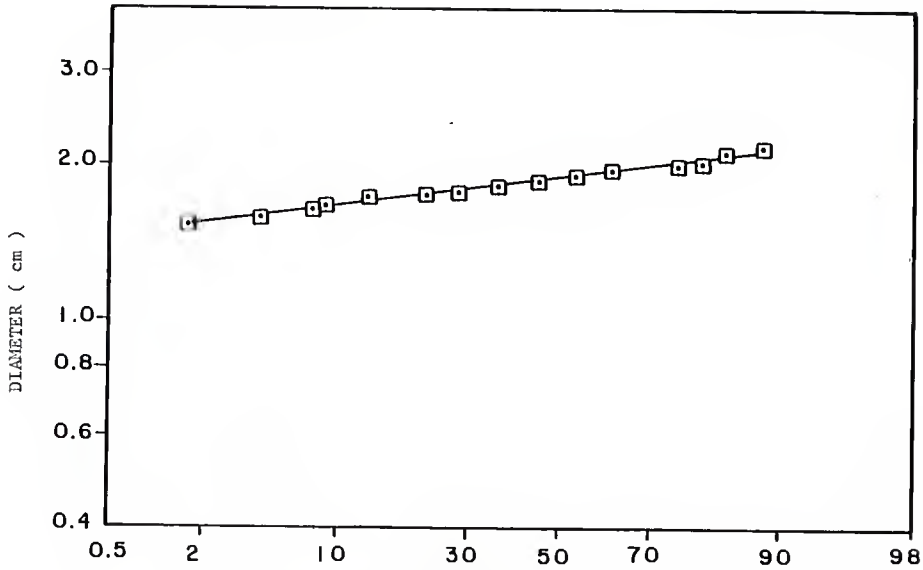

Cumulative weight fraction with diameter less than stated
for particle size #12-#14 based on perimeter of the particle

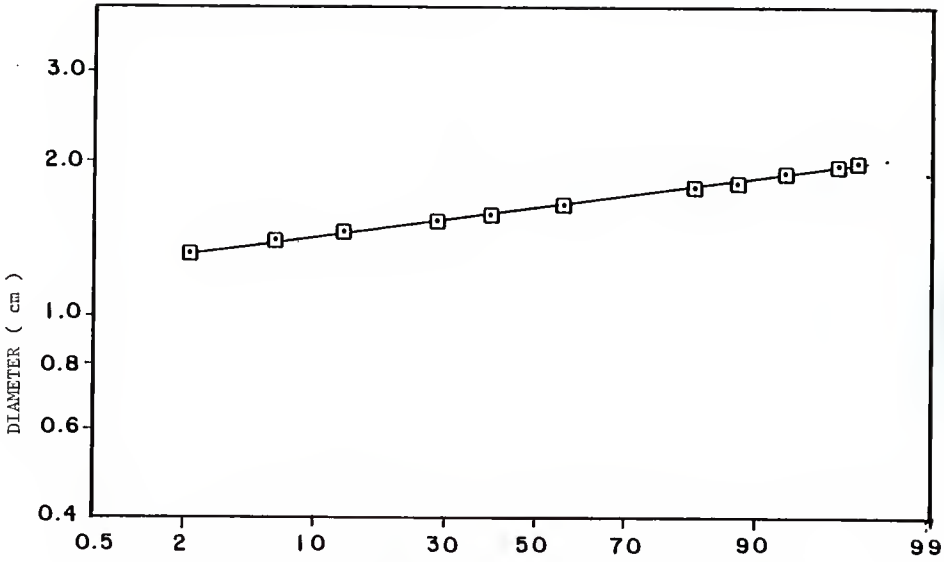

Cumulative weight fraction with diameter less than stated
for particle size #14-#16 based on perimeter of the particle

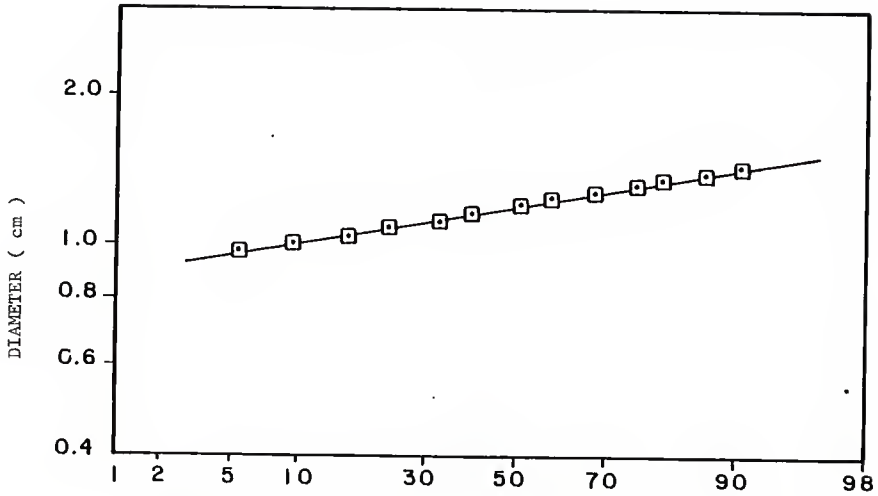

Cumulative weight fraction with diameter less than stated for particle size #16-#18 based on perimeter of the particle

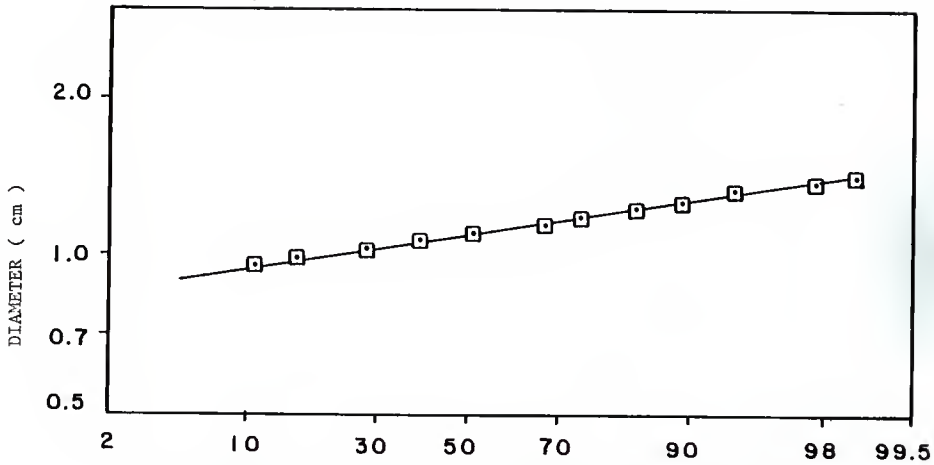

Cumulative weight fraction with diameter less than stated
for particle size #18-#20 based on perimeter of the particle

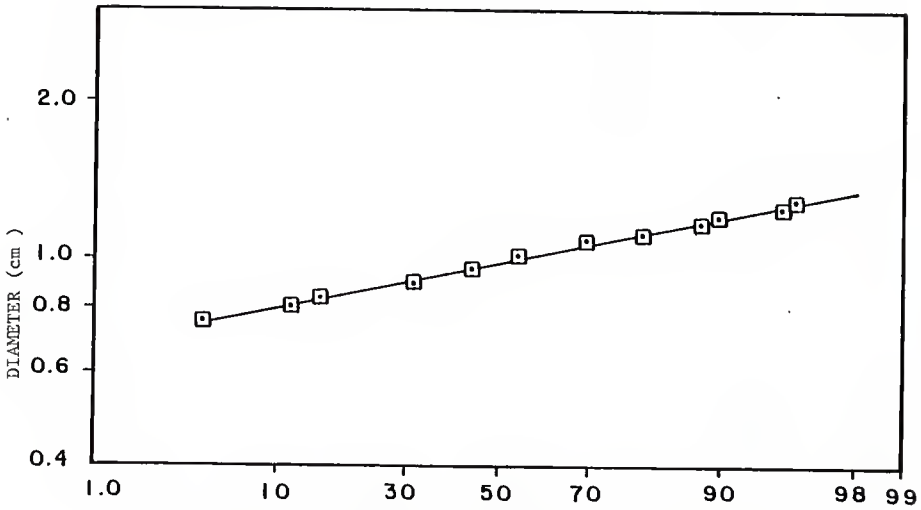

Cumulative weight fraction with diameter less than stated
for particle size #20-#25 based on perimeter of the particle

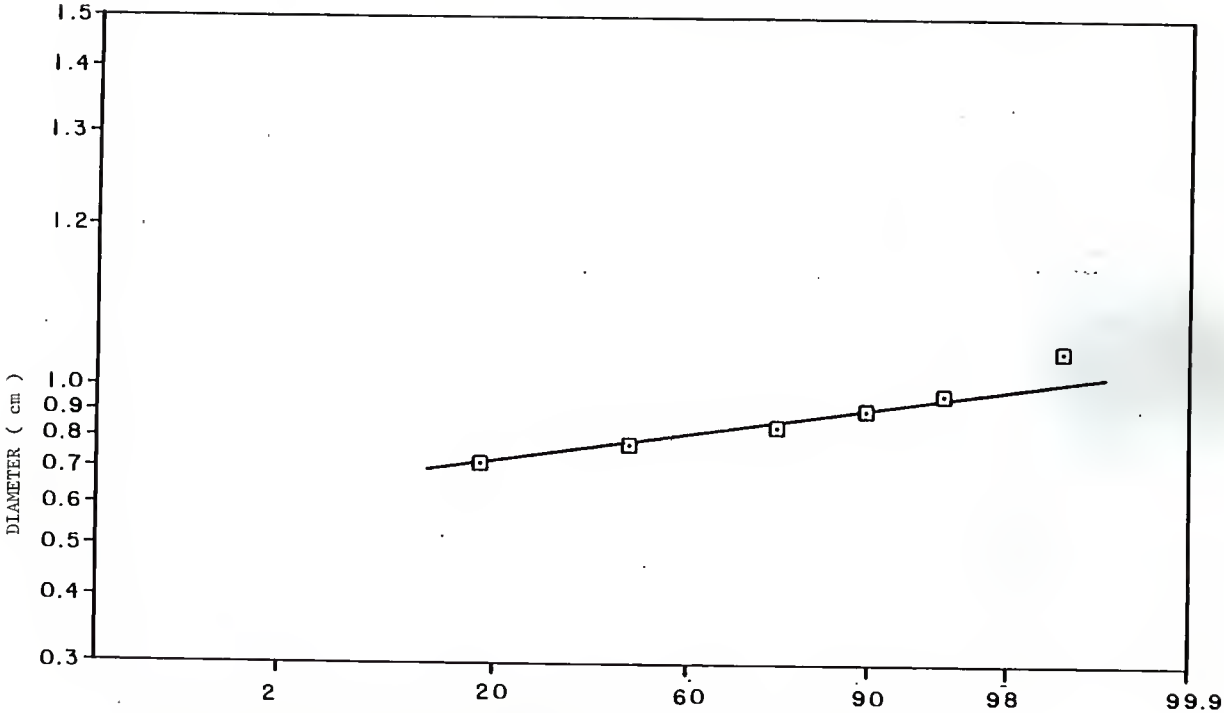

Cumulative weight fraction with diameter less than stated for particle size #25-#30 based on the perimeter of the particle

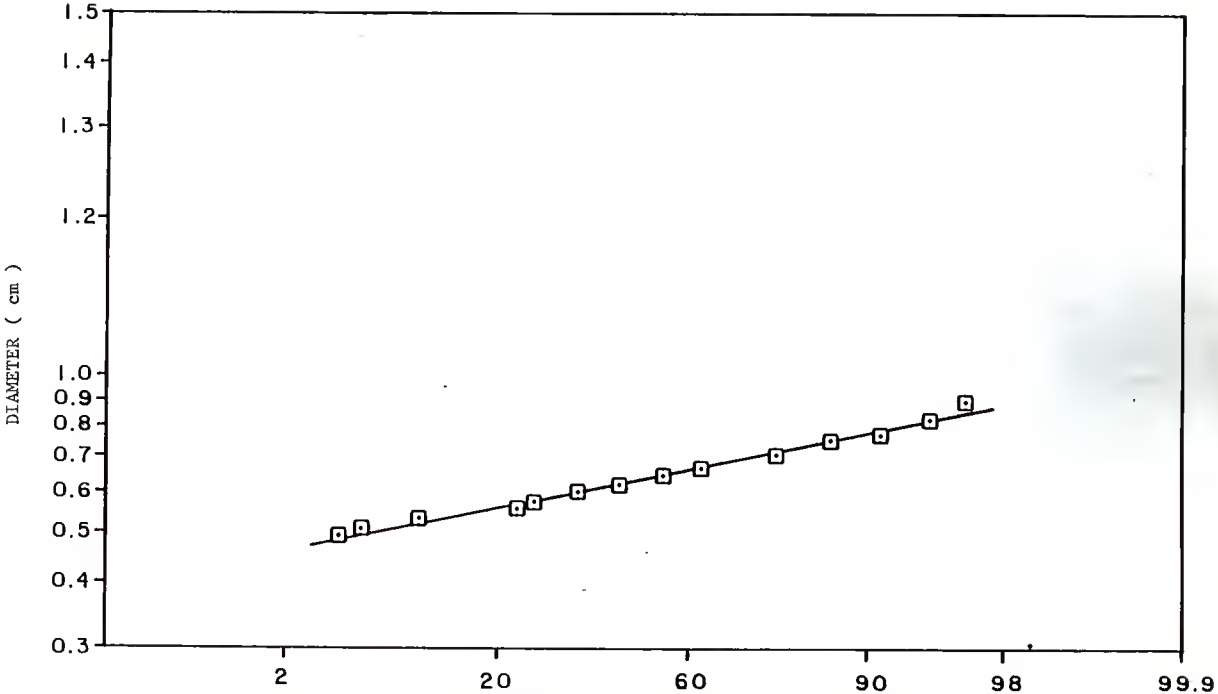

Cumulative weight fraction with diameter less than stated
for particle size #30-#35 based on perimeter of the particle

References

Allen T. (1973). Particle Size Measurment 2nd edition.

Butler, J. A. V. and C. Ockrent (1930). Studies in Electrolocapillarity. 3 J. Phys. Chem. 34,2841.

Cooney D. O. and F. P. Strusi (1972). Analytical Description of Fixed Bed Sorption of Two Langmuir Solutes Under Nonequilibrium Conditions. Ind. Eng. Chem. Fund., 11,123.

Crittenden J. C. (1976). Mathematical Modelling of Fixed Bed Adsorber Dynamics - Single Component and Multiconponent. PH.d. Thesis, Univ. of Michigan, Ann Arbor, MI.

Crittenden J. C. and W. J. Weber, Jr. (1978). Mathematical Modelling of Fixed Bed Adsorption Systems: Single Component and Multicomponent. 71st Ann. Meeting, Amer. Inst. Chem. Eng., Miami Beach, Florida.

Dietz F. , and J. Trand. Vom Wasser 51:233-257 (1978).

Digiano F. A. and W. J. Weber, Jr. (1973). Sorption Kinetics in Infinite Batch Experiments. J. Water Poll. Control Fed., 45, 713.

Dwiwedi P. N. and Upadyay S. N. (1977). Ind. Eng. Chem., Process Des. Dev., Vol. 16, No.2, 1977.

Famularo J., J. A. Mueller and A. S. Pannus (1980). Predictions of Carbon Column Performance from Pure-Solute Data. J. Water Poll. Control Fed. 52,2019.

Foust A. S., Wenzel L. A., Clump C. W., Maus L., Andersen L. B. Principles of Unit Operations. pg 525. Appendix B.

Fritz W., W. Merk, E. U. Schlunder and H. Sontheimer (1980). Competitive Adsorptions of Dissolved Organics on Activated Carbon. In: Activated Carbon Adsorption Of Organics From The Aqueous Phase.; Vol. 1. (M. J. McGuire and I. P. Suffet, Eds.). Ann Arbor Sci., Ann Arbor, MI.

Gleuckauf, E. and J. I. Coates (1947). Theory of Chromatography, Part 4. J. Chem. Soc., 1315.

Hall K. R., L. C. Eagleton, A. Acrivos and T. Vermeulen (1966). Pore and Solid Diffusion in Fixed Beds Adsorption

Under Constant Pattern Conditions. Ind. Eng. Chem. Fund. 5,212.

Harold Heywood, Symposium on Particle Size Analysis, pg 14. (1947), Inatitution of Chemical Engineers.

Heister N. K. and T. Vermeulen (1952). Saturation Performance of Ion-Exchange and Adaorption Columna. Chem. Eng. Prog., 48,505.

Holzel G., F. Fuchs and G. Baldauf (1979). Ubersuchunger Zur Optimierung der Aktivkohleanwendung bei der Trikwasseraufbereitung am Rhein unter besonderer Berucksichtigung der Regeration nach Thermischen Verfahven. In: Optimeirung der Aktivkohleanwendung bei der Trikwaaaeraufbereitung. Universitat Karlaruhe Deutschland.

Hseih J. S. C., R. M. Turian and C. Tien (1977). Multi-Component Liquid Phase Adsorption In Fixed Beds. Amer. Inst. Chem. Eng. J., 23,263.

Jain J. S., V. L. Snoeyink (1973). Adsorption From Bisolute Syatema on Activated Carbon. J. Water Poll. Control Fed.

Jossens L., J. M. Prausnitz, W. Fritz, E. U. Schlunder and A. L. Myers (1978). Thermodynamics of Multiaolute Adsorption From Dilute Aqueoua Solutiona., Chem. Eng. Sci., 33,1097.

Keinath T. M. and W. J. Weber, Jr. (1968). A predective Model for The Deaign of Fluid Bed Adsorbers. J. Water Poll. Control Fed. 40,741

Keinath T. M. (1977). Design and Operation of Activated Carbon Adaorbers Used for Industrial Waatewater Decontamination. Amer. Inst. Chem. Eng. Symp. Ser. 73,1.

Kyte W. S. (1973). Nonlinear Adsorption in Fixed Beds. Chem. Eng. Sci. 28,153

Langmuir J. (1918). The Adsorption of Gases on Planes of Glaas, Mica, and Platinum. J. Amer. Chem. Soc. 40,1361.

Larson A. C. and C. Tien (1983). Multicomponent Liquid Phase Adaorption in Batch . Part 2 Experiment on Carbon Adsorption From Solutiona of Phenol, O-Cresol, and 2,4-dichlorophenol. Chem. Eng. Commun. 27, 359-361

Lee M. C., J. C. Crttenden, V. L. Snoeyink and W. E. Thacker (1980). Mathematical Modelling Of Humic Substances Removal With Activated Carbon Beds. National Conference on Environmental Engineering. ASCE., NY.

Liapis A. I. and D. W. T> Rippen (1978). The Simulation of

Binary Adsorption in Activated Carbon Columns Using Estimates of Diffusional Resistances Within the Carbon Particles Derived from Batch Studies. Chem. Eng. Sci. 35,593

Mathews A. P. (1975). Mathematical Modelling of Multicomponent Adsorption in Batch Reactors. PH.D. Thesis, Univ. of Michigan, Ann Arbor, MI.

Mathews A. P. and W.J. Weber, Jr. (1977). Effects of External Mass Transfer and Intraparticle Diffusion on Adsorption Rates in Slurry Reactors. Americ. Inst. Chem. Eng. Symp. Ser., 73,91.

Mathews A. P. and S. R. Kulkarni (1983). Unpublished work, Department of Civil Engineering, Kanaas State University.

Mathews A. P. and C. A. Su, (1983). Prediction of Competitive Adsorption Kinetics for Two Priority Pollutants. Environmental Progress 2(4), 257.

Mathews A. P. (1983). Adsorption In An Agitated Slurry of Polydisperse Particles. AIChE Symposium Series 79, 18.

Mathews A. P. (1984). Unpublished work. Department of Civil Engineering, Kansas State University.

Mathews A. P. and W. J. Weber, Jr (1984). Modelling and Parameter Evaluation of Adsorption in Slurry Reactora. Chem. Eng. Commun. 25, 157.

Radke C. J. and J. M. Prausnitz (1972). Adsorption of Organic Solutes from Dilute Aqueous Solution on Activated Carbon. Ind. Eng. Chem. Fund., 11,445.

Radke C. J. and J. M. Prausnitz (1972). Thermodynamics of Multisolute Adsorption from Dilute Liquid Solutions. Amer. Inst. Chem. Eng. J., 18,761.

Schay G. J., F. P. Fejes and J. Szathmary (1957). Studies on the Adsorption of Gas Mixture, 1. Statistical Theory of Physical Adsorption of Langmuir type in Multicomponent Systems. Acta Chem. Sci. Hungary., 12,299.

Snoeyink, V.L. and W.J. Weber, Jr. (1968). Reaction of the hydrated proton with Active Carbon. In: Adsorption from Aqueous Solution, Advances in Chemistry Series, No. 79,112.

Suzuki M. and Kawazoe (1974). Batch Measurment of Adsorption Rate in an Agitated Tank - Pore Diffusion Kinetics with Irreversible Isotherm. J. Chem. Eng. Japan, 7,346.

Sweeny M. W., W. A. Melville, B. Trgovicich and C. P. L. Grady, Jr. (1982). Adsorption Isotherm Parameter Estimation.

J. Env. Eng. Div., ASCE, 108,913.

Thacker W. E. and V. L. Snoeyink (1978). On Evaluating Granular Activated Carbon Adsorption. Notes and Comments, J. Amer. Water Works Assoc., 70,45.

Thomas H. C. (1944). Hetrogenous Ion Exchange in a Flow System. J. Amer. Chem. Soc., 66,1664.

Van hall C. E., Ed. Measurments of Organic Pollutants in Water and Wastewater Treatment, ASTM Spec. Pub 686 (Philadelphia: American Society for Testing and Materials, 1979).

Van Vliet, B. M. and W. J. Weber, Jr (1979). Comparitive Performance of Synthetic Adsorbents and Activated Carbon for Specific Compound Removal from Wastewaters. 52nd Ann. Conf., Water Poll. Control Fed., Houston, TX.

Van Vliet, B. M. and W. J. Weber, Jr. (1980)., Modelling and Prediction of Specific Compound Adsorption by Activated Carbon. Water Research, 14(12),1719.

Vassiliou B. and J. S. Dranoff (1962). The Kinetics of Ion Exclusion. Amer. Inst. Chem. Eng. J., 8,248.

Vermeulen T. (1953). Theory for Irreversible and Constant Pattern Solid Diffusion. Ind. Eng. Chem. Fund., 45.

Weber W. J., Jr. Physicochemical Process For Water Quality Control. (1972), Wiley-Interscience.

Weber W. J., Jr. and R. R. Rumner (1965). Intraparticle Transport of Sulphonated Alkyl Benzenes in a Porous Solid: Diffusion with Nonlinear Adsorption. Water Resources Res., 1,361.

Westermark M. (1975). Kinetics of Actvated Carbon Adsorption. J. Water Poll. Control Fed., 47,704.

Zwiebel I., R. L. Gariepy and J. J. Schnitzer (1972). Fixed Bed Desorption Behavior of Gases with Non-Linear Equilibria : Part 1. Dilute, One Component Isothermal Systems. Amer. Inst. Chem. Eng. J., 18,1139.

EFFECT OF PARTICLE SIZE DISTRIBUTION ON ACTIVATED CARBON ADSORPTION

by

THOPPIL JOJO KUNJUPALU

B.E., College of Engineering Guindy, Madras University
India, 1983

AN ABSTRACT OF A MASTER'S THESIS

submitted in partial fulfillment of the

requirements for the degree

MASTER OF SCIENCE

Department of Civil Engineering

KANSAS STATE UNIVERSITY
Manhattan, Kansas

1986

Abstract

Batch and fixed bed experiments were conducted to study the effect of particle size on carbon adsorption. Three different types of diameters were used. They were geometric mean diameter of the sieve sizes, length mean diameter, and Sauter mean diameter. All these diameters were estimated based on area of the particles using Quantimet-720 image analysis. A mathematical model was used to compare the results of batch and fixed bed experiments. The model equations were formed considering film transfer and surface diffusion controlled adsorption rates. For fixed bed studies the model equations were solved by using orthogonal collocation technique.

Phenol and parachlorophenol were the two solutes used in the experimental studies. All experiments were conducted using tapwater at 25 deg. C and pH 7. Single solute isotherm data were fitted by the three parameter isotherm equation developed by Mathews and Weber (1977). Bisolute isotherm studies were conducted using Mathews model (1975) and the IAS model.

Kinetic studies were conducted on both single and bisolute systems for single adsorbent sizes as well as for a mixture of adsorbent sizes. The results were predicted by a computer program written by Mathews (1975) for single solute system. For multicomponent adsorption, results were predicted by a program written by Mathews (1983). It was seen from the

predictions that Sauter mean diameter gave better predictions than geometric mean diameter for both individual size fractions and mixture of sizes.

Fixed bed studies were conducted for single solute as well as for bisolute systems. A mathematical model of fixed bed was modified by Mathews (1984) so that the equilibrium could be represented by the three parameter isotherm. The model was employed to compare the performance of fixed beds for constant temperature and pH but varying particle sizes. Breakthrough curves were analyzed for geometric mean diameters and for Sauter mean diameters. In the case of mixture of sizes the model was analyzed for stratified bed layers also.

It was seen that when the stratified bed layer model was used the column predictions were better than for either geometric mean diameters or Sauter mean diameters. However, it was seen from the results of the predictions that the representation of particle size distribution by the Sauter mean diameter was better than that by geometric mean diameter.